COMMUNICATIONS

COMMUNICATIONS

https://doi.org/10.26552/com.C.2013.4.3-8

Rafal Melnik - Bogdan Sowinski *

APPLICATION OF THE RAIL VEHICLE'S MONITORING SYSTEM IN THE PROCESS OF SUSPENSION CONDITION ASSESSMENT

Rail vehicle's suspension determines riding dynamics, safety and comfort. Its condition should be checked regularly, and even monitored continuously. In order to acquire information on suspension condition during commercial operation, the rail vehicles' monitoring system has been developed at Monitoring of Technical State of Construction and Evaluation of its Lifespan Project (MONIT). The aim of the system is qualitative assessment of suspension condition based on acceleration signals recorded on bogie frames and body.

The experimental tests of the system were performed on wagons with introduced suspension damages: stiffness reduction of primary suspension in freight car and the loss of damper of secondary suspension in passenger car. The monitoring procedure and test results are presented in the work.

Keywords: *Suspension, condition monitoring, fault detection.*

1. Introduction

Currently used monitoring systems of the rail vehicles are directly related to the control of the vehicle, e.g. power supply, power train, braking system. Rail vehicles' suspension has not been an object of the monitoring although it determines significantly riding dynamics, safety and comfort. The rail vehicle monitoring system has been developed at Monitoring of Technical State of Construction and Evaluation of its Lifespan Project (MONIT). The main assumption for the system is qualitative suspension condition assessment by means of standard measuring equipment during normal operation.

The system has been tested on wagons with and without suspension damages. Recorded data during the test provided information on the vehicle dynamic behavior, affected by suspension faults.

2. Monitoring system

Expedient feature of the monitoring system of rail vehicle and track is versatility and modular architecture. It can be installed virtually on every type of rail vehicle. Its aim is qualitative assessment of the primary and secondary suspension, axle bearing temperature measurement and evaluation of track quality.

The system consists of:

- Central data acquisition computer MOXA V2406-XPE,
- Sierra Wireless AirLink GX400 router with GPS module,
- Local data acquisition units,
- Piezoelectric VIS-311A accelerometers,
- Pt100 temperature sensors,
- System server with operator's station.

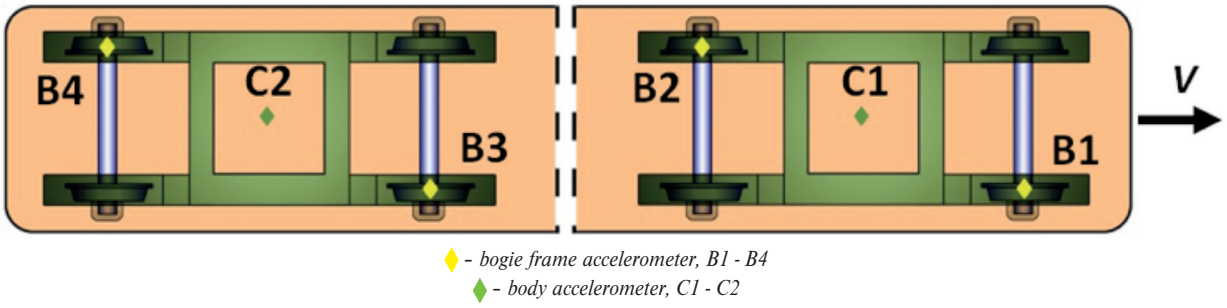

Fig. 1 The location of measurement points

* **Rafal Melnik, Bogdan Sowinski**
Warsaw University of Technology, Faculty of Transport, Department of Transport Equipment Construction Bases, Warsaw, Poland,
E-mail: rme@wt.pw.edu.pl

Location of measurement points is depicted in Fig 1. Acceleration signals recorded on a bogie frame above wheel sets (B1-B4) are used for primary suspension condition assessment. Regarding the system's architecture and cost of the equipment, the number of measurement points is reduced to two. This solution is still sufficient for qualitative assessment. Sensors installed on a body, above bogie center (C1, C2) are used in order to monitor secondary suspension condition. In each measurement point acceleration signals are recorded in vertical (Z) and lateral (Y) direction.

Length of a track section, on which monitoring system performs measurement, is adjustable and is set to 500 meters. The signals from all sensors are collected in the form of a data packet. This packet contains data re-sampled to spatial frequency fs = 5 m-1 which were previously analyzed. The data packet contains geographic coordinates of the place where the signals recording was triggered, and values of the signals. Exceedance of the diagnostic indicator limit value results in generation of a control packet containing warnings or alerts (depending on the exceedance value). Packets are sent to the operator's station (system's server) via GSM network where information occurs on warnings and alerts referring to the vehicle's condition. System enables vehicle localization by means of GPS module.

3. Suspension condition monitoring process

Suspension fault detection method for the monitoring system should be efficient, easy to implement and fast. There are a few methods, e.g. based on Kalman Filter [1 and 2] and multi-model approach [3 and 4] which are intended to solve the problem of suspension fault detection. These methods require mathematical model of the vehicle whose parameters: masses, moments of inertia, stiffness and damping coefficients may not be available. The proposed fault detection method does not require mathematical model since for qualitative assessment of suspension condition the analysis of the signals is incorporated.

The procedure, in terms of the running gear's dynamic properties and safety, is based on the requirements contained in UIC 518 leaflet [5] and in the standard EN 14363 [6]. The limit values of RMS and percentile 99.85% (maximal value) of acceleration signals, measured in specified points of vehicle, should not be exceeded.

The influence of suspension damages on acceleration signals is rather complex. The effect of stiffness or damping reduction on acceleration signals depends generally on the magnitude and frequency of the excitation (track geometrical irregularities, vehicle speed). Regarding damaged suspension, in certain circumstances the registered values of acceleration may be lower compared with a vehicle in undamaged condition. However, the change of speed or track section can result in the increase of the acceleration values for the damaged vehicle.

The normative parameters may not be sufficient for damage detection, therefore, monitoring procedure involves additional statistical parameters, which are not included in [5] and [6]. Various statistical parameters have been considered for this problem and it was concluded that the diagnostic process is more efficient when a set of parameters is used [7]. Finally, the set consisting of RMS, Interquartile range and Zero-Peak were chosen for the diagnostic process.

In papers [7, 8 and 9] there was a lack of algorithm that could link together all analyzed diagnostic parameters. Consideration of these parameters separately requires assigning limit values for each of them. In order to improve fault detection and to treat these parameters as one diagnostic indicator a multidimensional analysis is proposed.

The basic assumptions of multidimensional approach are listed below:

- Selected statistical parameters providing diagnostic information can be used in creation of multidimensional space,
- A point in multidimensional state space is defined by coordinates whose values correspond to the values of diagnostic parameters,
- The point representing a vehicle's faulty condition is distant from the point of a vehicle's nominal condition,
- The excess of certain (established) distance is a diagnostic symptom.

The current condition (at present time) of the vehicle is characterized by the parameters of acceleration signals recorded on a certain distance on a track of known maintenance quality.

For the vehicle in nominal condition (without suspension damages) we can obtain many Niv (1) points belonging to the diagnostic space. Each of these points refers to i-th passage on the same track section of known maintenance quality, at the same velocity v.

$$N_i^v = \left(x_{N1,i}^v, x_{N2,i}^v, ..., x_{Nn,i}^v\right) \tag{1}$$

where,

N_{iv}^i - a point referring to current condition at velocity v of coordinates $x_{N1,i}^v, x_{N2,i}^v, ..., x_{Nn,i}^v$,

i - the number of measurement,

$x_{N1,i}^v, x_{N2,i}^v, ..., x_{Nn,i}^v$ – the following values of diagnostic parameters for the current state from 1 to n, for velocity v.

The reference point S^v (2) is created by averaging the coordinates (diagnostic parameters' values) of many N_i^v points. This point represents a reference vehicle - vehicle in nominal condition which parameters' values are mean values obtained from many vehicle passages.

$$S^v = \frac{1}{n}\sum_{i=1}^{n} N_i^v \tag{2}$$

where,

$x_{S1}^v, x_{S2}^v, ..., x_{Sn}^v$ – the following values of the coordinates from 1 do n for the reference point and velocity v.

The point representing current state U_j^v (3) is described by coordinates (parameters) values of the signals recorded during j-th measurement during normal operation, on the same track section as for N_i^v point and at the same speed.

$$U_j^v = \left(x_{U1,j}^v, x_{U2,j}^v, ..., x_{Un,j}^v\right) \tag{3}$$

where,

U_j^v - a point representing current condition at velocity v of coordinates $x_{U1,j}^v, x_{U2,j}^v, ..., x_{Un,j}^v$,

j - the number of measurement,

$x_{U1,j}^v, x_{U2,j}^v, ..., x_{Un,j}^v$ - the following values of diagnostic parameters from *1* to *n*, velocity *v*.

Since three parameters were selected for diagnostic process, we get $i,j = 3$, a three-dimensional diagnostic space.

The fault detection of running gear, especially suspension, is based on the method of analysis of metric (distance) $d(S^v, U_j^v)$ from the reference point and point representing current state. The concept of the method is illustrated in Fig. 2. The diagnostic symptom is the excess of the permissible distance F from the reference point. The F value may be set upon results obtained from experiments in which suspension damages were studied. The distance can be calculated using different formulas, albeit Euclidean metric is used.

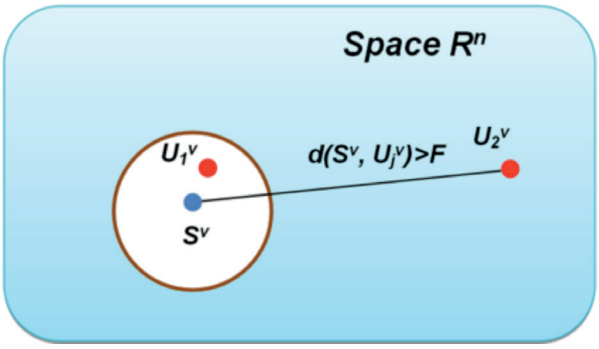

Fig. 2 The concept of the method

The points referring to current condition should be located within boundaries defined by F, of the reference point S^v. It is not crucial on which side of S^v the U_j^v point is located. This allows using this method in detection of faults that result in the increase and/or decrease of the parameters values. Since the range of values for the following parameters may be different, they should be normalized by dividing values of U_j^v by values of S^v, therefore, the reference points coordinates are (1, 1, 1).

4. Experimental tests

The aims of the experimental tests were validation of the monitoring system and studies of the influence of suspension damages on recorded signals. The monitoring system was installed on a passenger and freight car (equipped with Y25 bogies). The freight car was loaded up to 90 t. For validation purpose an additional measuring system was installed, which is used by the Railway Institute (Poland) for approval tests. The experiment took place on a test track in Zmigrod in Poland. The first stage of the experiment was carried out on vehicles in nominal condition in order to obtain reference signals. In the second stage, the test was performed on wagons with introduced suspension damages:

- passenger car - removal of one secondary suspension damper (Fig. 3),
- freight car - removal of one coaxial springs packet of secondary suspension, on the left side of axle bearing at one wheel (Fig. 4).

To minimize the risk of accident or even derailment, only one sort of damage was introduced during the test ride.

Fig. 3 Passenger car running gear with secondary suspension damper disconnected

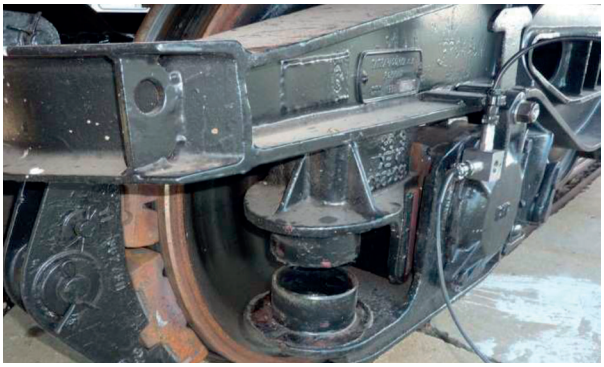

Fig. 4 Freight car bogie with removed springs on one side

5. Results of the experiment

The acceleration signals were analyzed using the proposed method. The number of markers in plots (points in Figs. 5 - 8) depends on the number of passages on chosen track sections. The F value (radius of the sphere) equals to standard deviation of the distances' value (of nominal vehicle) from the reference point and is calculated for different speed values and track sections. For commercial use it may be adjusted directly on the results of the experiment. Since the axes are not equal in Figs. 5 - 8, the sphere appears as an ellipsoid.

The case of damaged passenger car (damping reduction) condition is illustrated in Figs. 5 and 6. The blue star marker represents the reference point, blue point - condition assessed as undamaged, red point - condition assessed as damaged. The coordinates' normalized values are presented below plots. Vertical acceleration signals from four passages on the same tangent track section were used for condition evaluation. In these figures it can

be seen that not every point referring to a vehicle with suspension fault is classified as damaged. Nevertheless, for some passages (measurements) distances are substantial and faulty condition can be identified. For 80 km/h and vertical direction F=0.48 and F=0.232 for 100 km/h.

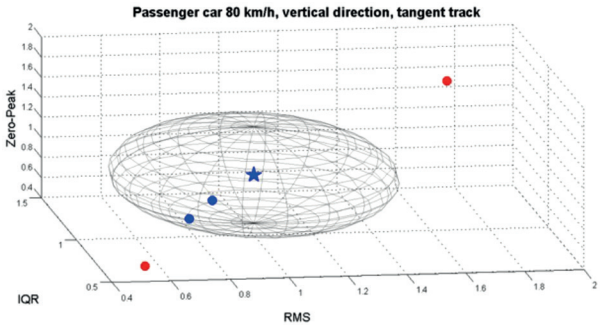

RMS (Z)	IQR (Z)	Zero-Peak (Z)	d(Sv,Ujv)
0.744	0.844	0.715	0.413
1.689	1.147	1.756	1.033
0.822	0.844	0.892	0.260
0.533	0.587	0.478	0.813

Fig. 5 Results of passenger car analysis, 80 km/h, vertical acceleration, tangent track

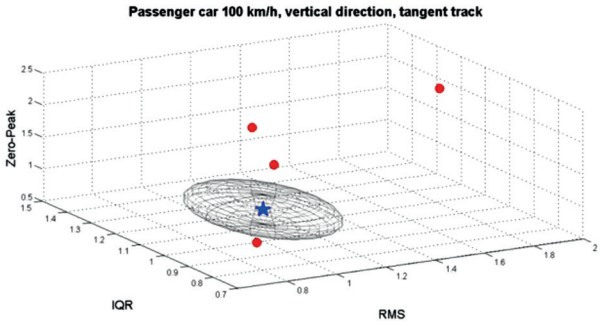

RMS (Z)	IQR (Z)	Zero-Peak (Z)	d(Sv.Ujv)
1.167	1.124	1.393	0.445
1.389	1.438	1.317	0.666
0.815	0.839	0.858	0.283
1.787	1.073	2.328	1.546

Fig. 6 Results of passenger car analysis, 100 km/h, vertical acceleration, tangent track

The results of the freight car condition analysis are depicted in Figs. 7 and 8. The results refer to a curved track section of R=900 m. The reduction of stiffness to the half of its nominal value caused that majority of the points is located beyond boundaries of the reference point and clearly indicate damage. In case of the freight car number of passages was greater than for a passenger car, entailing more points in the plots. The radius F=0.144 for 80 km/h in lateral and F=0.112 in vertical direction.

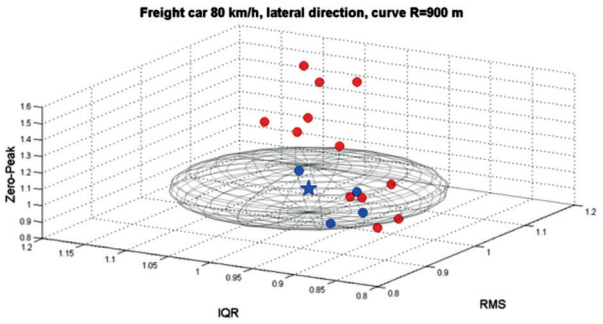

RMS (Y)	IQR (Y)	Zero-Peak (Y)	d(Sv,Ujv)
0.994	1.008	1.110	0.110
1.069	0.983	1.575	0.580
1.104	1.067	1.568	0.581
1.185	1.096	1.345	0.403
1.082	1.062	1.196	0.222
0.960	0.878	1.165	0.209
1.109	1.065	1.246	0.277
1.054	0.995	1.194	0.201
0.939	0.938	0.909	0.126
0.934	0.879	0.933	0.154
0.974	0.920	0.945	0.100
0.972	0.926	1.068	0.105
0.905	0.837	1.054	0.196
0.894	0.874	1.169	0.236
1.082	1.101	1.229	0.263
0.924	0.906	1.114	0.166

Fig. 7 Results of freight car analysis, 80 km/h, lateral acceleration, curve R=900 m

6. Conclusions

The method of multidimensional analysis of statistical parameters enables to detect faults of running gear (especially suspension). Vehicle condition is assessed on analysis of the metric between a reference point and a point representing current state. As the results have shown, it is necessary to take into consideration more points for the proper condition assessment. Although the vehicle may be damaged, some of the points might be located within permissible range (sphere) defined by F value. Setting the limit value of the metric should be preceded by statistical analysis of data acquired from nominal and damaged vehicle. For the experiment results analysis it was equal to standard deviation of distance from the points of current nominal condition to the reference point (averaged values for undamaged vehicle). In case of embracing too many points the F value should be adjusted.

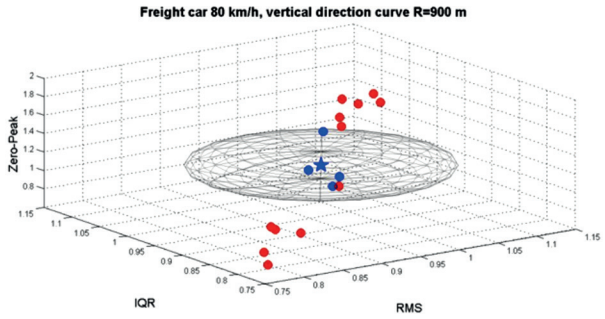

RMS (Z)	IQR (Z)	Zero-Peak (Z)	d(Sv,Ujv)
0.832	0.847	0.866	0.264
0.958	0.920	0.998	0.090
1.137	1.125	1.201	0.273
1.118	1.058	1.385	0.407
0.919	0.854	1.193	0.255
0.837	0.808	0.902	0.270
1.122	1.133	1.258	0.315
1.082	1.078	1.135	0.176
0.793	0.800	1.050	0.292
0.959	0.965	1.079	0.095
1.077	1.013	1.631	0.636
1.086	1.087	1.209	0.243
0.779	0.793	0.809	0.358
0.759	0.758	0.776	0.408
1.062	1.083	1.099	0.144
0.981	0.940	1.026	0.069

Fig. 8 Results of freight car analysis, 80 km/h, vertical acceleration, curve R=900 m

On track sections of low maintenance quality the established limits F may cause generation of false alarms. It is necessary to observe the vehicle's location and relate the alarms with its current position on track sections.

The further work will include development of progressive limits F according to track quality indicator - calculated upon the basis of accelration signals obtained from axle boxes.

Acknowledgement

The authors express their gratitude for the financial support by the Polish Ministry of Science and Higher Education for the support of research within the framework of the project MONITORING OF TECHNICAL STATE OF CONSTRUCTION AND EVALUATION OF ITS LIFESPAN – MONIT. Action Operational Programme Innovative Economy.

References

[1] GODA, K., GOODALL, R.: Fault-detection-and-isolation System for a Railway Vehicle Bogie. *Vehicle System Dynamics Supplement* 41 (2004), pp.468-476 Taylor & Francis Ltd.

[2] LI, P., GOODALL, R.: *Model-based Condition Monitoring for Railway Vehicle Systems*, Control 2004, University of Bath, UK, September 2004

[3] TSUNASHIMA, H., et al.: *Condition Monitoring and Fault Detection of Railway Vehicle Suspension using Multiple-Model Approach*. Proc. of the 17th World Congress, the Intern. Federation of Automatic Control, Seoul, 2008

[4] TSUNASHIMA, H., MORI, H.: *Condition Monitoring of Railway Vehicle Suspension Using Adaptive Multiple Model Approach*. Intern. Conference on Control, Automation and Systems 2010, Gyeonggi-do, Korea, 2010

[5] UIC 518: Testing and Approval of Railway Vehicles from the Point of View of Their Dynamic Behaviour - Safety - Track Fatigue - Ride Quality, 2003

[6] EN 14363: Railway applications - Testing for the Acceptance of Running Characteristics of Railway Vehicles - Testing of Running behaviour and Stationary Tests, 2005

[7] CHUDZIKIEWICZ, A., SOWINSKI, B.: *Problems of Choosing Statistical Parameters In the Process of Monitoring the System of Railway Vehicle*. Proc. of 8th Intern. Conference on Railway Bogies and Running Gears, pp.127-129, Hungary, Budapest, 8-10 November 2010

[8] CHUDZIKIEWICZ, A., SOWINSKI, B., SZULCZYK, A.: *Statistical Parameters of Vibrations as Measures of Rail Vehicle Condition*. Proc. of 17th Intern. Congress on Sound and Vibration, pp.73, Cairo, 2010

[9] MELNIK, R., KOSTRZEWSKI, M.: Rail Vehicle's Suspension Monitoring System - Analysis of Results Obtained From Tests of the Prototype. *Key Engineering Materials,* vol. 518, pp 281-288, 2012.

https://doi.org/10.26552/com.C.2013.4.9-17

Libor Izvolt - Peter Dobes - Martin Mecar *

CONTRIBUTION TO THE METHODOLOGY OF THE DETERMINATION OF THE THERMAL CONDUCTIVITY COEFFICIENTS λ OF MATERIALS APPLIED IN THE RAILWAY SUBBASE STRUCTURE

The paper focuses on the methodology of determination of thermal conductivity coefficients λ of the construction materials of railway subbase. The determination of the thermal conductivity coefficients λ depends on the determination of the specific heat capacity and the time interval as sub-parameters. The paper presents specialized equipment for the determination of these parameters, the stated procedures and the method of test evaluation.

The paper focuses on the presentation of the results of the experimental determination of the thermal conductivity coefficients λ of selected construction materials (clay, track ballast, fraction 32/63 mm, crushed aggregate fraction 0/32 mm and sandy gravel 0/32 mm). In the conclusion there is the confrontation of the values of the thermal conductivity coefficients λ stated by the experimental laboratory measurements with the values stated in TNZ 73 6312 and STN EN ISO 10 456.

Keywords: *Thermal conductivity coefficients, gravel sand layer, validation, railway structure.*

1. Introduction

The thermotechnical properties of construction materials are the basic characteristics for the design and assessment of the railway subbase structure with regard to non-transportation load (the influence of climatic factors, mainly adverse effects of frost). From this point of view the most important characteristic is the thermal conductivity coefficient λ of construction materials applied in the structural layers of railway subbase. As the adopted standard EN STN does not specify all the values of the thermal conductivity coefficients that are at present normally used in the subbase construction, it is necessary to specify them in the process of railway subbase dimensioning.

2. Verification of the thermal conductivity coefficients λ of railway subbase materials

In the Slovak Republic the design and assessment of the railway subbase structure is realized in accordance with TNZ 73 6312 [1]. This legislative document, binding for the design and assessment of ZSR lines to transportation load (static and dynamic load) and non-transportation load (influence of climatic factors, mainly frost), contains a section dedicated to the methodology of dimensioning and assessment of the railway

Design values of the thermal conductivity coefficients λ of railway subbase materials [1] Table 1

Material	Thermal conductivity coefficient λ [W/(m.K)]
Track ballast	2.00
Sandy gravel	2.30
Crushed aggregate, tailings, recovered material	2.00
Blast furnace slag	0.95
Stabilized soil	1.75
Asphalt coated aggregate	1.15
Cement concrete	2.55
Sandy clay	2.20
Clay	1.95
Silty clay	1.70
Mechanically compacted aggregates	1.80
Hydraulically bound aggregates	2.20
Polystyrene concrete	0.25
Polystyrene	0.15

* **Libor Izvolt, Peter Dobes, Martin Mecar**
Faculty of Civil Engineering, Department of Railway Engineering and Track Management, University of Zilina, Slovakia,
E-mail: libor.izvolt@fstav.uniza.sk

subbase structure to the non-transportation load, where it states the thermal conductivity coefficients λ of materials applied in the railway subbase structure. The stated coefficients are taken into account in the dimensioning procedure of railway subbase to adverse effects of frost - Table 1.

The Department of Railway Engineering and Track Management of the Faculty of Civil Engineering of the University of Zilina has been researching the relevancy and assessment of design of railway subbase to non-transportation load for several years. Not only because new structural materials and elements are applied into the railway subbase structure but also due to changes of some legislative documents dealing with the problem of thermotechnical proporties of construction materials and also due to recent climatic changes.

This verification is also important due to parallel modeling of the freezing process with SoilVision software for the experimental stand of the Department of Railway Engineering and Track Management of the University of Zilina. It contains a built-in subbase structure that was dimensioned for the non-transportation load according to the methodology stated in [1].

On the basis of long-term experimental measurements of the temperature regime of subbase layer that started in December 2002, conducted in the experimental stand of the Department of Railway Engineering and Track Management of the University of Zilina, it was proved that freezing of the subbase layer is not significantly influenced only by the origin and granularity, but also by the humidity of construction material built in the subbase structure. It is not known, which granulometric composition and mass moisture of the material the above stated thermal conductivity coefficients λ were gained for. Due to this fact and also due to the verification of the freezing process flow by the mathematical analysis using SoilVision software, at the same time it is necessary to verify the thermal conductivity coefficients λ that are used in the procedure of the design and asssessment of subbase related to adverse effects of frost according to TNZ 73 6312.

Since 2008 the laboratory of the Department of Railway Engineering and Track Management has been dealing with experimental measurements to verify the thermal conductivity coefficients λ stated in Table 1. Firstly, the testing devices that serve to determine the thermal conductivity coefficients λ were constructed. After development of these devices and their testing, the actual verification of individual construction materials took place. It included materials that normally occur in railway subbase structures or are applied there as new materials, such as clay, track ballast, fraction 32/63 mm, crushed aggregate, fraction 0/32 mm and sandy gravel 0/32 mm. This paper presents the procedures of experimental measurements and the achieved results of thermal conductivity coefficients λ of the stated construction materials in confrontation with the values stated in Table 1.

As stressed above, to determine the thermal conductivity coefficient λ it is necessary to develop the device for conducting the measurements of all the needed input characteristics that enter the relations for its calculation. These characteristics are primarily the time interval t and the specific heat capacity c. For each of the above stated mass moistures three measurements were conducted, they were averaged and the result was compared to the value of the thermal conductivity coefficient λ stated in [1].

2.1 Determination of the thermal conductivity coefficient λ of selected construction materials with the method of non-stationary heat flow

As in Slovakia after cancelling STN 72 1105 there is not any valid standard that can be applied in the measurements, the measurement procedure was realized according to the Czech standard CSN 72 1105 [2]. The stated standard only considers the maximum fraction 16 mm, so the procedure had to be partially adjusted to be suitable for fraction 0/32 mm and 32/63 mm. The determination of the thermal conductivity coefficient λ is based on the Fourier´s differential equation that describes the unidirectional heat transfer in homogeneous materials by spreading. The equation can be stated as:

$$q(x,t) = -\lambda \frac{\delta \theta_{(x,t)}}{\delta x} \tag{1}$$

where:
$q(x,t)$ - heat flow density in place x and in time t, (W/m^2),
λ - thermal conductivity coefficient, [W/(m. K)],
$\theta_{(x,t)}$ - temperature in place x and in time t, (K).

Depending on the environment, the heat flow can be expressed using the relation:

$$\frac{\delta q_{(x,t)}}{\delta x} = -\rho \bullet c \frac{\delta T_{(x,t)}}{\delta t} \tag{2}$$

where: ρ - volumetric mass, (kg/m^3),
c - specific heat capacity, [J/(kg. K)].

After some adjustment from the relations (1) and (2) an equation to characterize the temperature field development can be derived. This equation can be stated in the form:

$$\frac{\delta \theta_{(x,t)}}{\delta t} = \frac{\lambda}{\rho \cdot c} \cdot \frac{\delta^2 \theta_{(x,t)}}{\delta x^2} \tag{3}$$

By the adjustment of the relation (3), using the method of finite elements with the boundary conditions θ_0=10 °C, θ_M=0 °C, the time interval t between the 10 % and 50 % decrease of the initial temperature difference measured on the specimen bottom is determined.

This time interval is determined from the graphic assessment of the temperature flow measurements on the specimen bottom, in the place where the temperature decrease flow is the stablest in the given interval. After the adjustment, the relation (3) is stated as:

$$\frac{\lambda}{\rho \cdot c} = 0.249 \frac{h^2}{t} \tag{4}$$

where h is the specimen thickness in m.

By the mathematical adjustment the equation (4) obtains its final form for the calculation of the thermal conductivity coefficient λ and can be stated as:

$$\lambda = 0.249 \frac{h^2}{t} \rho \cdot c \qquad (5)$$

In this relation two main parameters become prominent, namely the specific heat capacity c and the time interval t. The procedure for their determination will be characterized in the further parts of this paper.

2.1.1 Calorimetric test [3]

The calorimetric test serves to determine the specific heat capacity c (J/(kg.K). This parameter is necessary for the indirect determination of the thermal conductivity coefficient λ. A special device demonstrated by Fig. 1 was constructed to specify it. The exact determination of the specific heat capacity c, as well the time interval t is a complex technological process and plays a crucial role in achieving overall results.

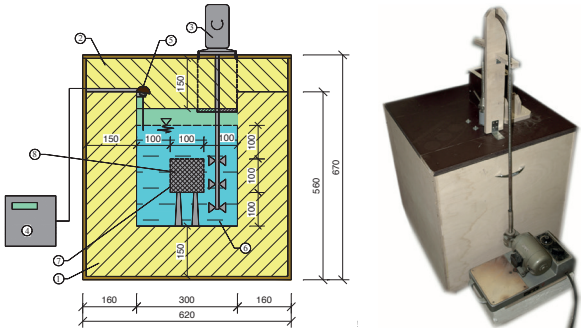

1 - polystyrene insulated container
2 - polystyrene insulated cover
3 - stirrer driven by a motor
4 - control and data centre MS4
5 - temperature measuring probe Pt1000
6 - water environment with θ ≈ 40 °C
7 - polyethylene cover
8 - tested specimen

Fig. 1 Calorimeter

Calorimetric test procedure:

- preparation of the necessary parts of a calorimeter,
- mass moisture adjustment of the tested material,
- specimen collection and its placement into the polyethylene foil,
- weighing the specimen and tempering its temperature at the value + 20 °C ± 2 °C

(placement into the sand layer of a given temperature),

- filling the calorimeter with water of temperature + 40 °C ± 2 °C and its constant stirring

(stirrer with an electric motor),

- temperature stabilisation in the calorimeter (approx. 45 min.),
- input of the tested specimen into the calorimeter,
- registering the specimen temperature consumption for the temperature compensation between the specimen and water (the constant temperature curve signifies the completion of collecting the heat from the water medium),
- determination of the difference between the initial and final temperature with the help of parallel lines (Fig. 2) that are the tangent curve (the use of AutoCAD),
- calculation of the specific heat capacity c0 of the sandy gravel specimen in a dry state according to the relation:

$$c_0 = \frac{m_v \cdot c_v + K}{m} \cdot \frac{\theta_P - \theta_K}{\theta_K - \theta} \qquad (6)$$

where:

c_0 - specific heat capacity of the dry specimen, [J/(kg.K)],
m_v - mass of water, (kg),
c_v - specific heat capacity of water, [J/(kg.K)],
m - mass of the tested specimen, (kg),
θ_P - initial temperature of water, (°C),
θ_K - final temperature of the system, (°C),
θ - specimen temperature prior to measurement, (°C).
K - heat capacity of calorimeter, (J/K)

For the conversion of the specific heat capacity of the sandy gravel specimen from the dry to the mass moisture state the following relation is valid:

$$c = c_0 + (c_v - c_0) \cdot \frac{w_m}{100 + w_m} \qquad (7)$$

where:

c - specific heat capacity of mass moisture material, [J/(kg.K)],
wm - mass moisture of specimen, (%).

The graphic record of the calorimetric test of the sandy gravel layer and the method of its evaluation is obvious from Fig. 3.

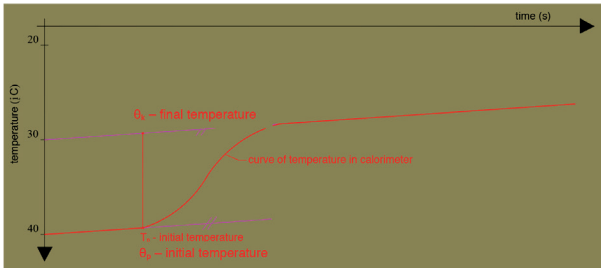

Fig. 2 Dependence of the thermal process flow on time and the method of measurement evaluation

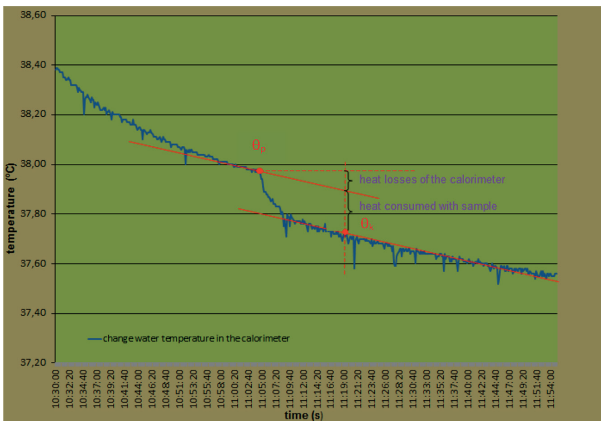

Fig. 3 Graphic record of the calorimetric test of the sandy gravel layer and the method of its evaluation

2.1.2 Measurement of time interval t [3]

The time interval t (s) is another characteristic necessary for the indirect determination of the thermal conductivity coefficient λ. This characteristic cannot be determined via standard laboratory tests and, therefore, in this case a special device for its determination had to be invented (Fig. 4).

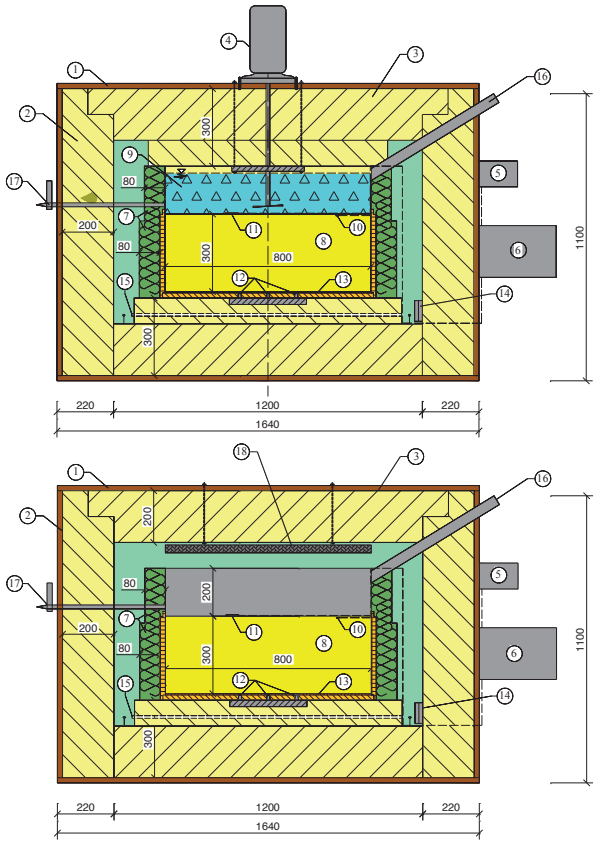

Fig. 4. Device for recording the time interval t

The procedure of determining the time interval t:

1 - thermo-insulated chamber the specimen surface (PT 100)
2 - polystyrene insulated cover
3 - polystyrene insulation of the chamber
4 - stirrer driven by an electric motor
5 - power supply
6 - control and data centre MS4
7 - thermal insulation
8 - tested specimen
9 - crushed ice of the crushed ice
10 - probe for measuring the temperature on
11 - heater element
12 - probes for temperature measuring on the bottom part of the specimen
13 - transfer plate
14 - probe for measuring the ambient air temperature
15 - resistance wire
16 - pipe for input of the ring for crushed ice
17 - pipe with a vent for the draining of the cooling mixture
18 - radiant panel for heating and thermoregulation of the specimen

- preparation of the device components necessary for the measurement of the time interval t,
- adjustment of the specimen mass moisture (drying, saturation with water),
- spreading out and compaction of the tested material in layers of 130 mm in the laminate container of a cylindrical shape, of diameter 800 mm and of height 300 mm,
- flattening of the specimen surface with the help of standard sand,
- placement of the container to the climatic chamber with the help of lifting equipment and embedding of a temperature sensor into its upper part,
- cleaning and treatment of the bottom contact area of a stainless-steel container (application of a vaseline layer) for the colling medium and its placement on the specimen surface,
- placement of the temperature sensor into the stainless-steel container and closing of the climatic chamber by the thermal insulation cover with a radiant panel,
- specimen heating setup to the value close to 35 °C and its tempering to +20 °C ± 2 °C (on the upper and bottom part of the specimen),
- exchange of radiant panel for the panel with the embedded stirrer,
- filling the stainless container with a cooling medium (water and crushed ice of the temperature 0°C) with a filling pipe (approx. 401 of the mixture),
- initiation of the stirring device and addition of the mixture to the volume of approx. 651,
- adding the ice as necessary up to the maximum volume 751 of the mixture.
- monitoring the temperature to the moment when the temperature in the lower part of the specimen decreases by 50 % compared to the temperature at the start of measurement,
- processing and evaluation of the graphic record from the measurements (Figs. 5 and 6) conducted with the help of COMET program(dependance of temperature on time),
- specimen collection for the determination of its granulometry and the test evaluation with SOILAB program,
- determination of the tested specimen mass moisture, drying the specimens in a drying room at the temperature of 105 °C, for 12 hours.

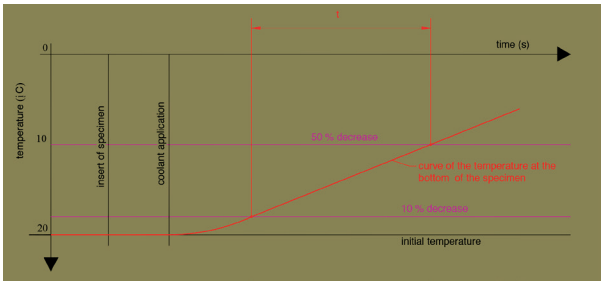

Fig. 5 Dependence of thermal process flow in the calorimeter on time and the method of measurement evaluation

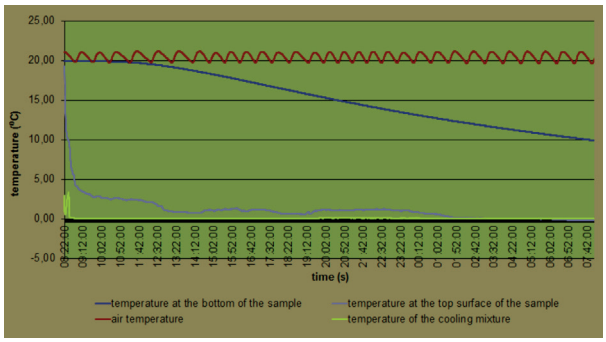

Fig. 6 Example of a graphic record of temperatures for measuring the time interval on a gravel sand specimen with wm ≅ 0 %

2.2 Evaluation of results of experimental measurements [3 and 4]

As previously stressed, by conducting the experimental measurements we aim to justify the relevancy of the values of the thermal conductivity coefficients λ W/(m.K) stated in [1] with regard to the new legislation. Moreover, in this way it is possible to obtain the values of the thermal conductivity coefficients for the materials that are at present applied into the subbase structure as new materials and are not included in the design values stated in [1]. Until now the following materials that are normally used in the subbase structure have been tested: track ballast, crushed aggregate, gravel sand and sandy clay. For each specimen of a given material a set of measurements was conducted while its evaluation was based on the correlation dependencies with determining parameters and influencing factors. Due to a high number of measurements done on the specimens, the detailed evaluation with the stated measured values is presented as a model evaluation on one specimen only, specifically for the railbed material (section 2.2.1). For all the other tested railway subbase materials only the obtained final average values of the input parameters for the calculation of the thermal conductivity coefficient as well as its final average values are stated.

2.2.1 Determination of the thermal conductivity coefficient λ of "new" track ballast fr. 32/63mm

The measurement of the thermal conductivity coefficient was conducted on the railbed material collected from the manufacture (track ballast, fraction 32/63 mm) at its natural mass moisture. The obtained results are valid for the pollution rate of the track ballast 1.86 % (washed away particles) and the mass moisture of 1.17 %. Within the measurements this material was also tested for the pollution rate 3.08 % and the mass moisture 1.31 %, for the sake of determination of the influence of the amount of the washed away particles on the value of the thermal conductivity coefficient λ.

Determination of the specific heat capacity c

The design value of the specific heat capacity of gravel sand was determined from the measurements stated in Table 2, while the given values were stated using the tested specimen that were dried in the laboratory dryer at the temperature 105 °C.

The design value of the specific heat capacity of the tested material with the pollution rate 1.86 % is c = 980 J/(kg.K) and for the material with the pollution rate 3.08 % it is c = 937 J/(kg.K).

Input data for the determination of the specific heat capacity c — Table 2

Measurement number	θ (°C)	θ_p (°C)	θ_k (°C)	m_v (kg)	m (kg)	c [J/(kg.K)]
1	11.76	40.76	40.404	18.09	0.80	1092
2	17.00	40.29	40.005	18.09	0.94	926
3	19.24	41.36	41.026	18.09	1.17	922
4*	17.77	41.34	41.007	18.09	1.12	905
5*	18.35	39.19	38.865	18.09	1.15	968
6*	19.22	40.81	40.348	18.09	1.81	937

**the measurements were realized on the material with the pollution rate 3.08 %*

Input values for the calculation of the thermal conductivity coefficient λ — Table 3

Measurement number	ρ (kg/m^3)	w_m (%)	c [J/(kg.K)]	t (s)	λ [W/(m.K)]
1	1702	1.17	1047	67 500	0.622
2	1718	1.17	1047	67 020	0.620
3*	1903	1.31	980	60 000	0.673
4*	1915	1.31	980	60 300	0.672

**the measurements were realized on the material with the pollution rate 3.08 %*

Determination of the time interval t and the value of the thermal conductivity coefficient λ

The character of the tested specimens regarding their granularity required a special adjustment of the contact surface area to prevent falling of the flattening material and filling the space among the grains. Due to this reason a very thin and adjustable foil was placed under this layer to copy the surface of the aggregate grains and also to prevent the formation of a relevant thermal insulation layer.

Table 3 shows the values that directly enter the calculation of the thermal conductivity coefficient λ, including their resulting values.

The design value of the thermal conductivity coefficient λ was obtained by the arithmetic average of the measurement results and it is λ = 0.621 W/(m.K) for the track ballast material with the pollution rate 1.38 %, and λ = 0.673 W/(m.K) for the material with the pollution rate 3.08 %.

2.2.2 Determination of the thermal conductivity coefficient λ of track ballast fr. 32/63 mm from the railway line in operation

In real conditions of railway track operation the rail bed is contaminated by various alien material that after reaching certain amount, (i.e. level of track ballast contamination), causes changes of not only physico-mechanical, but also thermo-technical properties of this structural layer. The alien material that causes the track ballast contamination enters the railbed in several ways. These are the results of operation (falling of the transported materials from leaking wagons), maintenance (tamping the sleepers), but also the influence of climatic factors (grain disintegration due to frost).

To determine the thermotechnical properties of the railbed material contaminated in this way the specimens from two different locations that differed in the pollution rate, were tested. The specimens No. 1 and No. 2 were collected from the running track of the railway line Zilina - Kosice, from the interstational section Zilina - Varín, specifically in the stop Teplicka n. Vahom, from the rail No. 2 (Fig. 7). The specimens No. 3 and No. 4 were collected from the identical line, specifically in the station Varín, from the loading rail No. 6 (Fig. 8). By the laboratory measurements it was found out that the specimens No. 1 and No. 2 reached the pollution rate 6.35 %, while the specimen No. 3 and No. 4 - 3.16 % only, which can be considered a benefit for the purposes of the verification of the thermal conductivity coefficient λ of the track ballast.

Fig. 7 Place of the collection of the specimen No.1

Fig. 8 Place of the collection of the specimen No.3

Determination of the specific heat capacity c

The design value of the specific heat capacity of the railbed material (track ballast, fr. 32/63 mm) was determined for the tested specimens from the railbed of mass moisture $w_m \cong 0$ %. The design value of the specific heat capacity of the material of the specimens No.1 and No.2 was determined as an average value from the results of 3 measurements and is stated as c = 1010 J/(kg.K). For the material of the specimens No. 3 and No. 4 this value was determined from 3 measurements and can be stated as c = 983 J/(kg.K).

Determination of the time interval t and the value of the thermal conductivity coefficient λ

The measurement was conducted at the natural mass moisture of the tested material (specimens No. 1 and No. 2 for wm = 3.98 % and specimens No. 3 and No. 4 for wm = 2.56 %). With regard to these mass moistures the specific heat capacity was recalculated to the value c = 1138 J/(kg.K) for the specimens No. 1 and No. 2 and c = 981 J/(kg.K) for the specimens No. 3 and No. 4. For the given mass moistures the time interval acquired the value t = 50950 s, and 52450 s for the specimens No. 1 and No. 2, respectively, and t = 63260 s, and 63700 s for the specimens No. 3 and No. 4, respectively. On the basis of the stated values of the partial parameters, the design value of the thermal conductivity coefficient λ for the material of the specimens No. 1 and No. 2, was obtained as an average value from 2 measurements - λ = 0.991 W/(m.K) and for the material of the specimens No. 3 and No. 4 this value is also obtained as an average from 2 measurements - λ = 0.750 W/(m.K).

2.2.3 Determination of the thermal conductivity coefficient λ of crushed aggregate fr. 0/32 mm and fr. 0/63 mm

With regard to the fact that in both cases the material was of the same mineralogical composition (melaphyr) and the materials only differed in granularity (and slightly different bulk density), the results of the testing mesurements are stated as a whole. The measurements of the time interval t were conducted at different mass moisture conditions (w_m = 2.41 % – 4.68 %), while the specific heat capacity c was determined for dry material ($w_m \cong 0$ %).

Determination of the specific heat capacity c

The design value of the specific heat capacity of the crushed aggregate, fr. 0/32 mm and fr. 0/63 mm was stated for the tested specimens of mass moisture wm ≅ 0 %. By the arithmetic average from 3 measured results the design value of the specific heat

capacity c = 1115 J/(kg.K) was stated. Due to the identical mineralogical composition this value can be considered for the fraction 0/32 mm as well as fraction 0/63 mm.

Determination of the time interval t and the value of the thermal conductivity coefficient λ

The measurement was conducted at different mass moisture of the tested material (w_m = 2.41 % – 4.68 %). On the basis of the given mass moistures the specific heat capacity was recalculated for the values in the interval c = 1190 J/(kg.K) to 1262 J/(kg.K) for the crushed aggregate, fraction 0/32 mm and c = 1115 J/(kg.K) to 1260 J/(kg.K) for fraction 0/63 mm. The values of the time interval t of the respective mass moisture varied from t = 43425 s to 61380 s for fraction 0/32 mm (2 higher values occurred due to the defective contact on the interface specimen/container and as a result of spill of the cooling medium) and t = 44790 s to 88500 s for fraction 0/63 mm. On the basis of the values of the partial parameters from 7 measurements for fraction 0/32 mm the design value of the thermal conductivity coefficient λ = 1.159 W/(m.K) and for fraction 0/63 mm its value is λ = 1.038 W/(m.K), which was acquired as an average from 9 measurements.

With the help of the obtained data it is then possible to express the average dependance of the thermal conductivity coefficient λ on the mass moisture w of the tested materials - Fig. 9.

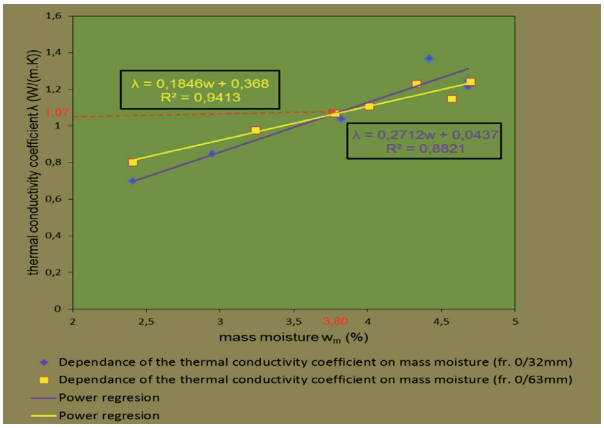

Fig. 9 Dependence of the thermal conductivity coefficient λ on mass moisture for crushed aggregate, fraction 0/32 mm and 0/63 mm

Figure 9 highlights the value of the thermal conductivity coefficient λ = 1.07 W/(m.K) for both fractions, for the material mass moisture w_m = 3.80 %, which is in this case considered a natural mass moisture.

2.2.4 Determination of the thermal conductivity coefficient λ of sandy gravel fr. 0/32 mm

At present the sandy gravel, fr. 0/32 mm is not normally applied in the subbase layer of the railway line structure, but the design nomograms stated in [1] were specifically made for this material. Due to the necessity of comparing the results acquired by the above stated methodology and verifying the reliability of the testing devices, this was really important. As it was necessary to revise the design nomograms for the materials of the subbase layer – crushed aggregate fr. 0/32 mm and 0/63 mm, it was also necessary to verify the thermal conductivity coefficient λ for the sandy gravel, too. The measurements of the time interval t were conducted at 3 different mass moistures (wm = 0 %, 2.46 % a 4.87 %), while the specific heat capacity c was stated for the dry material ($w_m \cong 0$ %).

Determination of the specific heat capacity c

The design value of the specific heat capacity of sandy gravel fr. 0/32 mm was stated for the tested specimens of mass moisture $w_m \cong 0$ %. By the arithmetic average from 6 measured results the design value of the specific heat capacity was determined as c = 854 J/(kg.K).

Determination of the time interval t and the value of the thermal conductivity coefficient λ

The measurement was conducted for 3 different mass moistures, specifically wm = 0 %, 2.46 % and 4.87 %. With regard to these mass moistures, the specific heat capacity was recalculated to the values c = 854 J/(kg.K), 934 J/(kg.K) and 1009 J/(kg.K). The values of the time interval t of the respective mass moistures ranged in the interval t = 56430 s to 60840 s for dry material, t = 21240 s to 21840 s for the mass moisture wm = 2.46 % and t = 22920 s to 23550 s for wm = 4.87 %. From the measured values it becomes obvious that the mass moisture wm considerably influences the values of the thermal conductivity coefficient λ, and that is why it is not possible to determine the average values by the arithmetic average from all the measurements, but it has to be stated for the individual mass moistures of the tested material. On the basis of the values of the partial parameters, the design value of the thermal conductivity coefficient for sandy gravel, fraction 0/32 mm was stated as λ = 0.753 W/(m.K) for dry material, λ = 2.074 W/(m.K) for material of mass moisture w_m = 2.46 % and λ = 2.362 W/(m.K) for material of mass moisture w_m = 4.87 %. The values of all the three thermal conductivity coefficients λ

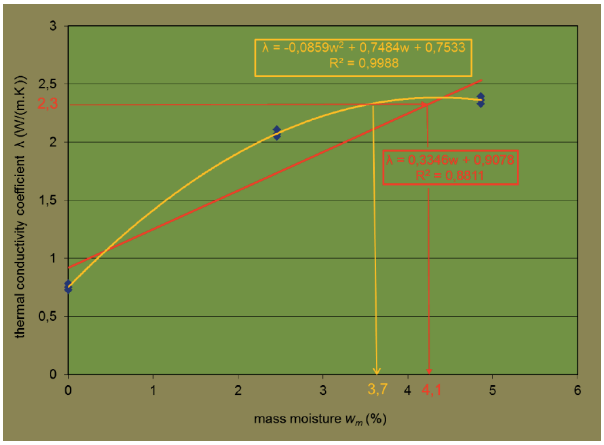

Fig. 10 Dependence of the thermal conductivity coefficient λ of a sandy gravel layer on mass moisture wm

were always acquired as average values of 3 measurements. The influence of humidity on the thermal conductivity coefficient λ of gravel sand, leading from the measured values is shown by Fig. 10. This evaluation clearly shows that the values of the thermal conductivity coefficient λ grow with increasing mass moisture and that is why the value of the thermal conductivity coefficient stated in Table 1 is valid for sandy gravel of mass moisture wm = approx. 3,7 (resp. 4,1)%.

2.2.5 Determination of the thermal conductivity coefficient λ of sandy clay

To detemine the thermal conductivity coefficient λ of sandy clay we used the material gained from the railway subbase – earthwork – of the testing stand of the Department of Railway Engineering and Track Management.

Determination of the specific heat capacity c

The tested specimens, as previously, were dried and subsequently the testing measurement was conducted. The design value of the specific heat capacity of sandy clay was acquired as an average value of 4 measurements and it is c = 1034 J/(kg.K).

Determination of the time interval t and the value of the thermal conductivity coefficient λ

The measurement was conducted for 2 different mass moistures, specifically: wm = 17.46 % and wm = 15.67 %. On the basis of different mass moistures that specific heat capacity was recalculated to the values c = 1582 J/(kg.K) and 1585 J/(kg.K). The values of the time interval t of the respective humidities ranged in the interval t = 50930 s to 52470 s. On the basis of values of partial parameters for sandy clay the design value of the thermal conductivity coefficient λ was determined as an average of 2 measurements and can be stated as λ = 1.211 W/(m.K) for mass moisture wm = 15.67 % and as the value of λ = 1.504 W/(m.K) for mass moisture wm = 17.46 %.

2.2.6 Determination of the thermal conductivity coefficient λ of sand

To detemine the thermal conductivity coefficient λ of sand we used the material gained from landfill sand.

Determination of the specific heat capacity c

The tested specimens, as previously, were dried and subsequently the testing measurement was conducted. The design value of the specific heat capacity of sand was acquired as an average value of 2 measurements and it is c = 1174 J/(kg.K).

Determination of the time interval t and the value of the thermal conductivity coefficient λ

The measurement was conducted for one mass moisture, specifically: wm = 3.73 % . On the basis of this mass moisture that specific heat capacity was recalculated to the value c = 1287 J/(kg.K). The values of the time interval t of the respective mass moisture ranged in the interval t = 29580 s to 29700 s. On the basis of values of partial parameters for sand the design value of the thermal conductivity coefficient λ was determined as an average of 2 measurements and can be stated as λ = 1.836 W/(m.K) for mass moisture wm = 3.73 %.

3. Conclusion

The thermal conductivity coefficient λ is a physical characteristic that indicates the substance ability to conduct heat, thus using it we can consider the material resistance against the heat flow. The design values of the thermal conductivity coefficient of the materials of railway subbase structure stated in Table 1 [1] are considerably different from the values measured with the help of the adjusted methodology of the non-stationary heat flow. Table 4 shows the stated standard (design) as well as measured values of λ (valid for the natural mass moisture of the material) for the tested railway subbase materials.

Measured and standard values of λ — Table 4

Material	λ (TNZ 73 6312) [W/(m.K)]	coefficient λ (measured) [W/(m.K)]
Track ballast 32/63 mm "clean"	2.00	0.62 – 0.67
Track ballast contaminated	–	0.75 – 0.99
Crushed aggregate 0/32 mm	2.00	0.70 – 1.37
Crushed aggregate 0/63 mm	2.00	0.64 – 1.28
Sandy gravel 0/32 mm	2.30	0.75 – 2.36
Sand	–	1.84
Sandy clay	1.70	1.21 – 1.50

Due to the verification of results of the experimental determination of the thermal conductivity coefficients λ of the selected railway subbase materials these were confronted. The independent and at the same time relevant source is at present the valid standard STN EN ISO 10 456 [5]. In this normative document, with regard to the specific properties of materials applied in the subbase structure, it is possible to conduct this verification of the thermal conductivity coefficient λ for clay and silica sand, fraction 0/2 mm. These soils also normally occur in the railway subbase structure. The comparison of the measured and standard values is done in Table 5, while both materials were tested at their natural mass moisture wm.

Measured and standard values of λ — Table 5

Material	λ (STN EN ISO 10 456) [W/(m.K)]	λ (measured) [W/(m.K)]
Clay, loam	1.50	1.21 – 1.50
Sand	2.00	1.84

Table 5 clearly shows that the value of the thermal conductivity coefficient λ for silty clay and sand corresponds roughly with standard values. It can thus be assumed that the measurement methodology is correct and the results are probably reliable. It is then possible to conduct the testing of other construction materials stated in Table1 or the ones that are at present applied in the railway subbase structure [6] and their thermal conductivity coefficient values are unknown and if applied it is not possible to conduct the structural assessment for the adverse effects of frost according to the design methodology stated in [1].

Acknowledgement

The presented results are the results of solving the VEGA grant project 1/0756/12 "Experimental monitoring and mathematical modelling of thermal regime of railway subgrade structure", which allows the realization of experimental measurements and consequently obtaining the relevant results that are presented in this paper.

References

[1] TNZ 73 6312 Design of Structural Layers of Railway Subbase (in Slovak), GR ZSR, August 2005

[2] CSN 72 1105 Determination of Thermal Conductivity Coefficient with the Method of Non-stationary Heat Flow (in Slovak), 1990

[3] KUPCULIAK, P.: *Design and Assessment of Railway Subbase from the Point of View of Load by Climatic Factors (in Slovak)*, Dissertation thesis, Zilinska univerzita, SvF, KZSaTH, Zilina, 2011

[4] DOBES, P.: *Optimization of Selected Conditions of the Railway Subbase Structure Design with Regard to Non-transportation Load (in Slovak)*, Diploma thesis, University of Zilina Faculty of Civil Engineering, Department of Railway Engineering and Track Management, 2012.

[5] STN EN ISO 10 456 Construction Materials and Products. Hygrothermal Properties. Tabulated Design (Calculated) Values and Procedures for the Determination of Declared and Design Values of Thermal Quantities, (ISO 10456: 2007).

[6] DURICA, P., VERTAL, M.: Verification of the Water Transport Parameter - Moisture Storage Function of Autoclaved Aerated Concrete - Approximately Calculated from a Small Set of Measured Characteristic Values, *Communications – Scientific Letters of the University of Zilina*, No. 4, 2011, pp. 92-97.

https://doi.org/10.26552/com.C.2013.4.18-20

Zbigniew Perkowski - Mariusz Czabak - Karolina Gozarska *

ESTIMATION OF SHEAR STIFFNESS OF INTERLAYER CONNECTION IN TWO-LAYER COMPOSITE BEAMS BASED ON ANALYSIS OF NATURAL FREQUENCIES

The paper shows possibilities of testing composite two-layer beams with flexible connectors (like bolts in steel-concrete beams and nails in wooden-concrete ones) offered by analysis of their natural frequencies. It enables an estimation of shear compliance for the interlayer connection if Young's moduli of layers are known thanks to finding the global minimum of function of errors between model and measured natural frequencies of beam. The considerations are illustrated by the results of our own laboratory-tests.

Keywords: *Composite beam, compliant shear connection, natural frequency, laboratory tests.*

1. Introduction

Composite structures like steel-concrete and wooden-concrete ones with compliant shear connection of their layers become more and more popular systems in civil engineering. First of all, a considerable increase of their load capacity and stiffness resulting from combining their components should be appreciated for this type of structures. Moreover, the problem of torsional-flexural buckling of more flexible steel (or wooden) profiles is eliminated thanks to connecting them with the rigid upper slab [1]. It should be stressed that these kinds of beam structures work correctly if the shear connection between the ferroconcrete slab and steel (wooden) bar elements shows enough low compliance. This characteristic is investigated, first of all, by means of push-out tests (for example [2]) or measurements of beam deflection under static load (for example [3]). The paper shows another method of estimating the shear compliance for the beam interlayer joints based on analysis of their natural frequencies which may be a complementary measuring method of the enumerated ones. The problem is illustrated by the experimental results obtained thanks to our own tests carried out in the laboratory-scale.

2. Mathematical description of the problem

Assuming the simplest linear elastic model for a two-layer composite beam with a compliant interlayer connection (for example [3]) the system of differential equations for functions: w, $u_{(1)}$ and $u_{(2)}$ (vertical displacement of centre line of the beam and horizontal displacements of centre lines of the lower and upper layer, respectively) may be written as follows (with neglected damping) (for example [4]):

$$\begin{cases} w^{IV}\left(E_{(1)}I_{(1)}+E_{(2)}I_{(2)}\right)-ke^2w^{II}-ke^2w^{I} & +keu^{1}_{(1)}+k^{1}eu_{(1)} \\ kew^{I} & +E_{(1)}A_{(1)}u^{II}_{(1)}-ku_{(1)} \\ -kew^{I} & +ku_{(1)} \\ -keu^{1}_{(2)}-k^{1}eu_{(2)} & =-q-\left(\mu_{(1)}+\mu_{(2)}\right)\ddot{w} \\ +ku_{(2)} & =\mu_{(1)}\ddot{u}_{(1)} \\ +E_{(2)}A_{(2)}u^{II}_{(2)}-ku_{(2)} & =\mu_{(2)}\ddot{u}_{(2)} \end{cases} \tag{1}$$

where: k – stiffness of the shear connection (in [N·m^{-2}]); $E_{(i)}$ – Young's modulus of layer (i); $I_{(i)}$ – moment of inertia of layer (i); $e=½(h_{(1)}+h_{(2)})$ where $h_{(i)}$ is a cross-sectional height of layer (i); $\mu_{(i)}$ – density over the length of layer (i); i=1,2 – index of beam layer; $(\,)^{I}$, $(\,)^{II}$, $(\,)^{IV}$ – the first, second and fourth derivatives along the x-axis; $(\ddot{}\,)$ – the second time-derivative, q – external vertical distributed load. In order to solve the above system for a specific problem it has to be completed by the proper boundary and initial conditions. Using the Finite Element Method (FEM) or Finite Difference Method (FDM), we can express the system (1) generally in the matrix form:

$$\mathbf{Ku = P - B\ddot{u}} \tag{2}$$

where: $\mathbf{K}$ – stiffness matrix, $\mathbf{u}$ – vector of node displacements, $\mathbf{P}$ – vector of forces (three terms in the node equations), $\mathbf{B}$ – inertia matrix. In order to formulate an eigenvalue problem for this case we assume in the equation (2) $\mathbf{P=0}$ and $\mathbf{u}=\mathbf{u}_0\sin(\omega t+\theta)$ (for example [5]). Then we can obtain the following equation for eigenvalues λ_i of matrix $\mathbf{KB}^{-1}$ (and the same for natural angular frequencies ω_i of the beam):

$$\begin{aligned} &\left(\mathbf{K}-\omega^2\mathbf{B}\right)\mathbf{u}_0\sin\left(\omega t+\theta\right)= \\ &=\mathbf{0}\rightarrow\det\left(\mathbf{KB}^{-1}-\lambda\mathbf{I}\right)=0\rightarrow\lambda_i=\omega_i^2 \end{aligned} \tag{3}$$

* **Zbigniew Perkowski, Mariusz Czabak, Karolina Gozarska**
Faculty of Civil Engineering, Chair of Physics of Materials, Opole University of Technology, Poland, Email: z.perkowski@po.opole.pl

where: **I** – unit matrix, **0** – zero vector, $\mathbf{u}_0$ – vector of free vibration amplitudes, t – time. If natural frequencies of the real combined beam are known from measurements (thanks to the Fourier analysis of accelerations at chosen points in the real structure excited to test vibrations) then it is possible to estimate its stiffness k finding the minimum of the following exemplary error functions:

$$F(k) = \sum_{i=1}^{n} \left| \frac{\omega_{i(\text{measurement})} - \omega_{i(\text{model})}(k)}{\omega_{i(\text{measurement})}} \right| \tag{4}$$

or

$$F(k) = \sum_{i=1}^{n} \left(\frac{\omega_{i(\text{measurement})} - \omega_{i(\text{model})}(k)}{\omega_{i(\text{measurement})} } \right)^2$$

where: $\omega_{i(\text{measurement})}$ – measured i-th natural angular frequency for the real structure, $\omega_{i(\text{model})}$ – i-th natural angular frequency calculated basing on the assumed model, n – number of the first natural frequencies taken into considerations.

3. Experimental results in the laboratory-scale

To illustrate the measuring possibilities offered by the free vibration analysis in the discussed scope, the experimental tests were carried out on cantilever beams in the laboratory-scale (at the temperature 20±2°C). The model of two-layer bar with sheared joint was made from two plexiglass layers 1.5m long of rectangular cross-sections (bxh=~40mm x 20mm) connected by the adhesive double-sided tape on the sides 40mm wide. The used plexiglass was characterised by the following parameters: dynamic Young's modulus E=3.99GPa, bulk density ρ=1174kg/m^3. The tape connection was used in the model to simulate the way of work of a real sheared joint.

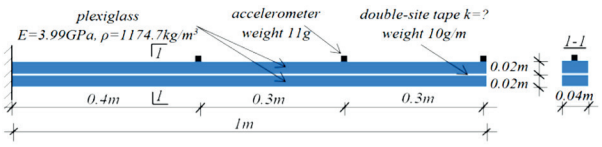

Fig. 1 The static scheme of plexiglass composite laboratory cantilever beam

The prepared two-layer bar was restrained on the solid steel element using the clamps so as to create the cantilever beam 1m long and three accelerometers (PCB 333B52 of external dimensions 11mm x 11mm x 11mm and weight ~11g with the connecting cables) were attached to the upper side of element as shown in Fig 1. Next, the cantilever was excited to vibrations by impacts applied to the lower side of element just under the accelerometers three times at each point. The accelerations were recorded on the PC computer using the software DASYLAB 10.0. An exemplary record of acceleration, which was obtained for the unbounded end of cantilever, is presented in Fig. 2. Using the Fourier transform for all the records it was found that the mean values of the first two natural frequencies were equal to:

$$f_1 = 10.43Hz,\ f_2 = 68.69Hz \tag{5}$$

Next, basing on the above values of frequencies, the minimum of function (4_2) (for n=2) was found by a direct search of domain for the physically possible solutions. The values for $\omega_{i(\text{model})}$ needed in the calculations were obtained by means of the own computer program written in the Matlab environment in which the eigenvalue problem, as defined by the equation (3), was solved using FDM. The diagram of function F vs. stiffness k is presented in Fig. 3. It can be noticed that one minimum was obtained in the analysed interval and it is situated at the value of stiffness equal to ~2·10^8 Pa.

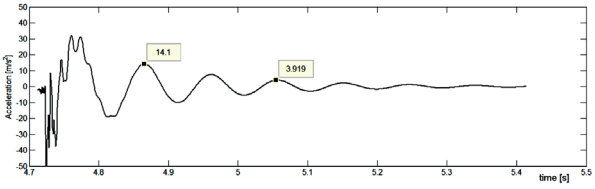

Fig. 2 The exemplary acceleration record at the unbounded end of cantilever beam

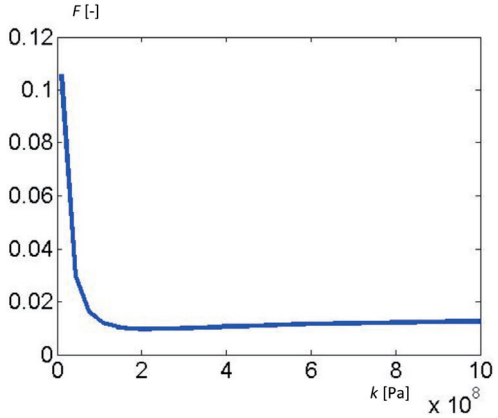

Fig. 3 The error function (4_2) vs. shear stiffness for n=2 in the case of tested cantilever

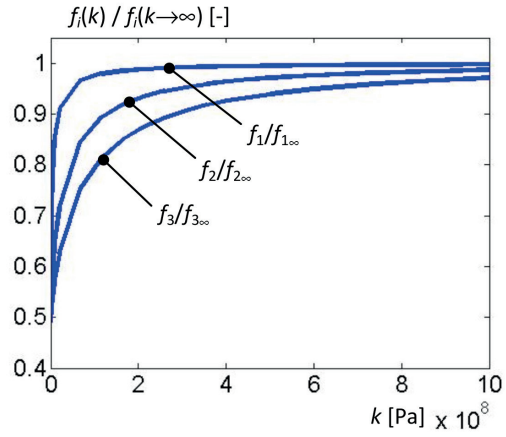

Fig. 4 First three natural frequencies vs. shear stiffness k for the data corresponding to the combined cantilever of scheme as shown in Fig. 1. The values of frequencies are normalised to their values at k→∞

Basing on these measurements it was also found that the mean value of fraction of critical damping ξ was equal to ~0.1 for the first mode of free vibrations. It is worth mentioning that the fraction ξ for the non-combined plexiglass cantilever 1m long of cross-sectional dimensions bxh=~40mm x 20mm was equal to ~0.04 which was measured by the authors in the same way as described above. The considerable increase of damping in the case of combined model was caused by viscous properties of the tape joint and introducing the mechanism of structural damping into the model in this way. However the damping for the two-layer cantilever characterised by the fraction ξ=~0.1 could not cause considerable errors in estimating the values of natural frequencies (for example [5]).

In order to show how a possible selection of number of the first natural frequencies taken into consideration (according to the pattern (4)) may influence the accuracy of results, the changes of the first three ones vs. shear stiffness k are presented in Fig. 4. The diagram was made for the data corresponding to the combined cantilever beam used in the tests described above and the values of frequencies were normalised to their values at $k\rightarrow\infty$. It can be noticed that the stiffness k can be determined more precisely if more natural frequencies are taken into account especially for its higher and low values. For example, taking only one frequency f_1 in the expressions (4) their global minimum may be found with a considerable error if input data are noised because an increase of frequency, related to a big increase of stiffness k, is very small starting from a certain value for k (in the analysed diagram approximately at k=10^8 Pa). The same goes for the next frequencies, but suitably at higher values of stiffness (in the analysed diagram approximately at k=$3\cdot10^8$ Pa for f_2 and k=$5\cdot10^8$ Pa for f_3). This fact may limit considerably the possibilities of application for the method if the number of the first measured frequencies is also limited due to the used equipment and measuring conditions. Basing on Fig. 4 one can state also that it should amount to 2 minimally.

4. Conclusions

The combined structures (especially two-layer beams) are more and more popular and willingly used in civil engineering applications because of their optimal use of materials with keeping required stiffness and load capacity. That is why laboratory- and non-destructive test methods should be intensively developed in this range, too. The method discussed in the work is based on the analysis of natural frequencies. It is investigated by the authors at the presented stage, first of all, from the point of view of its application in measurements of interlayer shear stiffness for combined beams in the laboratory conditions as a comparative method for the adequate push-out tests (for example [2]). The method, as formulated in the work, may be used in practice for diagnostic purposes under condition that a tested structural element can be described by a simple elastic beam model. Otherwise, it needs more advanced geometrical and physical models and software. The presented considerations illustrate also the fact that dynamic characteristics of layer structures may be determined with considerable errors if the problem of slip in their sheared interfaces is neglected.

Acknowledgements

The authors would like to thank Prof. Zbigniew Zembaty for making the part of measuring equipment available during the experiment.

References

[1] KUCHARCZUK, W., LABOCHA, S.: *Combined Steel-concrete Structures of Buildings (in Polish)*, Arkady, Warszawa, 2007.

[2] DURATNA, P., BUJNAK, J., BOUCHAIR, A., LACHAL, A.: *Modelling of the Steel-Concrete Push-out tests*, Proc. of the 8th PhD & DLA Symposium, Pecs, 2012.

[3] KUCZMA B., KUCZMA M.: Experimental Testing and Modelling of Adhesively Bonded Composite Beams of Steel and Concrete (in Polish), *Zeszyty Naukowe Politechniki Rzeszowskiej*, No. 254, Series: Budownictwo i Inzynieria Srodowiska, vol. 59, No. 3/2012/II, p. 381-388, Rzeszow, 2012.

[4] PERKOWSKI, Z., CZABAK, M.: *Estimation of Shear Compliance of Connectors for Composite Two-layer Beams Based on the Analysis of Free Vibrations*, Proc. of Conference PROGRESS 2013, Ostrava, 2013.

[5] CHMIELEWSKI, T., ZEMBATY, Z.: *Dynamics of Structures (in Polish)*, Series: Studia i monografie, vol. 97, Politechnika Opolska, Opole, 1998.

https://doi.org/10.26552/com.C.2013.4.21-26

Peter Janik - Josef Vican *

BEAM-COLUMN RESISTANCE ACCORDING TO SLOVAK STANDARD AND EUROCODES

The article deals with the verification of resistance of torsionally restrained hot-rolled beam-columns of H or I cross-sectional shape and also of the perpendicular hollow cross-section subjected to the biaxial bending and axial compression. Results of analysis of the beam-column resistances according to methods of former STN 73 1401 [1] and the current STN EN 1993-1-1 [2] are compared with results of numerical approaches. The observed members are subjected to the normal force and to the transverse loads uniformly distributed along the length of both axes. The cross-sections of HEB 300, IPE 300 and RHS 300x200x10 were chosen to compare obtained results.

Keywords: *Axial force, bending moment, torsional restraint, beam-column.*

1. Introduction

Nowadays, the development of new materials creates a competitive environment for the use of steel as a structural material in constructions. High-strength concrete and reinforced concrete cross-sections of high quality compete with steel with their dimensions. Therefore, many specialists are searching to improve the accuracy of design formulas for steel members, especially for members subjected to the combined actions. The beam-column subjected to combination of bending moments and axial compression is an example of this problem. Therefore, the possibility of using cross-sectional plastic reserve or improving and more specifying the design approaches to verification of beam-column resistance becomes more important. If the standard prescriptions do not meet criteria of the optimal structural design, then the determination of the structural resistance and its verification need necessarily to be more precise and often complex based on the numerical calculations using FEM models.

2. Analysis of beam-column behaviour

2.1. Analytical approach

Stability analysis of a beam-column has been done in the past using solution of the relevant homogeneous differential equations. The buckling resistance of initially deflected beam-column with double symmetric constant cross-section, subjected to combined constant axial compression and biaxial bending due to transverse load uniformly distributed along the length of the both axes, could be described by the system of inhomogeneous differential equations in accordance with [3]

$$\begin{aligned} &EI_y w^{(4)} + N(w + w_o)'' + \left[M_z(\theta + \theta_o)\right]'' = q_z \\ &EI_z v^{(4)} + N(v + v_o)'' + \left[M_y(\theta + \theta_o)\right]'' = q_y \\ &EI_w \theta^{(4)} - GI_t \theta'' + i_s^2 N(\theta + \theta_o)'' + \\ &+\left[q_y z_{g,y} + q_z z_{g,z}\right](\theta + \theta_o) + \left[M_y(v + v_o)'\right]' + \\ &+\left[M_z(w + w_o)'\right]' = 0 \end{aligned} \tag{1}$$

In the case of the torsionally restrained beam-column along its length, i.e. the member whose effects of lateral-torsional buckling are eliminated by the relevant supporting, and considering the initial deflection in the direction of the y-y axis only, the system of differential equations (1) can be rewritten into the following elementary pair of independent differential equations, describing the buckling resistance of beam-column respecting the above mentioned cross-sectional shape and load

$$\begin{aligned} &EI_y w^{(4)} + Nw'' = q_z \\ &EI_z v^{(4)} + N(v_o'' + v'') = q_y \end{aligned} \tag{2}$$

where

E	is the Young's modulus of elasticity,
G	is the shear modulus,
I_y, I_z	is the second moment of area about the y-y or z-z axis, respectively,
I_t	is the St. Venant torsional constant,

* **Peter Janik, Josef Vican**
Department of Structures and Bridges, Faculty of Civil Engineering, University of Zilina, Slovakia,
E-mail: peter.janik@fstav.uniza.sk

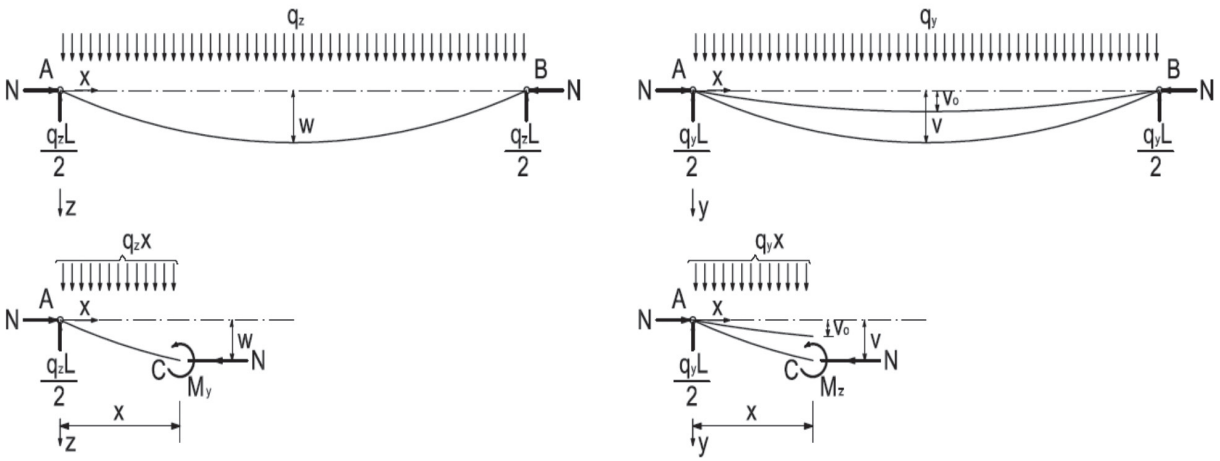

Fig. 1 Simply supported beam-column subjected to the constant axial compression and uniformly distributed transverse load

I_w is the warping torsional constant,
N is the normal compression force,
M_y, M_z are the bending moments about the y-y and z-z axis, respectively, induced by transverse loads,
i_s is the cross-sectional polar radius of gyration around to the centre of shear,
q_y, q_z are the transverse uniformly distributed loads in the direction of the y-y or z-z axis, respectively,
v_o is the initial deflection of a member in the direction of the y-y axis,
v is the deflection increment of a member in the direction of the y-y axis,
w is the deflection increment of a member in the direction of the z-z axis,
w_o is the initial deflection of a member in the direction of the z-z axis,
$z_{g,y}$, $z_{g,z}$ are the distances of the applied transversal load from the centre of shear measured in the direction of the y-y or z-z axis, respectively,
θ_o is the angle of the initial cross-sectional rotation of a member about the x-x axis,
θ is the angle increment of cross-sectional rotation of a member about the x-x axis.

Bending moments M_y and M_z depend on the type of transverse load and usually have the non-constant shape. According to Fig. 1, the bending moments at the point C at a distance of x from A (see Fig. 1) can be obtained by taking moments about C for the segment of member A-C using formulas

$$M_y = Nw + \frac{q_z L x}{2} - \frac{q_z x^2}{2}$$

and (3)

$$M_z = Nv + Nv_o + \frac{q_y L x}{2} - \frac{q_y x^2}{2}$$

The equations become even more inhomogeneous when the initial imperfections are implemented into the system. The member initial deflection of v_0 in the direction of the y-y axis was considered to simulate the shape of the member equivalent geometrical imperfection described by means of the sinusoidal function as follows

$$v_0 = e_{0,z} \sin(\pi x/L) \tag{4}$$

where the amplitude $e_{0,z}$ is defined according to the standard [2] in the following form

$$e_{0,z} = \alpha(\overline{\lambda} - 0,2) W_{el,z}/A \tag{5}$$

and the imperfection factor α_l depends on the cross-sectional shape.

Using the differential expression for bending moment, the equations (3) can be rewritten into the differential form [4] as follows

$$\begin{aligned} &w'' + \mu_1^2 w = \frac{q_z}{EI_y}\left(\frac{x^2}{2} - \frac{xL}{2}\right) \text{ with } \mu_1^2 = \frac{N}{EI_y} \\ &v'' + \mu_2^2 v = \frac{q_y}{EI_z}\left(\frac{x^2}{2} - \frac{xL}{2}\right) - \mu_2^2 e_{o,z} \sin\left(\frac{\pi x}{L}\right) \\ &\text{with } \mu_2^2 = \frac{N}{EI_z} \end{aligned} \tag{6}$$

The final solutions of the above described differential equations can be obtained using homogenous boundary condition, w = v = 0 for x = 0 and for x = L, in the form as follows

$$\begin{aligned} w &= \frac{q_z}{N\mu_1^2}\left(\tan\frac{\mu_1 L}{2}\sin\mu_1 x + \cos\mu_1 x - 1\right) + \\ &+ \frac{q_z}{2N}(x^2 - xL) \\ v &= \frac{q_y}{N\mu_2^2}\left(\tan\frac{\mu_2 L}{2}\sin\mu_2 x + \cos\mu_2 x - 1\right) + \\ &+ \frac{q_y}{2N}(x^2 - xL) + \frac{Ne_{o,z}}{N_{cr,z} - N}\sin\left(\frac{\pi x}{L}\right) \end{aligned} \tag{7}$$

where $N_{cr,z} = \pi^2 EI/L_z^2$ is the Euler flexural buckling force.

The displacement at any point of the member can be calculated by inserting appropriate values of *N, q* and *x* in these equations. The maximum deflections and maximum bending moment are in the mid-span of the observed beam-column and can be expressed by the following formulas

$$w_{\max,y} = \frac{q_z}{N\mu_1^2}\left(\sec\frac{\mu_1 L}{2} - 1\right) - \frac{q_z L^2}{8N} \text{ and} \quad (8)$$

$$M_{\max,y} = \frac{q_z EI_y}{N}\left(\sec\frac{\mu_1 L}{2} - 1\right)$$

$$v_{\max,z} = \frac{q_y}{N\mu_2^2}\left(\sec\frac{\mu_2 L}{2} - 1\right) - \frac{q_y L^2}{8N} + \frac{Ne_{o,z}}{N_{cr,z} - N} \text{ and}$$

$$M_{\max,z} = \frac{q_y EI_z}{N}\left(\sec\frac{\mu_2 L}{2} - 1\right) + \frac{Ne_{o,z}}{1 - \frac{N}{N_{cr,z}}}$$

Then, the maximum stress in the mid-span of the beam-column can be obtained using the relation

$$\sigma_{\max} = \frac{N}{A} + \frac{M_{\max,z}}{W_{el,z}} + \frac{M_{\max,y}}{W_{el,y}} \quad (9)$$

where $W_{el,y}$, $W_{el,z}$ are the elastic sectional modulus about the y-y or z-z axis, respectively.

2.2. Numerical approach

Due to the complexity of analytical solutions of system of inhomogeneous differential equations according to (1), the numerical analyses are used to obtain results. Numerical models are usually created using computer software based on FEM. In this case the Ansys-Workbench was used. Numerical model developed in this environment consists of one dimensional finite element BEAM 188 (see Fig. 2). The element is based on Timoshenko's beam theory including shear-deformation effects. The unrestrained warping of cross-section or restrained one respectively can be taken into account. This element is a linear, quadratic, or cubic two-node beam element in 3D. BEAM188 has six or seven degrees of freedom at each node. These include translations in the x, y, and z directions and rotations about the x, y, and z directions. The seventh degree of freedom - warping magnitude, is optional. This element is well-suitable for linear large rotation and/or large deflection nonlinear applications.

The sinus function was chosen in accordance with [2] to simulate the initial shape of bow imperfection of the member in the direction of the y-y axis. Its amplitude was taken in compliance with recommendation for flexural buckling in [2]. In the case of applied numerical model, the boundary conditions Rot,x = 0 were considered, allowing for torsionally restrained member with disabled rotation about the x-axis.

Ideal elastic-plastic material model was chosen. Material characteristics were used according to standard recommendations [2].

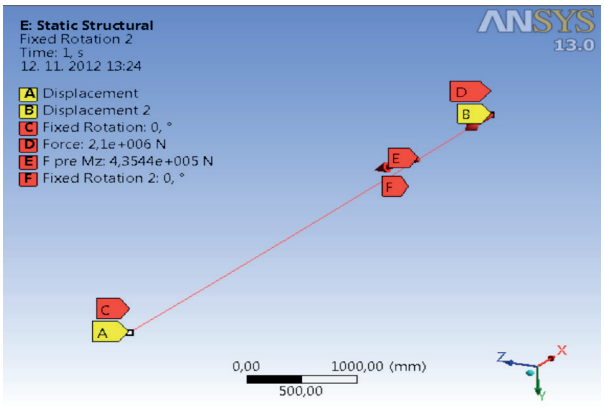

Fig. 2 The numerical model

To verify the described numerical model, the analytical solution of the problem derived in section 2.1 was used. The results of maximum stresses calculated by means of formula (9) and using the above mentioned numerical model for beam-column of IPE 300 cross-section having slenderness of $\overline{\lambda}_z$= 1.0 and 1.5 are compared in Table 1. The comparison is presented in the form of ratio of results of numerical calculations to results obtained using derived analytical solutions. The comparison presented in Table 1 is statistically evaluated to determine the error of the numerical approach.

Statistically evaluated comparisons of analytical calculations with results of numerical ones — Table 1

IPE 300		
$\overline{\lambda}_z$	1	1,5
Mean value	1.0086	1.0087
Maximum value	1.0160	1.0130
Minimum value	1.0041	1.0043
Σ calculations	27	27

The comparison presented in Table 1 shows a very good accordance insomuch that above described numerical model can be applied for parametric numerical study of the beam-column resistance determination. It was necessary to evaluate a large number of combinations of normal forces and transverse loads to create compact resistance surface of the observed members. Therefore, the following input values were taken into account for numerical calculations in frame of parametric study:

- yield strength of 235 MPa, the Young's modulus of elasticity of 210 GPa, the zero modulus of strain hardening and the Poisson ratio of 0.3;
- the amplitude of the initial bow imperfection was taken according to formula $e_{o,z} = \alpha_1(\overline{\lambda} - 0,2)W_{el,z}/A$ (A is the cross-sectional area of a member) with α_1 = 0.49 for HEB 300, α_1 = 0.34 for IPE 300 and α_1 = 0.21 for RHS 300x200x10;
- the geometric nonlinearity and torsionally restrained member with condition Rot,x = 0 was considered;

- cross-sectional characteristics of thin-walled sections were taken according to the table from [5].

2.3. Standard approach according to STN 73 1401

The standard procedures are used for assessment of members to achieve the greater extent. The resistance of member subjected to the combined biaxial bending and axial compression was verified by means of formulas according to STN 73 1401 [1]. The latest revision of this standard was valid from 23.03.1998. This latest version of the standard was applied in our country till 01.04.2010, when it was replaced, as well as the other Slovak structural standards, by Eurocodes.

In the parametric study, the analyses of the resistance of members with cross-sections of Class 1 and 2 were performed. Member not susceptible to torsional deformations with cross-sections of Class 1 or 2, respectively, shall satisfy the following single condition in accordance with [1]

$$\frac{N_{Ed}}{\chi_{\min} N_{Rk}/\gamma_{M1}} + \frac{k_y M_{y,Ed}}{\chi_{LT} M_{y,Rk}\gamma_{M1}} + \\ + \frac{k_z M_{z,Ed}}{M_{z,Rk}/\gamma_{M1}} \le 1,0 \qquad (10)$$

where

N_{Ed} is the design compression force,

$M_{y,Ed}$, $M_{z,Ed}$ are the design bending moments about the y-y or z-z axis, respectively,

N_{Rk} is the characteristic value of the resistance to normal compression force,

$M_{y,Rk}$, $M_{z,Rk}$ are the characteristic values of the resistances to bending moments about the y-y or z-z axis, respectively,

k_y, k_z are the interaction factors,

χ_{min} is the minimum of reduction factors due to flexural buckling to y-y or z-z axis, respectively,

χ_{LT} is the reduction factor for lateral-torsional buckling (in this case χ_{LT} =1.0),

γ_{M1} is the partial safety factor for material.

2.4. Standard approach according to STN EN 1993-1-1

Set of Eurocodes for the design of building structures has been successively implemented into the STN standard system since 2005. Translations of European standards to individual Slovak ones with the National Annexes were gradually published.

To verify resistance of the member subjected to combination of biaxial bending and axial compression, two methods named A and B are possible to apply according to standard [2]. A common form of equations for assessing the resistance of member with cross-section of Class 1 or 2 respectively, subjected to the axial compression and biaxial bending has the form as follows:

$$\frac{N_{Ed}}{\chi_y N_{Rk}/\gamma_{M1}} + k_{yy}\frac{M_{y,Ed}}{\chi_{LT} M_{y,Rk}/\gamma_{M1}} + k_{yz}\frac{M_{z,Ed}}{M_{z,Rk}/\gamma_{M1}} \le 1,0 \\ \frac{N_{Ed}}{\chi_z N_{Rk}/\gamma_{M1}} + k_{zy}\frac{M_{y,Ed}}{\chi_{LT} M_{y,Rk}/\gamma_{M1}} + k_{zz}\frac{M_{z,Ed}}{M_{z,Rk}/\gamma_{M1}} \le 1,0 \qquad (11)$$

where the following designations are used in addition to ones under relation (10)

$k_{i,j}$ are the interaction factors,

χ_y, χ_z are the reduction factors due to flexural buckling to y-y or z-z axis, respectively.

Methods A and B differ from each other by the approach to calculating the interaction factors $k_{i,j}$. Equations for individual interaction factors $k_{i,j}$ were calibrated by means of many geometric and material nonlinear computer simulations (GMNIA) based on the finite element method, [6]. For practical design in Slovakia, the utilization of method B was recommended in the National Annex [7].

3. Comparison of approaches to verification of beam-column resistance

The comparison of the results obtained using different standard approaches to results of the numerical calculations is shown in Figs. 3-8. The numerical values represent the size of the third axis in the selected levels of N_{Ed}/N_{Rd}. Ratios $M_{y,Ed}/M_{y,Rd}$ and

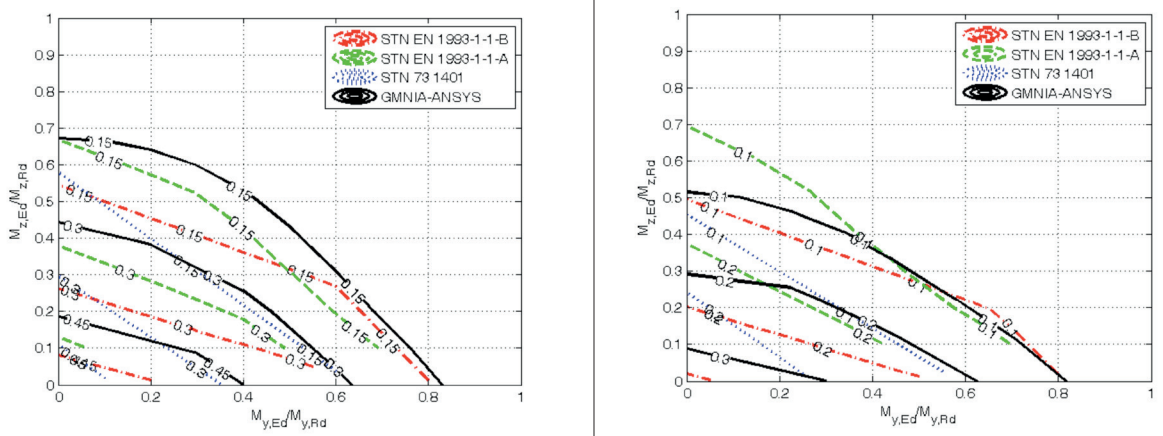

Fig. 3 Comparison of member resistance curves, $\overline{\lambda}_z$=1.0;1.5 - HEB 300

$M_{z,Ed}/M_{z,Rd}$ are shown on the horizontal and vertical graph axes. Characteristic values of resistances without partial safety factor γ_{M1} for material were considered as the standardized member resistances for all normative approaches to compare the obtained results of numerical calculations. Graphs are processed for non dimensional slenderness $\overline{\lambda}_z$=1.0; 1.5 and 2.0.

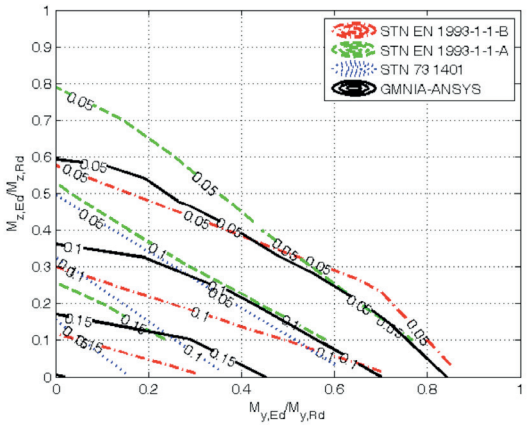

Fig. 4 Comparison of member resistance curves, $\overline{\lambda}_z$=2.0 - HEB 300

The investigated member is subjected to the axial compression and bending due to the uniformly distributed transverse load for both axes of symmetry of the cross-section so that the shape of the bending moment is parabolic. Calculations were considered with torsionally restrained cross-section HEB 300 and IPE 300, i.e. the effect of lateral-torsional buckling was neglected. The cross-section of RHS 300x200x10 is not susceptible to torsional deformations.

4. Conclusions

Conservative approach to the resistance verification according to the standard [1] is evident from all the result's comparisons. In accordance with this standard, the spatial display creates approximately "planar resistance surface" connecting the borderline cases lying on the axes of the graph.

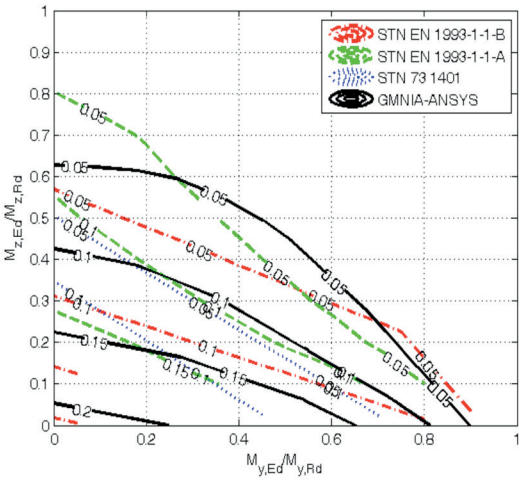

Fig. 6 Comparison of member resistance curves, $\overline{\lambda}_z$=2.0 - IPE 300

Resulting isoclines of methods A and B show that the standard [2] uses the plastic reserve of members more accurately. Surface resistance of these approaches is already convex describing more realistic beam-column resistance. Both methods for assessing the combination of biaxial bending and axial compression according to [2] describe the resistance of member with the closed cross-section of RHS 300x200x10 better. In the cases of the higher levels of normal forces, standardized approaches show reserve of resistance compared to results of numerical calculations. If members are subjected to the smaller bending moment M_y, the method A provides higher levels of the member resistance for non-dimensional slenderness $\overline{\lambda}_z$ greater than 1.0 than numerical calculations for open cross-sections IPE 300 and HEB 300. Assessments of members with torsional restraints according to method A are less suitable for members with non-dimensional

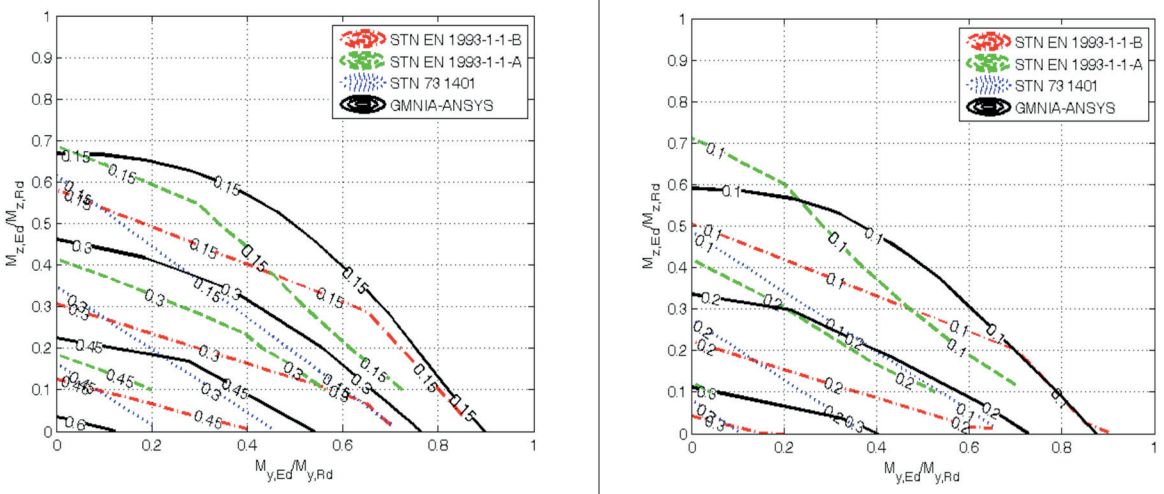

Fig. 5 Comparison of member resistance curves, $\overline{\lambda}_z$= 1.0;1.5 - IPE 300

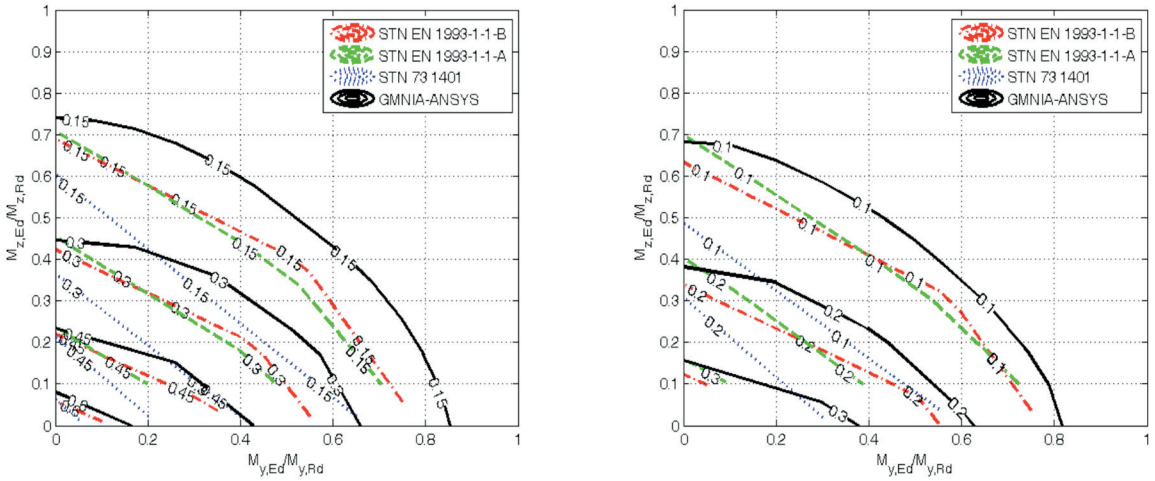

Fig. 7 Comparison of member resistance curves, $\overline{\lambda}_z$=1.0;1.5 - RHS 300x200x10

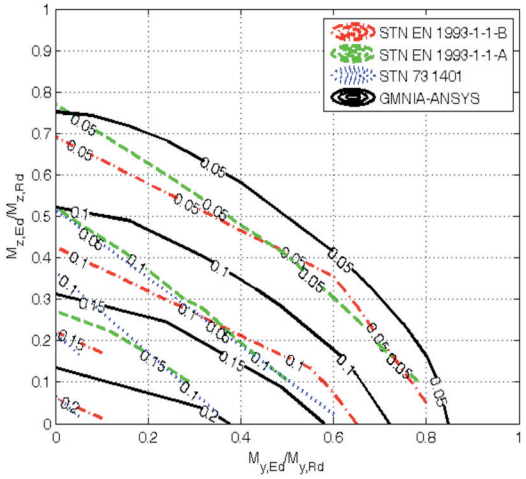

Fig. 8 Comparison of member resistance curves, $\overline{\lambda}_z$=2.0 - RHS 300x200x10

slenderness $\overline{\lambda}_z$ greater than 1.0. The recommendation to use the method B in Slovakia seems to be correct from this point of view [8].

Acknowledgements

This paper presents results of works supported by the Slovak Research and Development Agency under the contract No. APVV-0106-11 and by the Scientific Grant Agency of the Slovak Republic under the project No. 1/0364/12.

References

[1] STN 731401: *Design of Steel Structures. Bratislava*, SUTN, 1998.
[2] STN EN 1993-1-1: *Design of Steel Structures - Part 1-1: General Rules and Rules for Buildings*. Bratislava, SUTN, 2006.
[3] BREZINA, V.: *Buckling Strength of Structural Steel Members*, Prague, SNTL, 1963, 384 p.
[4] ALLEN, H. G. et al.: *Background to Buckling*, McGraw-Hill Book Company (UK) Limited. 1980, 582 p.
[5] http://www.staticstools.eu
[6] BOISSONNADE, N.: *Rules for Member Stability in EN 1993-1-1*, Background documentation and design guidelines. ECCS 2006, 259 p.
[7] STN EN 1993-1-1/NA: *Design of Steel Structures. Part 1-1: General Rules and Rules for Buildings*, Bratislava, National Annex, SUTN, 2006.
[8] VICAN, J., ODROBINAK, J, GOCAL, J., HLINKA, R.: Design and Stability of Long Span Railway Arch Bridge, *Communications - Scientific Letters of University of Zilina*, No. 4, 2013 (in print).

https://doi.org/10.26552/com.C.2013.4.27-31

Renata Korenkova - Peter Krusinsky - Peter Pisca *

ANALYSIS OF THE IMPACT OF MICROCLIMATE IN A ROOF SPACE ON A GOTHIC TRUSS CONSTRUCTION

The research in the field of historical trusses, carried out at the workplace of authors for a long time, is focused on monitoring and analysing microclimate with the aim of specifying environmental conditions that would be suitable for preservation of a historical structure for further generations. Currently, this investigation is running together with a blanket screening of historical trusses in Slovakia [1 and 2]. In each truss, there was recorded the general technical state as well as the way of ventilation in a roof space. To define the impact of microclimate in a roof space on the lifetime period and sustainability of a historical truss, long-term measurements of features regarding both a roof space and its surroundings are made. The gothic truss over the gothic Roman-Catholic church of the Most Holy Body of Christ was chosen as an experimental truss for this type of analysis because it is very well-preserved.

Keywords: *Historical truss, timber construction, relative air humidity, air temperature, absolute moisture of wood.*

1. Introduction

With the effort of achieving the sustainability of the good technical condition of an involved truss, it is needful to analyse the effect of air humidity on moisture of timber structural elements. The object is to determine admissible (optimal and critical) conditions of microclimate in a roof space which are to be met to prevent arising acute moisture states in dependence on the way of ventilating in such a space. The marginal conditions that are taken into account are as follows:

- external environment (outdoor air temperature, relative air humidity, wind, rain, altitude, location)
- internal environment (temperature, relative air humidity, air circulation)

Acute moisture states occur when exceeding the level of relative moisture on a surface, achieving the condensation point on the surface of a construction, and transcending equilibrium moisture in building materials with sorptive features (wood). Our study pays attention mainly to timber constructions which are historically valuable and are damaged due to the influence of acute moisture states. It is known that absolute moisture that is critical for occurring biotic forms of damage is as follows: around 10% for ligniperdous insects, more than 20% for dry rot, depending on the length of exposure [3]. The long-lasting influence of unfavourable conditions has a negative effect on physical and mechanical characteristics of timber components, and it consequently leads to degradation or other unwanted changes in statics of a building.

2. The building and its truss in an experiment

The Roman-Catholic church of the Most Holy Body of Christ was built as a stand-alone building, situated from the north to the west, in the middle of a fenced area in the historical centre of the village of Bela-Dulice (see Fig. 1). It probably arose in the first half of the 14th century. It has two separated truss structures, over the nave and the sanctuary. The truss over the nave was a subject of our investigation [2]. The steep truss over the nave has a rafter construction with collar beams, it is longitudinally bound with a central framed trestle (see Fig. 2), and it is dated from 1409d. It has 10 bonds, where 4 are full with 2 intermediate ones among them. In full bonds, central posts intersect collar beams; they are lapped over with rafters in the top. Symmetrical struts stabilize the post and join it with a tie beam. Rafters are mortised into the ends of tie beams. Tall oblique struts are used as a lateral reinforce. All joints are made using treenails. Central standing trestle is composed of a frame consisting of a sill beam, 4 posts which are, approximately in 3/5, divided with horizontal struts. Symmetrical bottom struts stabilize the posts in longitudinal direction, like in transversal one. Diagonal struts serve as a bracing for the entire framed structure. There are 3 larger openings in the roof space: the passage opening in the parting gable between the trusses over the sanctuary, and a smaller one in the upper part over the roof ridge of the sanctuary. Additional openings are: an entrance into the tower, a continuous slot between roofing and a profiled cornice – Fig. 3. The truss was renovated more times in the past; about 60% of original wall plates were replaced in 2011. Approximately 80% of the truss construction preserved its originality up to the present days.

* [1]**Renata Korenkova,** [1]**Peter Krusinsky,** [2]**Peter Pisca**
[1]Department of Building Engineering and Urban Planning, Faculty of Civil Engineering, University of Zilina, Slovakia,
E-mail: renata.korenkova@fstav.uniza.sk
[2]Department of Geodesy, Faculty of Civil Engineering, University of Zilina, Slovakia

Fig. 1 The church of the Most Holy Body of Christ in the village of Bela-Dulice

Fig. 2 View into the truss space

3. Venting in the roof space

The issue of venting in a roof space of a loft type is rather difficult. To make an airflow simulation in such a place, it is necessary to take account of all openings through which the air exchange between a roof space and the exterior could happen [4]. Most cases are difficult to definite openings like these; they are very often disordered, or they are irregular. In addition to the openings shown in Fig. 3, it is also needed to reckon with permeability of roofing, especially if it is made up e.g. of tiles. Then it is considered a permeable roof deck.

Nowadays, closed air layers are often used as a thermo-insulation. The air layer can be thought closed, when there isn´t any opening leading to a space and roofing is compact or it is airtight. Thermal resistance of the air layer depends on the thermal conductivity coefficient, and also on air circulation and heat radiation. Since the temperature of surfaces is various, the air on the warmer side is heated and moves up while the air on the colder side is cooled and moves down. This is air circulation - i.e. the exchange of heat by natural airflow (convection).

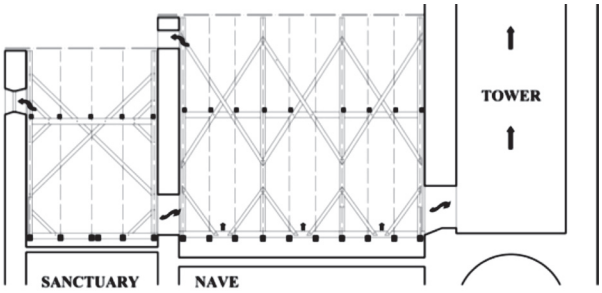

Fig. 3 The dispositional scheme of vents in the investigated truss; right - the truss cross-section, left - the truss longitudinal section

4. Experimental measurements

4.1. The measuring system

The examined pitched roof has a slope of 59°64´ [5] with gable walls. The roof deck comprises sheet copper roofing used in strips; the joints of particular strips have standing seams. As the roof space is open towards the outside - it has openings as in the lower so in the upper part of the roof deck, in the top of the gable wall, passage openings in the tower gable wall and in the truss gable wall over the sanctuary - the roof can be considered as a ventilated double-cladding pitched roof.

To enter reliable and real data into the airflow simulation, and to detect an actual as well as a long-term impact of microclimate in a roof space on the moisture accumulation in timber elements, the measuring system with two types of sensors for a particular space was designed. Particular temperature and relative air humidity sensors, and also sensors for scanning the temperature and absolute moisture of timber elements are found on spots where there is a precondition of airflow. Their disposition is symmetrical in relation to the roof ridge, i.e. they are disposed evenly on the western and southern side in the roof space. Some sensors are located in the lowest roof part, exactly in the exterior under the gutter cornice (sensor 01 and 02). Additional sensors have their positions in the exterior near the opening in the eastern

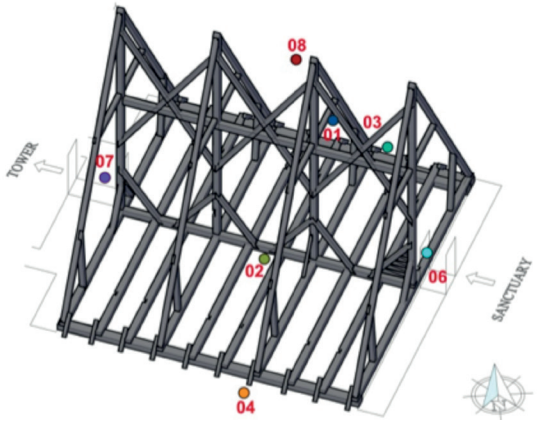

Fig. 4 The dispositional scheme of sensors V1 used as a measuring system

gable wall, in openings in gable walls leading into trusses over the sanctuary (06) and into the tower (07). Other sensors are found in the roof space - in the middle of the object under the roof ridge (08), and in the midpoint of the roof plane length (03 and 04) - see the scheme in Fig. 4.

4.2. Microclimate in the roof space

Temperatures and relative air humidity are monitored with sensors at 15-minutes intervals. For calculations, data gathered at 7:00, 14:00 and 21:00 o'clock within summer time, and at 8:00, 15:00 and 22:00 o'clock during winter time was considered – Fig. 5 and Fig. 7. Average day temperatures and relative air humidity are calculated using obtained data – Fig. 6 and Fig. 8. All evaluated data from sensors, as in spring so in autumn season, reached temperature maximums at 14:00 o´clock – Table 1. Most sensors recorded temperature minimums at 7:00 o´clock; and all sensors in autumn season. As to complete evaluation, sensor No. 8 (located closely to the roof ridge) recorded the highest temperatures at 7:00, 14:00 and also at 21:00 o´clock. Relative air humidity goes to minimum in these spots. The roof ridge has no ventilation, thus there isn´t any obvious airflow. There is sheet copper roofing used in strips on wooden slabs. The sensor No.07, found in the gable wall opening running into the tower, registered temperature minimums at 14:00 o´clock. At the same time, temperatures that were monitored with this sensor showed the smallest differences.

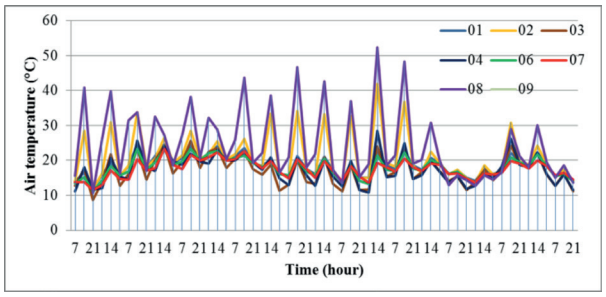

Fig. 5 The course of air temperatures recorded at 7:00, 14:00 and 21:00 o´clock - spring season 2012 (18.5.2012 – 5.6.2012)

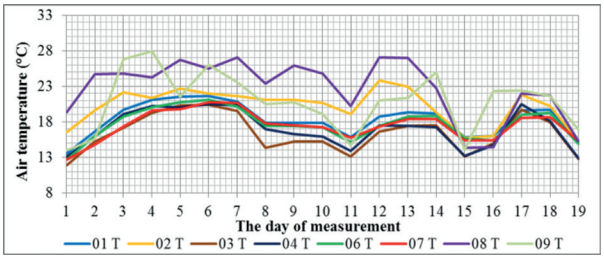

Fig. 6 Average day temperatures - spring season 2012 (18.5.2012 – 5.6.2012)

The tower has a square ground plan. It is made of stone and its walls are 800 mm thick. During daytime, there isn't any air overheating, and for the wall has high ability of accumulation, there isn´t either any significant air cooling. And that´s why there is no markedly cool air in early morning, in contrast to the truss space.

In most cases, temperature minimum was recorded with sensor No. 04, position of which is in the exterior on the northern side of a building, and with sensor No. 03 located near eaves in the exterior on the northern side of the building. Lowest temperatures in both seasons were found out using the outdoor sensor on the northern side of a building under the gutter cornice. Sensors No. 08 (under the roof ridge) and No. 02 (under roofing on the southern side of building) monitored considerable temperature fluctuations. It is these spots in the truss that air overheating occurs, which is caused by the effect of sunrays during the day.

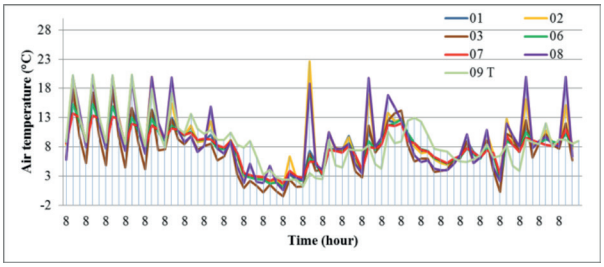

Fig. 7 The course of air temperatures recorded at 7:00, 14:00 and 21:00 o´clock - autumn season 2012 (18.10.2012 – 13.11.2012)

Measured values of maximal and minimal temperatures in particular openings according to the scheme in Fig. 4 Table 1

Sensor No.	Spring (18. 5. 2012 – 5. 6. 2012)			Autumn (18. 10. 2012 – 13. 11. 2012)		
	7:00	14:00	21:00	8:00	15:00	22:00
01	Min	Max		Min	Max	
02	Min	Max		Min	Max	
03		Max	Min	Min	Max	
04	Min	Max		Min	Max	
06	Min	Max		Min	Max	
07	Min	Max		Min	Max	
08		Max	Min	Min	Max	

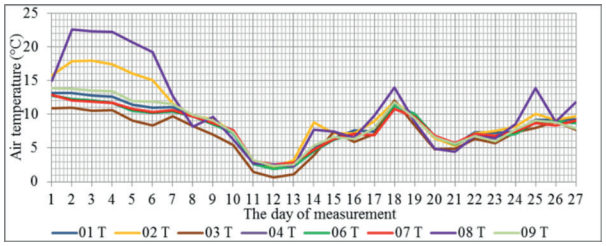

Fig. 8 Average day temperatures - autumn season 2012 (18.10.2012 – 13.11.2012)

4.3. The impact of microclimate on moisture of timber

Moisture of timber that is used in the roof space as a supporting truss structure ranges between 10 - 16%. Its value is depending on relative air humidity in the space. Wood is a hygroscopic material that has the ability to change its moisture according to ambient air humidity - equilibrium moisture (sorption, desorption). Moisture of wood has direct effect on various forms of its deterioration. In praxis, it is not very easy to define its natural durability because it is affected by many factors. The most significant are factors like its constitution and an exposure to loading. The dependence of equilibrium moisture of wood on relative air humidity at the steady temperature is called the sorption isotherm. It can be defined by DEBOER and ZWICKER [6] as follows:

$$\ln \frac{1}{\varphi} = A.\exp(-B.w) \quad (1)$$

where φ is the relative air humidity (%), w is the absolute moisture of wood (%),

A,B are the coefficients having a linear shape [7], T is the thermo-dynamical temperature (K)

$$A(T) = 7.7317 - 0.014348.T \quad (2)$$
$$B(T) = 0.0087 + 0.000567.T \quad (3)$$

The comparison of measured values of timber components in relation to relative air humidity and thermo-dynamical air temperature may be set by the following formula:

$$w = -\frac{\ln\left(\frac{\ln\left(\frac{1}{\varphi}\right)}{A}\right)}{B} \quad (4)$$

In accordance with calculations, absolute moisture of timber during the spring period in 2012 (see Fig. 9) fluctuated from 9.5 to 19.8%. The highest values of moisture (average moisture of 13.2%) are related to the timber elements on the northern truss side near eaves; the lowest ones (average moisture of 8.23%) regards the elements under the roof ridge. The highest values of moisture do not go over the critical limit which is optimal for arising such conditions that could cause damage of timber, e.g. ligniperdous insects, dry rot etc. [3].

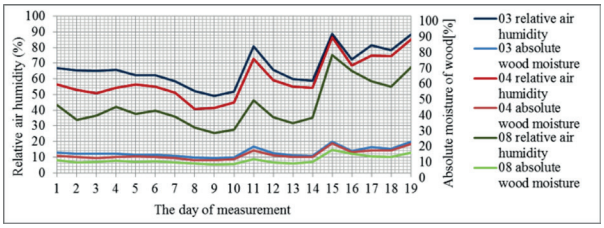

Fig. 9 The dependence of relative air humidity and absolute moisture of wood - calculated values, spring season 2012 (18.5. - 5.6.2012)

Absolute moisture values during the autumn period in 2012 (see Fig. 10) ranged between 10 - 27%. Generally, relative air humidity is higher than in the spring and therefore moisture of timber elements is noticeably higher. The highest values of moisture (average 23.22%) were found out in timber elements on the northern side of the truss structure near eaves; the lowest ones (average 13.61%) concerned the timber elements under the roof ridge. In the view of the fact that moisture of timber elements exceeds critical values for the activity of ligniperdous pests, and the time during which the effect of higher relative air humidity is much longer, there is a high risk of occurring biotic damage of timber components.

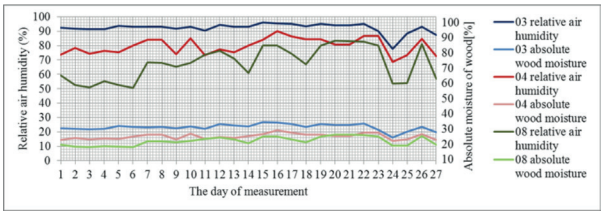

Fig. 10 The dependence of relative air humidity and absolute moisture of wood - calculated values, autumn season 2012 (18.10. - 13.11.2012)

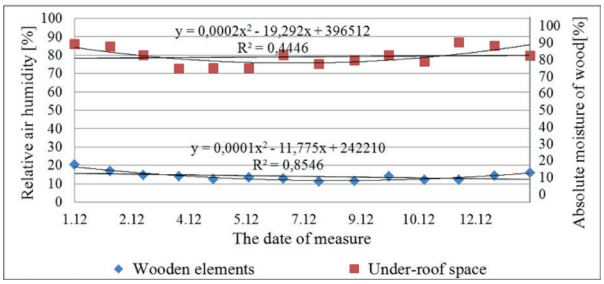

Fig. 11 Behaviour of relative air humidity in the roof space and values of absolute moisture, measured in timber elements of the fourth bond - the village of Bela-Dulice [8]

Values of moisture in timber components were confronted with the values that were obtained by direct measurements with the device Greisinger. Measured relative air humidity in the roof space reached the values of outdoor air characteristics. Year-long measurements regarding moisture in timber components of the fourth bond indicated that average values of absolute moisture of wood exceeded 20% only in one case - in January. Next month average moisture was 17%, and after that time values of moisture did not go over 13%. As late as in winter season the values were higher than 16% - see Fig. 11.

Calculated values were compared with values of absolute moisture of timber elements that were measured with the hand-device within experimental measurements using resistant hygrometer Greisinger. Measured absolute moisture of wood moved on lower level, in critical seasons it did not overrun critical values of absolute moisture of wood. On the basis of data confrontation it is possible to suppose that under the influence of venting in specific spots or areas in the truss space, there is a local change of conditions in microclimate, which can be seen as a change of moisture in particular timber elements.

6. Concluding remarks

This case study describes the system of measuring characteristics of microclimate relating to the roof space of a historical truss and moisture in timber elements. It brings the results of temperature and relative air humidity measurements in two seasons - spring (18.5.2012 - 5.6.2012), and autumn (18.10. 2012 - 13.11.2012). Obtained data obviously indicate that there are considerable differences in air characteristics for individual openings in truss spaces during daytime; there are also noticeable temperature fluctuations in terms of building´s location regarding the cardinal points. In respect to the comparison of measured characteristics in particular openings of the truss space, it is possible to define the way of air circulation in this space and subsequently mark the spots wherein there is no airflow. This fact has a fundamental impact on the moisture content in involved timber components which are found on such places of the truss structure. The data differences associated with absolute moisture of timber elements, recorded by actual measurements as well as obtained by calculations, point out presumable effect of ventilating in the truss space on the moisture content in timber. Thus, the influence of microclimate in the roof space on moisture of timber components can be evaluated with consideration of their position. The lifetime of used timber components is connected with moisture affecting them for a long time. Measurements of airflow velocity in selected openings were also made in the evaluated spring period. They ranged from 0.25 to 1.15 m.s-1 [8], while wind velocity in the exterior at the time of measurements reached 3.3 m.s-1. It is very important to know real air circulation in spaces of historical trusses for creating such conditions that are convenient for preservation of valuable timber constructions. All data, which were got by methodical long-term measurements, form the groundwork for making airflow simulation in given space. This simulation is the second step of our experiment. Inputs for simulation will be specified with respect to actually measured airflow velocities.

This contribution is the result of the project implementation under the Culture Ministry of the Slovak Republic with number MK-5913/2011/1.3.

References

[1] SUCHY, L., KRUSINSKY, P., GRUNOVA, Z., DURIAN, K., ZACHAROVA, D., KORENKOVA, R.: *Historical Trusses in Region of Orava and Kysuce*, Zilina: M. Gibala KNM, ISBN 978-80-970171-1-8, 2010

[2] SUCHY, L., KRUSINSKY, P., BABJAKOVA, Z., DURIAN, K.: *Historical Trusses of Sacral Objects in Turiec*, Zilina: M. Gibala KNM, ISBN 978-80-965547-9-7, 2008

[3] REINPRECHT, L.: *Wood Protection*, TU Zvolen, 2008

[4] KORENKOVA, R.: Analysis of Historical under Roof Space Trusses, 36. *Mezinarodni vedecka konference kateder a ustavu pozemniho stavitelstvi*, Brno : VUT Brno 2012, ISBN 978-80-214-4536-9, pp. 49-52

[5] CAPKOVA, E., KRUSINSKY, P.: *Geometric Analysis of Gothic Roman Catholic Church Roof in the Village of Bela-Dulice*, IX. intern. scientific conference FCE TUKE, May 22-25, 2012, ISBN 978-80-553-0905-7

[6] CHRISTEN SKAAR: *Wood-Water Relations, Springer Verlag*, Berlin, 1988, ISBN 978-3-642-73685-8

[7] SIAU, J. F.: *Transport Processes in Wood*, Springer Verlag. ISSN 0043-7719, 1984

[8] KORENKOVA, R.: Effect of Microclimate Historic Truss under Roof Space on the Timber Construction, *Stavebne hmoty*, ISSN 1336-6041, vol, 9, No. 1, pp. 24-27, 2013.

https://doi.org/10.26552/com.C.2013.4.32-38

Josef Vican - Jozef Gocal – Jaroslav Odrobinak – Richard Hlinka *

DESIGN AND STABILITY OF LONG SPAN RAILWAY ARCH BRIDGE

The bow-string arch bridge across the Vah River was designed on the main Slovak railway line. Total length of the bridge is almost 451 m, while the lengths of two main spans are 124.8 m. To analyse behaviour of the bridge, spatial transformation model was developed using FEM software. The Eurocodes were applied for all verification procedures. Bridge global analysis and verification of arches against buckling is discussed in more detail. The variation of upper bracing system and its influence on out-of-plane buckling of the arches is presented. Together with an architecture point of view, a minimum load amplifier to reach the elastic instability α_{cr} is used to estimate the suitability of the bracings.

Keywords: *Arch bridges, bow-string girder, buckling, stability of arches, bracings.*

1. Introduction

The main traffic lines in Slovakia, which have been included into European railway corridors, are under reconstruction and modernization during last decade. The speed 160 km/h is required, at least, [1]. In this context, our department has participated on design and processing of project documentation of several railway bridges. Given the nature of the line, majority of touched bridges are of small and medium spans [2]. But, there are also several bridges, which are dominant due to their spans or used technology [3]. Considering great number of relatively large bridges around Nosicka Dam, the concept of maximum utilisation of arched bridges in this area has been agreed during preliminary design work in order to achieve consistent bridge structures in this attractive location. One of such bridges, located in the line section between towns Puchov and Povazska Bystrica, will be bridging the Nosicky Canal at the Vah River. Experiences and remarks from design of this bridge are presented in this paper. The main attention is paid to global analysis and verification of the arches under buckling and the associated system of bracing arches.

2. Conception of the bridge structure

2.1. Preliminary design

The bridge will cross the Nosicky Water Canal just directly behind the railway station Puchov under very acute crossing angle 19.5°. A demand of the State Navigation Administration

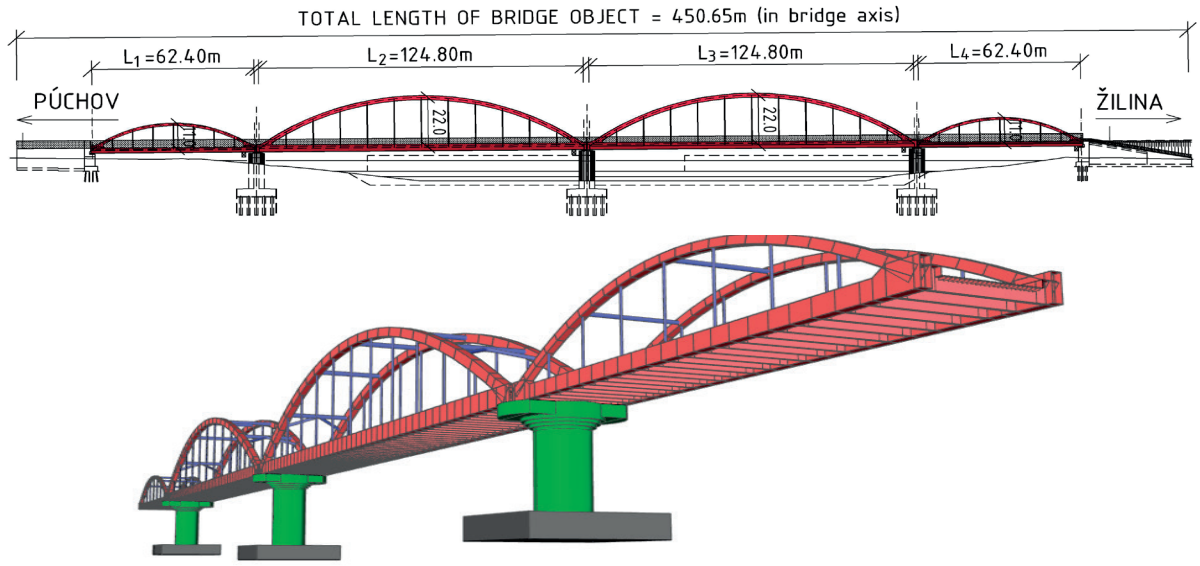

Fig. 1 Longitudinal view and FEM model visualisation of the bridge - the first proposal

* **Josef Vican, Jozef Gocal, Jaroslav Odrobinak, Richard Hlinka**
Department of Structures and Bridges, Faculty of Civil Engineering, University of Zilina, Slovakia, E-mail: vican@fstav.uniza.sk

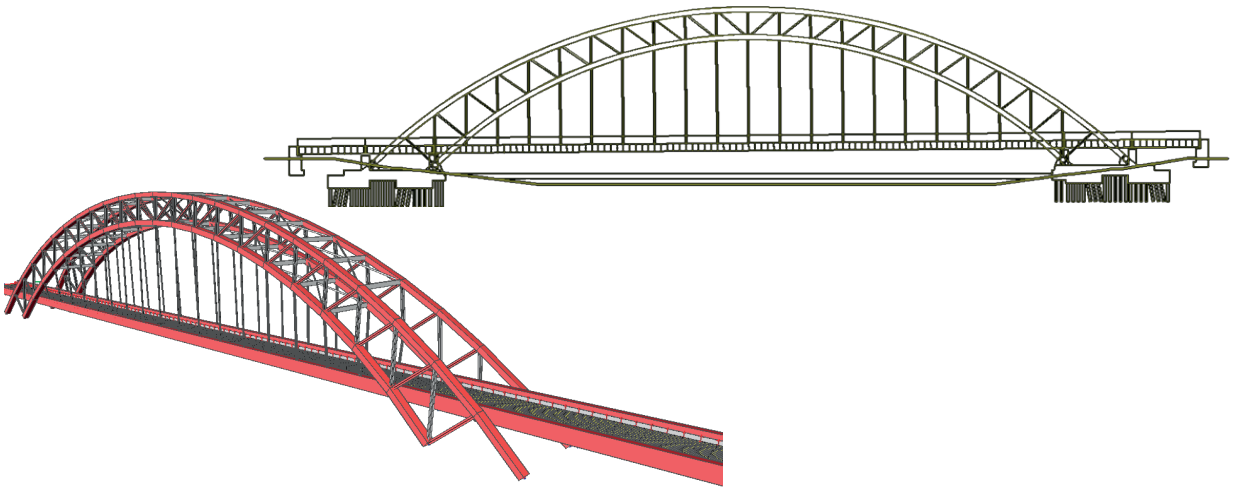

Fig. 2 Longitudinal view and a FEM model of the superstructure – the second proposal

to ensure navigability of Vah Waterway of class *Va*, at least, had to be necessarily satisfied. In addition, because of the navigable waterway in the future, excavating the river bottom of the value of 1.93 m had to be taken into account, as well. The small distance from the end switches of the railway station together with request for minimizing the piers in the canal induced the need of two-line bridge. Based on the adopted concept of arch bridges, two alternatives for bridging the water canal were presented in the first design stage.

The first proposal was based on conventional solution, where a set of bow-string arch bridges (Langer`s beams) was considered. Four simply supported steel beams reinforced by arches have spans 62.40 + 124.80 + 124.80 + 62.40 m long, see Fig. 1. The total length of the bridge is 450.65 m. Bottom steel orthotropic deck was designed to redistribute loads from ballast bed to the main girders. Unfortunately, this solution required an establishment of three piers in the canal-basin. Accordingly, to find a compromise with the State Navigation Administration, a splitting shipping space from the original width of 50 m perpendicular to the river was negotiated into the two parts with the width of 2 × 30 m. Such solution would allow shipping on both sides of the middle pier.

The second alterative of the proposed draft led into the fixed trussed through-arch bridge, see Fig. 2. This solution had the ambition to bridge the entire main obstacle - the river, with the superstructure of a single bridge span. An interesting structure consists of two truss arches with a span of their lower chord of 240.00 m and a suspended deck, which continued with two spans of 2 × 25.00 m on both ends. The total rise of upper arch chord has the value of 52.60 m. Both arches were designed in inclined planes at a distance of 11.40 m at the top of the arches and 17.50 m at the level of bearings. Although expensive, it represents a very courageous design without need for construction of a substructure in the bed of canal.

To choose the most favourable solution from the economic, aesthetic and structural point of view, rather time-consuming negotiations with representatives of the Railway Administration took place. Finally, the first proposed alternative introducing four single-span bridges consisting of stiff beams reinforced by arches and combined with the bottom orthotropic plate decks was found as the better one. Despite of any other arguments, the main reason was clear. The second alternative was more expensive than the first version proposed. Nevertheless, the two middle spans of this chosen two-line railway bow-string arch bridge still belongs to the unique structures in the design practise in our region.

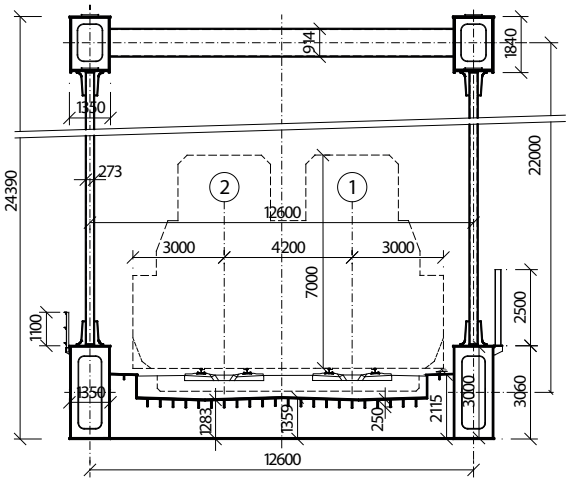

Fig. 3 Cross-section of the superstructure in the middle of the 2nd span

2.2. Basic parameters of superstructures of the final proposal

The steel superstructures of two internal fields 2 and 3 (Fig. 3) with theoretical spans of 124.8 m consist of two bow-string arch girders with the lower orthotropic bridge deck and the upper longitudinal bracing. The plate beams are designed from passable

box-section with external dimensions of 1350 × 3100 mm. The arches are designed as the circular curved with theoretical rises of 22.00 meters. Above the supports they are centrically connected to the beams of passable box-section with internal dimensions of 1220 × 1710 mm. The vertical hangers are designed from steel tubes R 273/20 mm, filled with concrete C 20/25 in order to increase dynamic resistance to the transverse vibrations.

The steel superstructures of two edge fields 1 and 4 with theoretical spans of 62.4 m are similar to the previous one. The plate beams are also designed as the passable box-section with external dimensions 1000 × 2410 mm. Theoretical rises of the circular curved arches are 11.00 meters. Above the supports they are connected to the beams with the eccentricity of 460 mm. The passable cross-sections of arches have internal dimensions of 900 × 1020 mm. The vertical hangers are from steel tubes R 219/17.5 mm, filled with concrete C 20/25.

The superstructures have a bottom steel plate orthotropic bridge deck with continuous ballast bed. The deck plate of thickness 16 mm is shaped into the profile of ballast bed channel with vertical webs. Flat longitudinal stiffeners located at distances of 420 mm are designed from plates 25 × 250 mm. Transverse stiffeners are arranged at distances of 2600 mm and they have a variable cross-section of an inverted T shape.

3. Analysis of the bridge superstructure

3.1. Global analysis model

For the global analysis, the spatial transformation model of the bridge structure given in Fig. 1 was developed using software based on Finite Element Method. Considering the size of the structure, the member finite elements were used for modelling main girders, arches, hangers and upper bracings, respectively. A steel plate of the deck was meshed by 2D shell finite elements. The plate was stiffened by the ribs in the longitudinal and transversal way, approximating in this manner the longitudinal and transversal stiffeners of the deck. Variation of thickness of all plates through the length, the changes of stiffness and all relevant eccentricities were considered in the numerical model, too. Considering the actual structural detail, the arch-to-beam joint were considered as a rigid, while the connections of hangers were approximated by the hinge joints (Fig. 4).

3.2. Stability of arches

Firstly, it was necessary to optimise the main dimensions, especially to find the optimal ratio of arc rise to its length. Then, the configuration of upper longitudinal bracings was varied from common truss systems to frame ones. After the preliminary design and optimisation process, more complex static analysis, analysis of stability and dynamic analysis could be performed.

3.2.1. Variation of upper bracings

In order to observe an influence of upper longitudinal bracing on the stability of the arches, a parametric study was performed. Different types of the bracing system were incorporated into the spatial computational models of the both bridge superstructures. The first comparative model was considered without any upper bracing system (I). Then, two basic types of upper bracing systems were taken into account: the frame system (II) with different number of cross-beams and the truss system (III) with various arrangements of diagonals. All considered bracing systems are summarized in Fig. 5. Besides, better understanding can be obtained from Fig. 7. In all cases, the bracing members were designed of circular hollow sections. In case of truss bracing system, the slenderness of members did not exceed the value of 150.

3.2.2. Stability analysis

Implementation of the imperfections as well as the second order effects into global analysis was found as a very time-

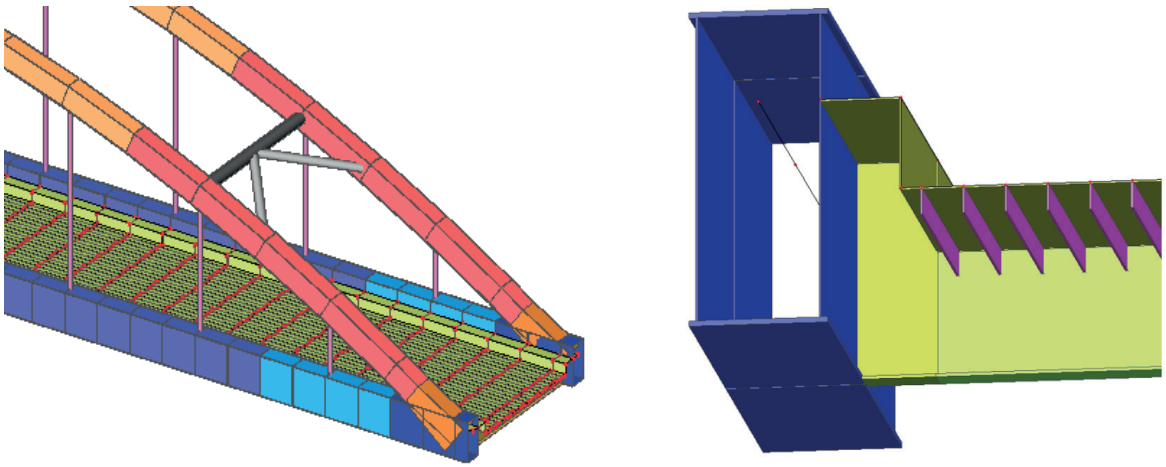

Fig. 4 Detailed look on FEM model visualisation of the longer superstructure

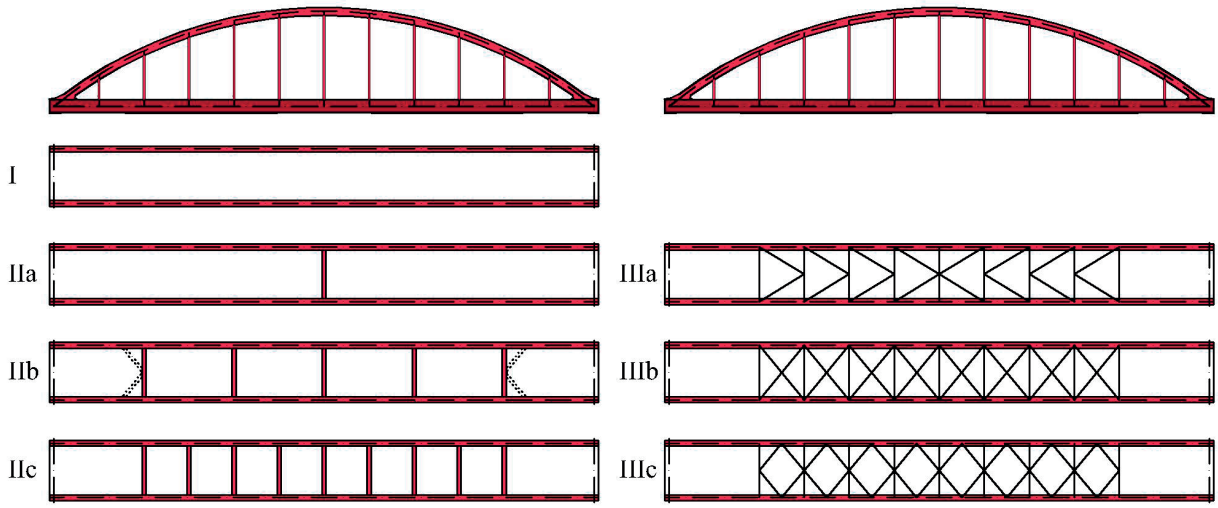

Fig. 5 Considered types of upper longitudinal bracings

consuming procedure because of full geometry models. Therefore, it was decided to take into account the imperfections of arch in the global analysis and the second order effects to allow for during a verification process. Buckling effects can be then included by introduction of equivalent buckling lengths, corresponding to a global eigenmode of the loss of structural stability, particularly the arches. In that case, the first order analysis may be used to find the factor α_{cr}, by which the design load should be increased to cause the elastic instability in a global mode.

The critical buckling length $L_{cr,z}$ of arch member for buckling about z axis can be then obtained from the well-known equation:

$$L_{cr,z} = \pi \sqrt{\frac{E \cdot I_z}{\alpha_{cr} \cdot N}} = k_z \cdot L_{arch} \qquad (1)$$

The unknown parameters in the equation (1) not mentioned hereinbefore are: E - the steel modulus of elasticity; I_z - the second moment of area about z axis of the arch cross-section; N - the value of normal force in the arch element, for which the stability is analysed; k_z - the coefficient of buckling length for buckling about z axis; L_{arch} - the theoretical length of arch axis.

Similarly, the influence of deformed geometry, so called "the second order effect" can be expressed by means of multiplying horizontal bending moments in arches determined using the first order theory by the factor k_{II}, according to equation:

$$k_{II} = \frac{1}{1 - 1/\alpha_{cr}} = \frac{\alpha_{cr}}{\alpha_{cr} - 1} \qquad (2)$$

Calculated values of the factors α_{cr} and k_z for various bracing systems — Table 1

Span of the bridge [m]			**62.4**		**124.8**	
Span-to-width ratio			5.07		9.90	
Upper bracings of the arches			α_{cr}	k_z	α_{cr}	k_z
Without bracing		I	4.57	0.31	1.76	0.33
Frame bracings	One in the middle	IIa	5.06	0.30	1.94	0.32
	In every 2nd hanger	IIb	**5.25**	**0.29**	2.85	0.26
	IIb + portal diagonals	IIb*	5.38	0.28	**3.22**	**0.24**
	In every hanger	IIc	5.46	0.28	3.43	0.24
Truss bracings	K - truss	IIIa	12.61	0.19	5.69	0.18
	X - truss	IIIb	13.10	0.18	5.64	0.18
	rhombic truss	IIIc	13.34	0.18	5.71	0.18

* Values for the finally adopted solution are in bold

The equation (2) is authorised by Eurocode 3 [4] only for values of amplifier α_{cr} higher than 3.0. In-plane buckling of the arches is controlled by tension hangers. This was also confirmed by stability analyses. Moreover, second order effects in vertical direction could be regarded as inessential, because the amplifier to reach the elastic in-plane instability α_{cr} was far above the value of 10.0 in both cases of arch structures.

3.2.3. Comparison of the parametric study results

The results of stability analyses of both superstructures stiffened by all aforementioned types of bracing systems are presented and compared in Table 1. Denotation of the particular bracing systems is shown in Fig. 5. As could be expected, the frame bracing system is generally less effective than the truss one [5]. The arch stability is also affected by the span-to-width ratio of the bridge superstructure. The comparison in Table 1 outlines dominant role of rigid model of arch-to-girder connection, as well. Actually, the out-of-plane buckling lengths of non braced arches could be considered under the one third of the theoretical arch length for all analysed cases. When using the truss bracing, the rhombic system seems to be the most effective, but only small differences were observed between particular truss types.

Calculated values of the amplifier α_{cr} from Table 1 are graphically compared in Fig. 6. It is clearly seen that, in the case of shorter spans, the use of truss bracing would significantly stabilize arches. If the span comes longer, the difference between frame and truss bracing is less evident.

The results of stability analyses of the final proposal are illustrated in Fig. 7 in the form of a mode of stability lost.

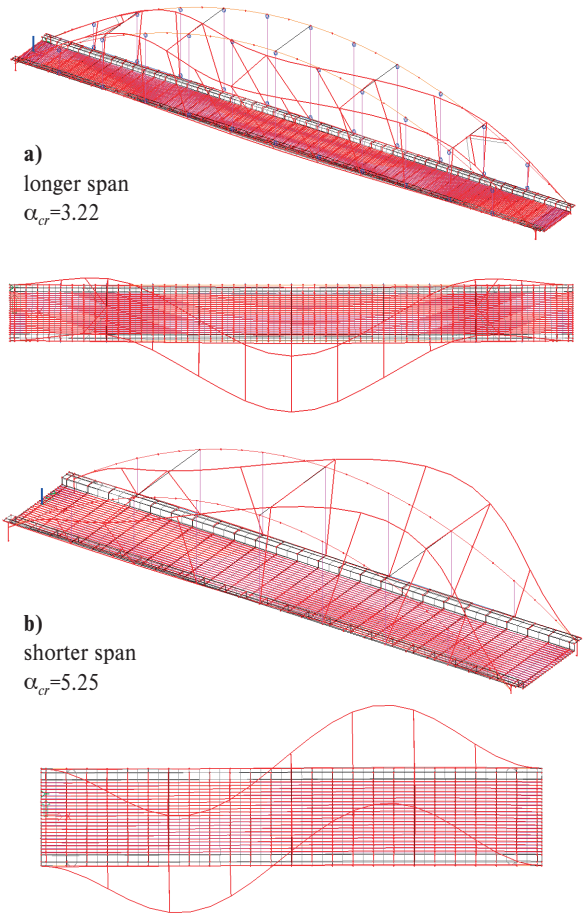

Fig. 7 Shapes of stability lost - bifurcation eigenmodes of the structures: a) for longer spans with α_{cr} = 3.22; b) for shorter spans with α_{cr} = 5.25

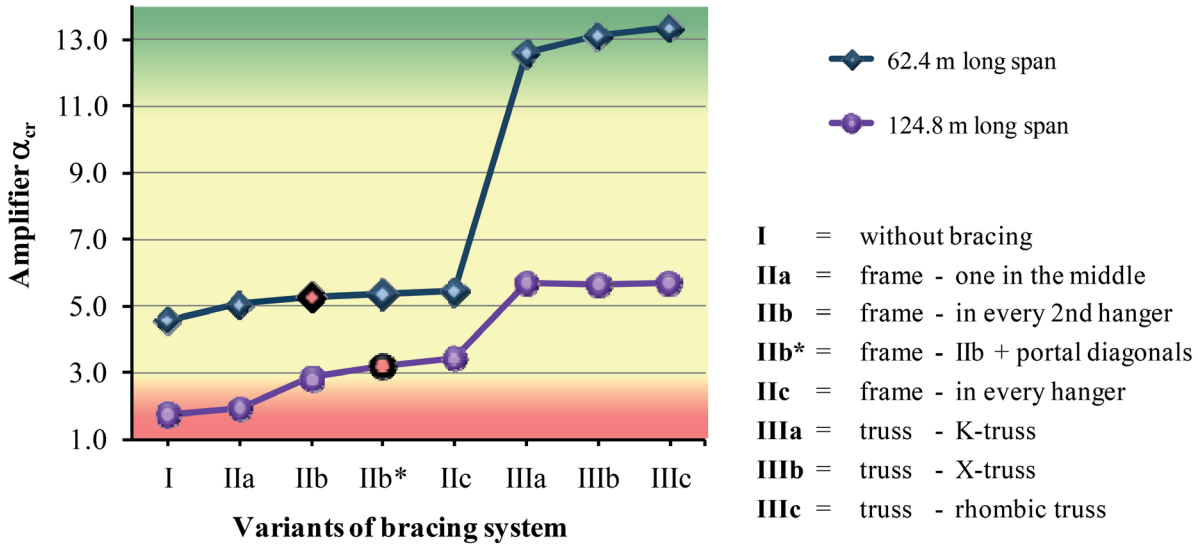

Fig. 6 Comparison of minimum load amplifiers α_{cr} to reach elastic instability

3.2.4. Discussion of aesthetic look of bracings

The aesthetics and architecture is commonly considered as universal opinion for attractive solution. Upper bracing of bow-string arch bridges is placed on visible part of the bridge and usually plays a dominant role in look of the bridge. In Fig. 8, the arrangement of bracing in the case of the superstructure with longer span (124.8 m) is compared.

Based on the human nature, many opinions on the best solution would be certainly found. As could be expected, the truss bracing seems to be less attractive. If the frame bracing is applied, it can be stated that the fewer cross members are installed the more beautiful sight is achieved. The mission is if the question: "Which is the nicest bracing?" is the most accurate in the case of the railway bridge not placed just in the middle of a big city. If the ability to stabilise arches is taken into account, the question can be probably turned into "which bracing with high level of stiffness has still acceptable look?"

Finally, the concept of frame bracing in every second hanger (variant IIb) was adopted for the bridge over the Nosicky Canal in Puchov city, where the rigid joint of the box arch to the box cross-section of girder plays very important role in the arch stability. In the case of longer superstructure with theoretical span of 124.8 m, the both portal cross-braces are reinforced with a pair of diagonals in order to increase the stability and to push up amplifier α_{cr} over the value 3.0 (variant IIb*).

4. Conclusion

A dominant bridge, which is being prepared for construction within the scope of modernisation of corridor lines on the Slovak Railways, is presented in the paper. Because of the space limitation, a special attention was paid only to the stability of arches. The results of the stability analysis show that except of system of bracing, some other parameters are important, as well. The stiffness of joint between the arch and the main girder seems to be also essential. A stiffer box-to-box connection of arch-to-girder joint can notable increase the arch stability in comparison with the arch fixed to a common plate I-girder. The span-to-width ratio has significant influence, as well.

From the description of the concept of bridging the Nosicky Canal, the analysis of the structure and its technical parameters, it is clear that the bridge represents a very ambitious and challenging structure. After the successful erection, the bridge will surely go down in history of Slovak bridge building.

Acknowledgements

This paper presents results of works supported by the Slovak Research and Development Agency under the contract No. APVV-0106-11 and by the Scientific Grant Agency of the Slovak Republic under the project No. 1/0364/12.

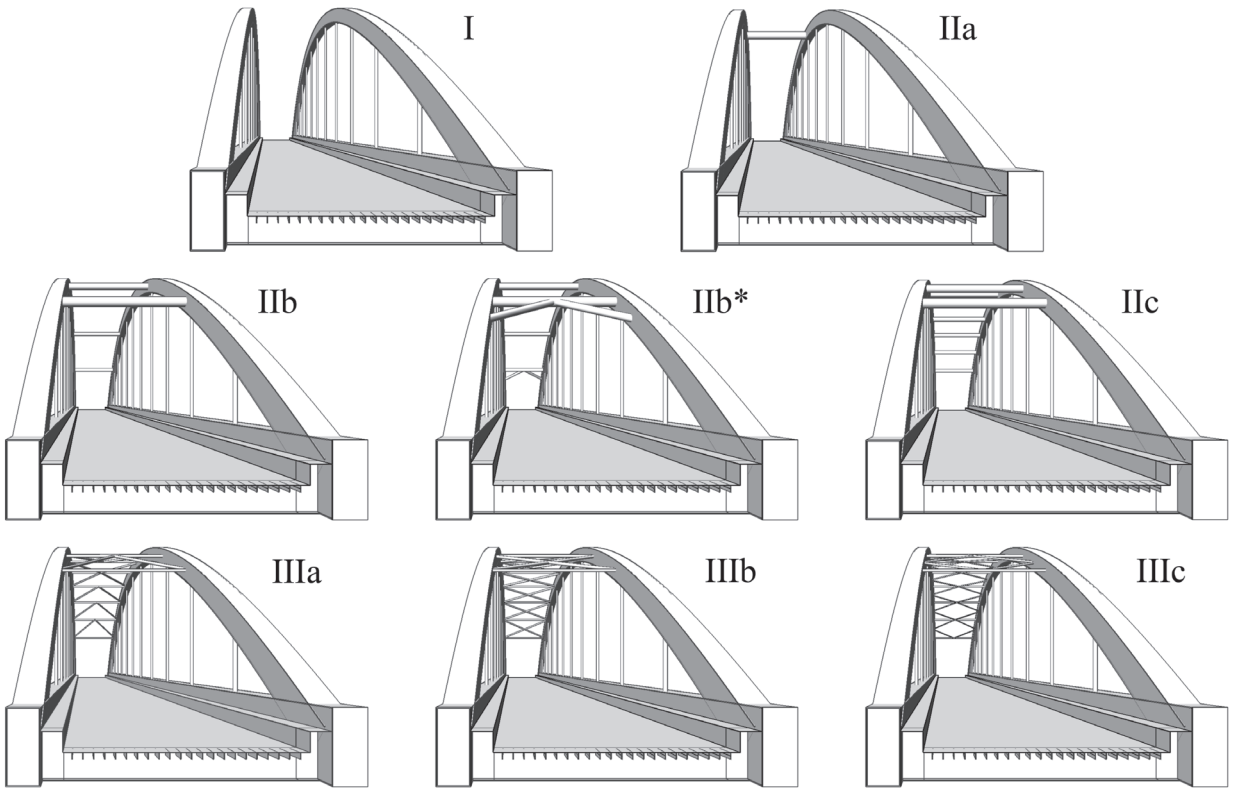

Fig. 8 Aesthetic look of bracings in the case of the 124.8 m long span superstructure (for denotation, see Fig. 5 and Table 1)

References

[1] IZVOLT, L., KARDOS, J.: Influence of Parameters of Railway Track Construction on Vertical Dynamic Interaction Vehicle/Track, *Communications – Scientific Letters of the University o Zilina,* vol. 13, No. 3, 2011, pp. 63-70.

[2] VICAN, J., ODROBINAK, J., GOCAL, J., HLINKA, R.: *Remarks from Diagnostics and Load Carrying Capacity Estimation of Existing Railway Bridges*. Proc. of 8th Intern. Conference on Short and Medium Span Bridges, Niagara Falls, CSCE, 2010, p. 150-1/150-9.

[3] VICAN, J., GOCAL, J., ODROBINAK, J., HLINKA, R.: *Reconstruction of Bridges at Corridor Lines of the Slovak Railways*, Eurostav: Bratislava, vol. 15, No. 9, 2009, pp. 8-12.

[4] STN EN 1993-1-1: Design of Steel Structures. Part 1-1: General Rules and Rules for Buildings, CEN, Brussels, 2005.

[5] DURATNA, P., BOUCHAIR, A., BUJNAK, J.: Analysis of the Behaviour of Steel-concrete Composite Truss, *Communications - Scientific Letters of the University of Zilina*, vol. 13, No. 4, 2011, pp. 46-50.

https://doi.org/10.26552/com.C.2013.4.39-43

Dusan Halaj - Stefania Semanova *

APPROPRIATE INFORMATION SYSTEM IN ROAD FREIGHT TRANSPORT BASED ON THE CARRIERS' REQUIREMENTS AND COSTS

The article is focused on the carriers' requirements and costs of the information systems in road freight transport. Based on the carriers' requirements for information and services as well as the costs of individual information systems, a recommended system or a combination of information systems, which are the most advantageous for carriers, is proposed.

Keywords: *Information system, carrier, costs, functions and services.*

1. Introduction

Individual information systems offer different functions and services to carrying agents for various costs. For the carrier it is, therefore, important whether a concrete information system which he buys, offers the required functions for the reasonable costs. It is important to avoid such situation that the purchased information system often connected with high costs, doesn't meet the carrier's basic requirements and needed functions.

2. Information systems that can be used by Slovak carrying agents

In the Slovak Republic carriers can use navigation and information systems, which are offered by individual vehicle manufacturers or, on the other hand, information systems which are independent from the vehicle mark and are focused on the monitoring of transport and vehicles. There are also information systems that cannot be used by Slovak carriers because they are intended only for selected foreign carrying agents. An example for such an information system is Frotcom, which is focused on the monitoring of vehicles and transport.

2.1. Information systems offered by vehicle manufacturers

Information systems (Table 1) that are offered by individual vehicle manufacturers can be classified together with the subsystems for operational control and are designed to monitor operating parameters of vehicles. A part of such subsystem is, for example, fuel management – management and control of the fuel consumption. These information systems also provide carriers with different levels of services which provide a variety of information and can be focused on the vehicle, the driver or the transport management. At each level of service some hardware is needed. It may be a part of the new vehicle or not. Monthly fees are also different according to these levels.

Information systems offered by vehicle manufacturers [1] Table 1

Vehicle manufacturer	Information system
IVECO	BLUE&MEFleet
Mercedes Benz	FleetBoard
Volvo	Dynafleet
Scania	C200
MAN	Telematics
DAF	
Renault	Infomax

Functions focused on the vehicle

These functions are included in the basic packages of information systems. For their usage there is no need for the purchase of a new hardware for the carrier, because it is already a part of the vehicle (Fig. 1). He pays only a monthly fee that is approximately 15 €/ month per each vehicle. A carrier therefore obtains the following functions: vehicle journey recording (speed, braking, fuel consumption, and travelled distance), remote data downloading, failures assistance, maintenance planning, log book.

* **Dusan Halaj, Stefania Semanova**
Department of Road and Urban Transport, Faculty of Operation and Economics of Transport and Communications, University of Zilina, Slovakia,
E-mail: dusan.halaj@fpedas.uniza.sk

Fig. 1 Hardware IVECO for use of functions focused on the vehicle and driver [2]

Functions focused on the driver

Functions of this level of information systems are designed not only to monitor the operating parameters of vehicles, but also to control the work of individual drivers. For the usage of these functions, once again, it is not necessary to purchase and procure hardware, because it is also a part of the vehicle. The carrier pays a monthly fee from 25 to 30 €/month per each vehicle. Besides the previously mentioned functions he also receives the following functions: time records – all information about the working hours of drivers and the length of their drives, tacho-management – remote data downloading from the driver cards and mass memory tachograph.

Functions focused on the transport management

These functions are not used by Slovak carriers as often as the previous ones because they require to purchase hardware – GPS module (Fig. 2) that is not a part of the vehicles and its price including installation is around 2 500 €. The carrier pays for the usage of such functions a monthly fee, which is 35 €/month per each vehicle. The carrier receives, in addition to the previously mentioned functions, the following functions and services: processing of messages between the driver and the control centre, on tracks – this function signalizes the dispatcher that the vehicle is close to its final destination, navigation, workflow – this feature integrates data about transport with the navigation, trailer&refeer – information about trailer – temperature, disconnection, connection, geofence – possibility of setting geographical areas including the reporting of exceptions.

Fig. 2 Hardware Mercedes Benz for use of functions focused on the transport management [3]

2.2. Information technology for monitoring of transport and vehicles in road transport

Information technologies for monitoring of transport and vehicles are designed mainly to monitor the vehicle movement, control the work of the drivers, record and monitor the operational status of vehicles. These information technologies, however, do not allow navigation [3]. In the Slovak Republic the carriers can use the following information technologies: Commander, DeMoTech, GENETECH, INFOCAR, TAMEX and EMTEST. In road freight transport, the most widely used system is Commander. For carriers, it offers the following functions and services: on-line monitoring of the vehicles, visualization of the vehicles on the map in the real time, automatic generation of the log book for tax purposes, unlimited storage of the drives history, automatic calculation of the fuel consumption according to data about refuelling, automatic creation of transport orders with their accounting, monitoring of the operational status of the vehicles, the possibility to trace a vehicle after theft, car service management, the ability to track problems on the journey (e.g. congestions, accidents, and etc.) and to inform drivers about the impassable sections, communication with drivers, the possibility of setting alarm when entering restricted areas – waypoint function, simple and accurate report about the service of the vehicle, the possibility to search for stolen vehicles.

In order to use individual levels of services and functions, the carriers need to have a GPS unit installed in their vehicle, which is connected to the bus. The price of this hardware equipment is 547.60 € for each vehicle. Its maturity is about 6 years. Besides one-time payment for the purchase, the carriers also pay a monthly fee of 20 € per each vehicle.

2.3. Navigation systems

Information technologies for the navigation should be distinguished from the information technologies designed for monitoring vehicles and transport. Navigation systems are used to search for the shortest, fastest or the most economical journey of transport from the place of loading to the final destination. Its advantage is mainly navigation of the driver in cities, because the driver can be fully focused on driving and the voice navigation guides him directly to the place of unloading in a concrete area. Navigation manufacturers developed special devices designed for trucks and their price is around 400 €. Navigation systems also allow receiving actual information about the traffic conditions and in case of impassable sections they can suggest another journey in order to avoid long delays [4].

3. Transport companies´ requirements for various functions and information

The carriers have different requirements for information systems, their functions and services. If the carrier procures some information system, it should meet the most of his requirements

for its functions and the costs should not be higher than the savings achieved. For carriers it is the most important to know the location of their vehicles during its transport performance. They put on this function even greater emphasis than on the fuel consumption, because in the present competition the utmost importance is put on the customer, delivery deadlines and reduction of empty runs. The fuel consumption is also important because this cost factor builds up to 40% of all costs. The problem is that the information systems that can be used by carriers in Slovakia do not allow monitoring the fuel consumption on-line. The information system Frotcom enables to monitor the consumption on-line but it cannot be used in the Slovak Republic. Other functions and services that are important for carriers are: warning of the dispatcher when the vehicle is approaching its final destination, information about the drivers working hours, remote data downloading, navigation, which is important mainly to the driver, caution for the dispatcher if the vehicle is deflecting from the journey or approaching the final destination to a mobile phone (smart phone), information about the traffic density and congestions, failure assistance.

Requirements of carriers for information [5] Table 2

Requirements of carrying agents	Amount	Percentage
Actual vehicle location	58	92.06
Fuel consumption – Online	55	87.3
Fuel consumption – Offline	40	63.49
Navigation	40	63.49
Information about the traffic density and congestions	35	55.56
Information about the drivers working hours	28	44.44
Caution when approaching final destination	15	23.81
Information to a mobile phone	6	9.52
Failure assistance	5	7.94

Individual requirements according to their importance are shown in the following Table 2. They are based on the requirements of 63 carriers.

4. Comparison of costs associated with using information systems

The carriers use mainly navigation systems that are determined for road freight transport. When the carriers want to optimise their operation, they can procure either information technologies for monitoring transport and vehicles or information technologies focused on the vehicle and the driver in addition to the navigation system. The technologies are offered by individual vehicle manufacturers. For these cases, the costs associated with the use of information systems are determined. The Slovak carriers do not use the functions focused on transport management, because hardware is much more expensive than a navigation device, although, the information systems focused on transport management offer much more functionality.

Costs, which are invested by the carrier into the information system, should not be higher than the savings achieved by the carrier during the utilization of the functions of the information system. Based on average costs shown in Table 3, it is possible to calculate the cost increase in €/km and €/year when using various information systems; the calculation with classification of costs on variable and fixed costs is used [6].

Average costs €/year a data for the articulated vehicle [7] Table 3

Fuel costs – 42 500	Other direct costs (ODC) – 5 200
Oil costs – 800	Depreciation of vehicle– 13 500 (DoV)
Tires costs – 2 500	
Maintenance, repair and treatment (M, R and T) – 5 950	Overhead– 7 000
Wages with levies – 14 000	Toll – 12 000
Travel compensation (TC) – 7 000	Driving performance - 110 000 km
Heating vehicle costs (HV) – 495	Time of operation– 3 000 h/year
Coefficient of drives utilization– 0.80	Technical speed – 55 km/h

Comparison of the rates when using individual information systems [authors] Table 4

	Navigation		Navigation and Commander		Navigation+ management functions of vehicle and driver		Management functions of vehicle, driver, and transport	
Rates	Skm(€/km)	Sh(€/h)	Skm(€/km)	Sh(€/h)	Skm(€/km)	Sh(€/h)	Skm(€/km)	Sh(€/h)
Fee	-	-	0.0015	0.08	0.002	0.11	0.0025	0.14
Hardware	0.0004	0.02	0.001	0.05	0.0004	0.02	0.0025	0.14
Costs	0.8660	15.75	0.8680	15.86	0.8680	15.86	0.8706	16.01
Cost increase in % (€/km)	0.05		0.28		0.28		0.58	
Cost increase per year	44 €/year		265 €/year		265 €/year		558 €/year	

Comparison of the carriers' requirements with the information systems functions [5] Table 5

Carrier's requirements	Blue& MeFleet	C 200	Fleet Board	Dyna fleet	Commander	Navigations	Frotcom
Actual vehicle location	X	X	X	X	X		X
Fuel consumption – online							X
Fuel consumption – offline	X	X	X	X	X		X
Navigation	X	X	X	X		X	
Information about the traffic density and congestions					X	X	X
Information about the drivers working hours	X	X	X	X	X		X
Caution when approaching final destination (area)	X	X	X	X	X		X
Information to a mobile phone			X				
Failure assistance	X	X	X	X			

Table 4 contains the calculated costs in €/km and €/h of operational downtime (idle time) when the carrier uses information or navigation systems. The rates calculated from the average costs without the use of information systems are 0.8656 €/km and 15.73 €/h of operational downtime. These rates may vary depending on the level of costs and vehicle operational data of individual carriers. The rates do not include a profit margin and coefficient of drives utilization.

5. Conclusion

Most of the carriers already use navigation and they have it procured before the individual vehicle manufacturers came out with the transport management function. Based on the analysis it can be concluded that in the Slovak Republic there is no information system, which allows on-line monitoring of the fuel consumption. The carriers receive the information whether the journey was in the standard consumption level or above it in certain period after the transportation. Receiving information about vehicles by mobile phone (smart phone) is enabled only b the information system Fleet Board designed for Mercedes Benz trucks. Individual functions and services of information systems required by carriers are shown in the following Table 5. Based on the comparison of functions and costs (Fig. 3), it is possible to recommend obtaining the Commader Information System in addition to the navigation because it provides best balance of functions for carrier and the costs are lower than for a complete package of managerial functions provided by different vehicle manufacturers.

Determination of the costs was based on average costs which arise to the carriers during operating in road freight transport. Costs €/km (basic rate – 0.8656 €/km without using any information system) were determined by the calculation with classification of costs on variable and fixed costs. Individual rates may vary according to the amount of individual cost items and operational parameters of carriers. In Fig. 3 we can see the comparison of costs €/km when the carriers use only a navigation, navigation and the information system commander, navigation and managerial vehicle and driver functions or complete service of transport management, which also includes navigation. Costs that are connected with the usage of navigation and commander system are comparable with costs of navigation and vehicle and driver managerial functions. In the case of the managerial vehicle and driver functions with navigation, the carrier receives failure assistance service, but he does not get the actual vehicle location function that is much more important.

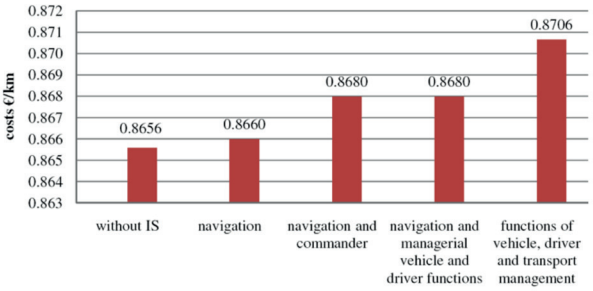

Fig. 3 Costs in €/km when using individual information systems [authors]

Based on the costs and carriers' requirements, it can be concluded that the most appropriate combination is to use the navigation and information system Commander, which is designed to monitor vehicles and transport.

The carriers can optimise their operation by using information systems. They can decrease numbers of empty kilometres (increase β coefficient) or increase annual driving performance based on acquiring new customers. Table 6 shows about what percentage should be increased β coefficient or driving performance to cover costs of IS. A carrier achieves gain of 12 980 €/year for price of

Increase of β coefficient and driving performance to cover costs on IS [authors] Table 6

	Without IS	Navigation	Navigation and Commander	Navigation+ management functions of vehicle and driver	Management functions of vehicle, driver, and transport
Rates	Skm(€/km)	Skm(€/km)	Skm(€/km)	Skm(€/km)	Skm(€/km)
Without β	0.8656	0.8660	0.8680	0.8680	0.8706
With β (0,8)	1.0820	1.0825	1.0850	1.0850	1.0882
β increase to cover costs of IS	-	0.8004	0.8022	0.8022	0.8046
β increase to cover costs of IS in %	-	0.0462	0.2773	0.2773	0.5777
Increase of driving performance to cover cost of IS	-	110 468	112 870	112 870	116 100
Increase of driving performance to cover cost of IS in %	-	0.4255	2.6087	2.6087	5.5456

1.200 €/km, driving performance of 110 000 km/year, and costs without using information systems of 1.0820 €/km. For example, if the carrier uses navigation and Commader information system, he must increase driving performance to 112 870 km/year in order to achieve gain of 12 890 €/year at an unchanged price.

Acknowledgement

This paper was developed under the support of project: MS SR VEGA 1/0144/11 Vplyv zmeny kvality poskytovanych sluzieb verejnej hromadnej osobnej dopravy na zvysovanie jej konkurencieschopnosti vo vztahu k individualnemu motorizmu.

References

[1] HALAJ, D., POLIAK, M.: *Analysis of Selected Information Systems in Road Transport (in Slovak),* CMDTUR 2012 : Almanac of papers and posters: the 6th Intern. Scientific Conference, Zilina - Straza, University of Zilina, in EDIS, 2012, ISBN 978-80-554-0512-4. - S. I-89-I-99.

[2] Internal resources of IVECO Zilina

[3] Internal resources of Mercedes Benz Banska Bystrica

[4] GNAP, J., KONECNY, V., POLIAK, M.: *Application of Information Systems in Road Transport (in Slovak),* University of Zilina, 2007

[5] HALAJ, D., POLIAK, M., KOLAR, J.: *Carrying Agents´ Requirements for Information Systems in Road Freight Transport*, TRANSCOM 2013 : 10th European conference of young research and scientific workers, University of Zilina, 2013, 2013, ISBN 978-80-554-0690-9, pp. 53-56.

[6] GNAP, J.: *Calculation of own Costs and Pricing in Road Transport – 3rd edition(in Slovak),* University of Zilina, 2006

[7] POLIAK, M., KONECNY, V.: *Economy of Road and Urban Transport - Guidelines for Exercises (in Slovak),* University of Zilina 2008.

https://doi.org/10.26552/com.C.2013.4.44-47

Katarina Sulovcova - Jozef Jandacka *

OPTION OF SOLID POLLUTANTS ABATEMENT IN FLUE GAS PATH

Biomass combustion produces gaseous and solid pollution. Solid pollutants are small particles which are getting into the air with smoke and may be harmful to the environment, the human and animal health. Therefore, it is important to decrease their amount in the ambient atmosphere. Particulate matter sources are not only big combustion devices but also small combustion devices which are quite common and widely used. It is necessary to mention that the small boilers are not as monitored as bigger ones. Therefore, they are potentially a large source of pollution. The main objective of this work is to reduce particulate matter concentration produced by small residential combustion appliances by making a change of the geometric parameters in a flue gas path.

Keywords: *Pollution from biomass, particulate matter, separation.*

1. Introduction

There is nowadays worldwide high encouragement of taking up of the biomass as a heat and energy source. The renewable energy sources replace fossil fuels in order to reduce the amount of total pollution in atmosphere. The combustion is the most developed and the most frequently applied thermochemical technology of conversion of biomass into the useful energy. The combustion of solid biomass produces less pollution than the combustion of fossil fuels, but there are still some pollutants [1].

The air quality is very important not only for humans, but also for all organisms living on the Earth and for general function of all ecosystems. Previous observations show that there are problems with a higher particulate matter concentration in many countries [2]. As a consequence of this fact, European countries make changes in legislation that regulate the amount of emissions. The monitoring of pollution and stricter emission legislation should help to decrease their amount.

One of the pollutants which extensively effects air quality is particulate matter that is generally coming into the ambient atmosphere from various sources, for instance, traffic, factories and volcanoes. But there is also one potentially big source of particulate matter pollution - small combustion appliances. The domestic heating sources have a big potential because they are numerous and, especially during winter heating season, produce particulate matter pollution. Those uncontrolled combustion appliances (because they are not monitored) contribute to the air pollution on a large scale and it is estimated that those small sources produce from 20% to 90% of the total emission of particulate matter in the winter [1 and 3].

In many cases small combustion boilers do not have any additional appliances to reduce pollution. There is high probability of incomplete combustion leading to the production of fine particles and hazardous organic compounds in small heat sources. During process of biomass combustion the solid particles are formed and emitted together with smoke into the ambient air. In many European countries the problems with increased amount of the particulate matter persist and, as a consequence, this may cause various diseases [3].

With view to minimize the production of particulate matter emission and improve air quality various ways of their reduction are used. Filters or external separators can be used, but they are costly; sometimes the same price or even more expensive than the heat source itself. Therefore, new solutions which are not so costly and are effective enough to decrease the amount of solid particles are looked for. Such a solution can be a change of a construction and design parameters of a heat source, especially change of a design parameter in the combustion chamber and flue gas path.

1.1. Particulate Matter

Many of the scientific studies deal with particulate matter pollution and its influence on human being. Exposure to such particles can affect both lungs and heart, especially fine particles – containing microscopic solids that are so small that they can get deep into the lungs (Fig. 1) and cause serious health problems [4, 5 and 6].

Particulate matters may generally increase the risk of respiratory and cardiovascular diseases, higher mortality, more allergies, aggravated asthma, nonfatal heart attacks, irregular heartbeat, decreased lung function, and increased respiratory symptoms, such as irritation of the airways, coughing or difficulty

* **Katarina Sulovcova, Jozef Jandacka**
Department of Power Engineering, Faculty of Mechanical Engineering, University of Zilina, Slovakia, E-mail: katarina.sulovcova@fstroj.uniza.sk

with breathing etc. [4, 5 and 6]. Mortality associated with air pollution is about 15-20 % higher in cities with high levels of pollution compared to relatively cleaner cities. In the European Union, average life expectancy is estimated to be 8.6 months lower due to exposure to $PM_{2.5}$ resulting from human activities [7].

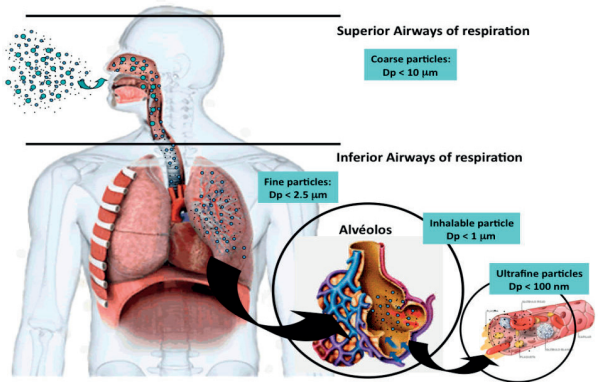

Fig. 1 The areas where particulate material is deposited in the body [6]

Behavior of particulate matters in the air and also the influence on human body is determined partly by their size. Coarse particulates can be filtered by natural human defense system in nose or they are sneezed or coughed out of body. But there are also smaller ones, the fine particles. The biggest attention is paid to PM_{10} (particulate matter less than 10 microns in diameter) and $PM_{2.5}$ (less than 2.5 microns in diameter). Those small particles are able to get deep into the lungs and into the alveolus. The smallest ones are even able to get into the blood stream. For better imagination particulate matter PM_{10} is at average 7 times smaller than human hair in diameter and $PM_{2.5}$ is even 28 times smaller than human hair [4 and 5].

Particulate matter emissions from biomass combustion have various sizes. Higher concentration of the particles is with the finer sizes. Particles with size PM_{10} make around 35% of total particle matter emission of combustion [8, 9 and 10].

2. Separation of Particulate Matter

In order to minimize amount of particles emitted into the ambient atmosphere various solutions are researched. Usually the appliances which produce particles are connected with filters or external separators. It is effective but it can be expensive. Sometimes this technology is more costly than the appliances itself. Therefore, solutions which could decrease particle concentration and still would not be so costly are looked for.

One of the options how to decrease particulate matter concentration is trapping particles before flying out of the combustion devices. It can be achieved by making construction changes of the combustion chamber and flue gas path.

The essential thing of every separation process, in which solid particles are separated, is to remove solid particles away from flue gas and get them into a trapping place. The trapping of particles is theoretically explained by cooperation of few together working separation processes.

2.1. Separation Process

The separation of solid particles has several steps. The first step, as already mentioned, is to separate the solid particles from a fluid flow into the wall of separator. In this step various principles and forces are important, for example, the force of gravity, centrifugal force, inertia force, electrostatic force, diffusive force and others. The second step is to get the solid particulate matter into the trapping place and avoid getting it back to the stream of fluid. It is also carried out in various ways. For example, a dry mechanical separator uses flow of carrier gas. The particles are carried close to the separation wall and taken away into the trapping place [11].

This type of separator is interesting because its principles can be applied in small heat sources. The scale of separation is from 3 to 30 µm [11].

3. CFD Modeling as Option of Reducing Pollution

Simulation of various physical processes is necessary for many experiments from economic, ecological and safety point of view. Modeling together with experiments, enables a cost-effective approach not only for future biomass combustion application designs [1].

CFD program offers a possibility to solve numerically the essential physical equations as conservation of mass, energy and momentum etc. Modeling improves our understanding of the fundamental process involved in combustion appliances and may significantly reduce the “trial and error” development time needed when experiments are used for design optimization only. By combining modeling with experiments, an improved design is possible with respect to the reduction of emissions from combustion. Parametric studies can be carried out to reveal the relative influence of different combustion processes and flow variables on emission levels and energy efficiency [1].

This type of program can simulate various physical processes which can help also with a particulate matter concentration. We can simulate the flow in small combustion devices too.

To simplify the model of the particulate matter flow and reduce computational time needed, it is possible to make modeling without combustion. Some of the input parameters are given in Table 1.

Input data for simulation Table 1

Number	Input parameters	Value	Unit
1	Pressure on inlet	0	Pa
2	Pressure on outlet	-12	Pa
3	Temperature	25	°C
4	Density	1.185	Kg.m-3

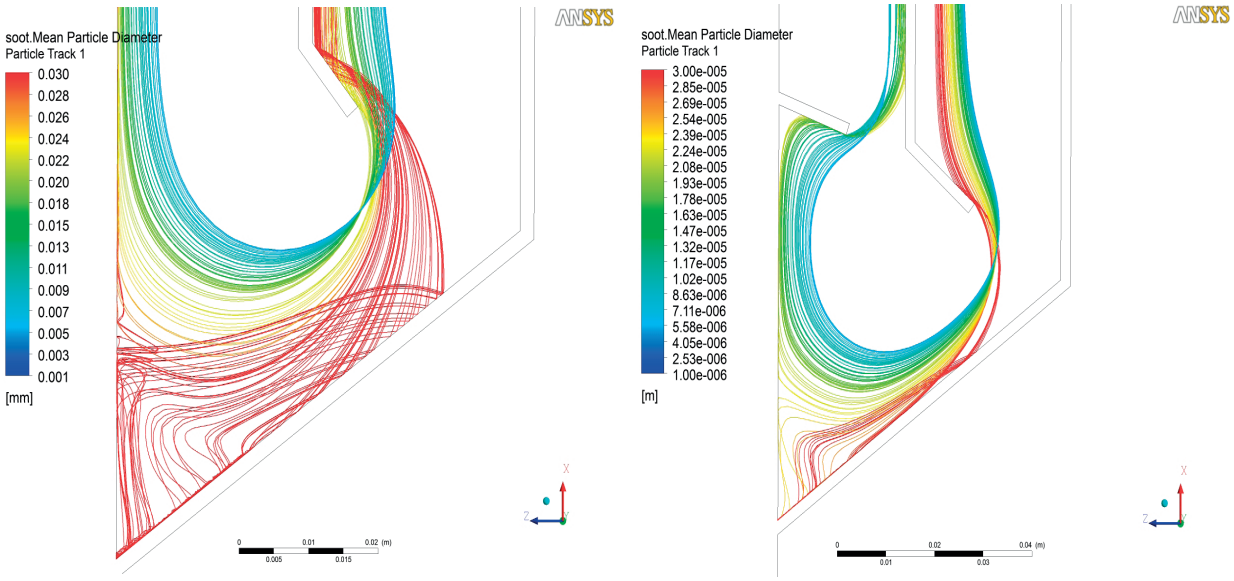

Fig. 2 Idealized flow of particles

The source of particulate matter emission with the certain amount of mass flow is given into the model. It is necessary to consider the gravity force in the model because it is important for trapping particles and, therefore, we are able to observe behavior of those solid particles in the flue gas path. It is also assumed that the process is time independent, steady; the fluid is incompressible air in the simulation [12].

Solid particles in the model are defined by Rosin-Rammler distribution in order to see various sizes of those particles. Just flow of fluid and trajectory of particle is sufficient for simplification.

In the flue gas path variable constructions can be performed. The influence of this construction on flow and on trapping of the particles can be closely observed by this program. It allows to see the effect of the construction changes on velocity, pressure, turbulence, etc. This helps to make useful changes in order to improve the construction of the small combustion devices with respect to minimizing particle emission.

A fireplace with a special tunnel placed in flue gas path was used in this work. In Fig. 2 we can see an idealized flow of particles in the trapping place in the special tunnel with two various constructions. The bigger particles are trapped at the bottom and the smaller particles are flowing away with smoke. There is possibility to trap more particles with appropriate construction changes.

4. Experimental Verification

Verification of the simulation results is possible to make by a gravimetric measure method, a laser measurement or other similar measurements of a particle concentration. Gravimetric method (Fig. 3) where multiple sampling is done by observance of the isokinetic conditions can be used. Samples are taken during several measurements. This method is based on determination of the mean concentration of particulate matter by manual taking of samples from time cross section of measurement and its consistent gravimetric interpretation. Representative sampling is performed by a sampling probe with a proper shape right from the gas stream [8 and 13].

Two series of measurements have to be made. One series before the construction changes, second series of the measurements after the construction changes. These two series are necessary for the comparison of values of a particulate matter concentration from the first series with those from the second series. This comparison shows whether the construction changes helped to avoid the solid particle production into the ambient air or not.

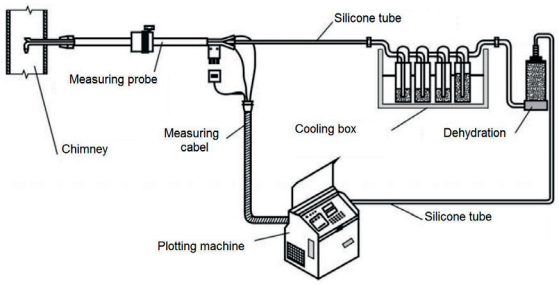

Fig. 3 Gravimetric method scheme [10]

5. Analysis of Results

Two various constructions were chosen for measurements. The first construction is the original one, without changes, while the second construction underwent some changes. This changed one seems to have better separation properties in the

Value of gravimetric measurement Table 2

	First series of measurements	Second series of measurements	Unit
Average weight of wood	2.994	2.952	kg
Average concentration calculated on 13% O_2	56.31	49.63	$mg.m^{-3}$

modeling results than the original one, therefore it was selected for comparison.

Gravimetric measurements were made on a fireplace with beech wood combustion. Isokinetic condition and other conditions for gravimetric method were followed. The conditions were the same for both series of measurements. The average values of measurements are presented in Table 2.

The average particulate matter concentration in the first series is $56.3mg/m^3$, in the second series the average value is $49.6mg/m^3$. The second series of measurements showed lower concentration of particulate pollution then the first ones. We can assume that it is due to construction changes which were made in compliance with the previous simulation.

6. Conclusion

The widespread biomass usage brings problems connected with the particulate matter production resulting from biomass combustion, especially in small domestic heat sources. Their contribution to particulate matter concentration is remarkable mainly during winter heating season. As the amount of those appliances increases, the particle pollution produced by them also increases.

Particulate matter emissions formed in heat sources impair the air quality and have harmful influence on human health; therefore, it is very important to reduce the concentration of solid and also gaseous emissions.

The use of CFD simulation in combination with experiments seems to be a good way to reduce particles emission. It not only enables to see particulate matter flow in combustion devices but also to see how particulate matter concentration can be dependent on construction changes. It can help to decrease air pollution.

Acknowledgement

This work is supported by the financial assistance of the project VEGA No. 1/1290/12.

References

[1] VAN LOO, S., KOPPEJAN, J.: *The Handbook of Biomass Combustion and Co-firing*, Earthscan, London: Washington, p. 442, 2008. ISBN 978-1-84407-249-1.

[2] Euractiv: *Air in Europe Contains Many Harmful Substances (in Slovak),* 2012, online: http://www.euractiv.sk/zivotne-prostredie/clanok/ovzdusie-v-europe-obsahuje-vela-skodlivych-latok-020019

[3] TISSARI, J.: *Fine Particle Emissions from Residential Wood Combustion*, online: Doctoral dissertation, Kuopio University Publications, *C. Natural and Environmental Sciences 237,* 2008. p. 63. ISBN 978-951-27-1090-4 (PDF), Finland, Kuopio 2008 < http://wanda.uef.fi/uku-vaitokset/vaitokset/2008/isbn978-951-27-0975-5.pdf>

[4] ABBOT, J., STEWART, R., FLEMONG, S., STEVENSON, K., GREEN, J., COLEMAN, P.: *Report to the Scottish Government.* Measurement and Modelling of fine particulate emission (PM10 & PM2.5) from wood – burning biomass boilers, Edinburg 2008, ISBN 978-0-7559-7296-8

[5] EPA United States Environmental Protection agency, Particulate matter, online : www.epa.gov/airquality/particlepollution/

[6] GUERREIRO, C., DE LEEUW, F., FOLTESCU, V., SCHILLING, J., VAN AARDENNE, J., LUKEWILLE, A., ADAMS, M.: *European Environment Agency, Air quality in Europe – 2012 report*, ISBN 978-92-9213-328-3

[7] EC - European commission, *Air Quality Standards*, 2013Environment – Air – Airquality. online: http://ec.europa.eu/environment/air/quality/standards.htm

[8] JANDACKA, J., NOSEK, R., PAPUCIK, S., HOLUBCIK, M.: *Analysis of the Particulate Matter Emission Measurement of Small Heat Sources by Various Methods (in Slovak),* 30. setkani mechaniky tekutin a termomechaniky.

[9] MOLNAR, L.: *Environmental Protection (in Slovak)*, 2011 online

[10] JANDACKA, J., MALCHO, M., MIKULIK, M.: *Ecological Aspects of Substitution Fossil Fuels for Biomass (in Slovak)*, 2008, ISBN 978-80-969595-5-6, Jozef Bulejcik, 01001Mojs 94

[11] CERNECKY, J., NEUPAUEROVA, A., JANOSKO, I., SOLDAN, M.: *Environment Engineering (in Slovak),* Technicka univerzita vo Zvolene, 2010, p. 274, ISBN 978-80-228-2161-2, 2010.

[12] LENHARD, R., MALCHO, M.: Numerical Simulation Device for the Transport of Geothermal Heat with Forced Circulation of Media. *Mathematical and Computer Modelling*, No. 1-2, vol. 57, 2013, ISSN 0895-7177, pp. 111-125.

[13] HUZVAR, J., NOSEK, R.: *Impact of Fuel Supply to Concentrations of Missions in Domestic Boiler,* Power control and optimization, Proc. of fourth global conference, 2010, Kuching, [S.l.: s.n.], 2010. - ISBN 978-983-44483-32.

https://doi.org/10.26552/com.C.2013.4.48-53

Juraj Machaj - Peter Brida *

SURVEY OF DEVICE CALIBRATION TECHNIQUES FOR FINGERPRINTING LOCALIZATION ALGORITHMS

In the paper device calibration algorithms for indoor positioning systems based on fingerprinting localization framework are discussed and compared. Device calibration should play important role in development of localization systems based on Wi-Fi since heterogeneous devices have different receiver parameters. This fact causes that the positioning system cannot provide position estimates with sufficient accuracy. In this paper different calibration approaches will be described and two state of art automatic calibration techniques will be compared in the simulations.

Keywords: *Indoor positioning, localization, fingerprinting, device calibration.*

1. Introduction

In the recent years many localization systems for indoor positioning were proposed and developed [1]. The main reason is that satellite navigation systems, which are widely used, are not feasible for use in the indoor environment [2]. This is caused by the fact that signals from the satellites are highly attenuated by the building walls and ceilings, so the receiver is not able to accurately estimate its position [3]. This leads many research teams to work on localization systems based on wireless technologies [4 and 5] e.g. GSM, UMTS, ZigBee, UWB and Wi-Fi.

The most popular indoor localization systems are based on Wi-Fi (IEEE 802.11b/g) technology in combination with fingerprinting approach. The main advantages are that there is no need to build new infrastructure in order to deploy the positioning system and that fingerprinting approach seems to be immune to the multipath phenomenon. Most of fingerprinting based localization systems uses RSS measurements to create a radio map and estimate position. Measurements of RSS can be performed on all devices without any additional modification [6].

However, the use of RSS measurements has one huge drawback. Due to lack of standardization of receivers each device has different parameters and antenna gain. These differences are not only caused by different hardware implemented in devices, but can be also caused by the use of different software. For the successful deployment of the localization system based on Wi-Fi and fingerprinting framework, it is important to use device calibration. Calibration should decrease negative impact of receiver differences on the functionality and accuracy of the localization system.

In this paper we will describe the state of art methods for device calibration in indoor positioning systems based on fingerprinting framework and test proposed methods in order to find optimal solution for device calibration. We assume that optimal calibration technique should provide the same positioning accuracy for different devices without interaction with the user.

The rest of the paper is organized as follows; in the next section the state-of-art fingerprinting localization algorithms will be described. In section 3 device calibration methods will be described and compared. Simulation model used for comparison of chosen calibration methods and simulation scenarios will be introduced in section 4. Results of simulations will be shown in section 5 and section 6 will conclude the paper.

2. Fingerprinting localization

The fingerprinting localization technique consists of two phases, the first phase is called offline or training phase and the second is called online phase. During the offline phase a radio map is created and stored in the database. During the online phase the position of mobile device is estimated using localization algorithm and radio map database.

A Offline phase

The radio map construction process (Fig. 1) can be divided into three main steps. The first step is to choose reference points. This can be done by dividing the area of interest into cells and choose one reference point for each cell; another very common approach is to choose reference points in the grid with fixed distance between them.

* **Juraj Machaj, Peter Brida**
Department of Telecommunications and Multimedia, Faculty of Electrical Engineering University of Zilina, Slovakia
E-mail: juraj.machaj@fel.uniza.sk

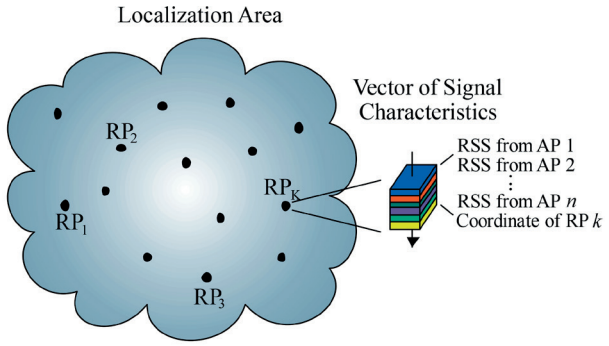

Fig. 1 Construction of radio map

The second step is measurement of RSS values from all Access Points (APs) in the radio range for a certain period of time. The measured RSS vector together with position of the reference point is called fingerprint:

$$P_j = (N_j, \alpha_{ji}, \theta_j), \quad j = 1,2,...,M\,, \tag{1}$$

where N_j is the number of j-th reference point, M is the number of all reference points, α_{ji} is the vector of RSSI values and parameter θ_j obtains additional information which can be used during the localization phase, e.g. device orientation or information about time [7].

Last step of the offline phase is to save the measured fingerprints from all reference points to the radio map database. The radio map database can be modified or preprocessed before online stage to reduce memory requirements or computational cost of localization algorithm.

B Deterministic Algorithms

In the deterministic algorithms, the state is assumed to be a non-random vector. The main objective is to compute the position estimate $\hat{x}$, which is a combination of reference points p_i, that is:

$$\hat{x} = \sum_{i=1}^{M} \omega_i . p_i \Big/ \sum_{j=1}^{M} \omega_j\,, \tag{2}$$

where all weights ω_i and ω_j are nonnegative [8]. Weights ω_i and ω_j are computed as inverted value of distance between RSS vector from the online phase and vectors stored in the radio map. Euclidean distance is commonly used as a measure between these RSS vectors.

The estimator (2), which keeps the K highest weights and sets the others to zero is called the WKNN (Weighted K-Nearest Neighbor Method) [1]. WKNN with all weights $\omega_i = 1$ is called the KNN (K-Nearest Neighbor) method. The simplest method, where $K = 1$, is called the NN (Nearest Neighbor) method [1]. KNN and the WKNN can perform better than the NN method, particularly with parameter values $K = 3$ and $K = 4$ [8].

C Probabilistic Algorithms

In the contrast to the deterministic approach in the probabilistic (or statistical) framework the state is assumed to be a random vector [8]. Let us assume that there are M location candidates ω_1, ω_2, ω_3, ..., ω_M. This means there are M classes from which the most appropriate one is the chosen based on the posteriori probability. These M locations represent reference points where RSS values were measured during the off-line phase. Vector S represents the observed RSS during the on-line stage. The location candidate ω, is chosen in case that its posteriori probability is the highest. The decision rule from Bayes' theorem can be written as:

$$P(\omega_i \mid S) = \frac{P(\vec{S} \mid \omega_i) P(\omega_i)}{P(\vec{S})}, \tag{3}$$

where posteriori probability $P(\omega_i \mid S)$ is the combination of likelihood $P(S \mid \omega_i)$, prior probability $P(\omega_i)$, and observed evidence $P(S)$. The observed evidence keeps the same during the one positioning process, and the prior probability is assumed to be the same for all over the target environment. Based on this the comparison of the posteriori probability could be considered as the comparison of likelihood.

The likelihood of each location candidate is assumed to have the Gaussian distribution. Therefore, means and standard deviations of each location candidate could be calculated from the sample data. The APs in the environment are assumed to be independent, so the overall likelihood of one location candidate can be calculated by multiplying the likelihoods of all APs:

$$P(\vec{S} \mid \omega_i) = P(S_1 \mid \omega_i) \times P(S_2 \mid \omega_i) \times P(S_m \mid \omega_i), \tag{4}$$

where m is the number of APs and S_j represents the RSS from the j-th AP [8]. In order to get more accurate results the position can be computed as average of all locations by adopting their posteriori probabilities as weights.

3. Device calibration methods

Device calibration methods can be divided into three main groups based on the calibration process. First group called manual calibration methods requires a collection of data at several known locations. Quasi-automatic calibration methods require a collection of data at unknown locations, but complex algorithms are needed to find the mapping of RSS values to reference device. Calibration methods which can automatically obtain fitting parameters based on unsupervised learning are marked as automatic calibration methods.

In the most cases differences in RSS measurement on devices are assumed to be linear and thus can be formulated as:

$$RSS_{ref} = a_x * RSS_u + b_x, \tag{5}$$

where RSS_u stands for RSS value recorded by an unknown device and a_x, b_x are parameters of linear transformation between the

unknown device and reference device. The main goal of the device calibration methods is to find the transformation parameters.

A Manual calibration

The basic idea for the manual calibration of mobile devices is to measure RSS data at the known calibration points and use these data to find a transformation function between the user device and reference device used for the radio map construction.

Vaupel et al. [9] introduced a manual calibration method which was used during the development of their localization system. Measurements in an anechoic chamber were used to find offset of RSS measured on different devices. RSS measurement offset $b_{x,i}$ for device x and AP i was calculated as:

$$b_{x,i} = mean(RSS_{ref,i}) - mean(RSS_{x,i}), \tag{6}$$

After measurements for all AP in every direction the measurement offsets were combined using all N offsets:

$$b_x = \frac{1}{N}\sum_{i=1}^{N} b_{x,i}, \tag{7}$$

Measurements from the different directions and different APs were performed due to imperfect omni-directional antenna characteristics of the antennas used in devices and non-linear scaling of the Wi-Fi cards within the measurement range.

In [10] Haeberlen et al. proposed a manual calibration scheme. In this scheme the calibration measurements are performed at several different reference points. The measurements are performed manually and after the device collects a few scans the user must indicate the current reference point on a floor plan of the building. The calibration function is then computed by applying least-squares method.

B Quasi-automatic calibration

It is clear that even manual calibration methods are effective, but they have the disadvantage of requiring the user to perform measurements at a known position. However, calibration can be performed even without this information, based only on calibration measurements. Calibration methods, which use only calibration measurements, are called quasi-automatic.

In [10] authors propose the use of a calibration method using least-squares algorithm to estimate the transformation function without a known position of the user during calibration measurements. This solution is based on assumption that there is no linear mapping between observations from different positions. Based on this assumption it is given that if the chosen reference point is incorrect, the confidence value of Markov localization is low for all reference points. Algorithm must choose reference point in a way that the confidence value is maximized.

Kjaergaad proposed a quasi-automatic calibration method based on least-squares method in [11]. Since in quasi-automatic calibration the measurement positions are unknown the measurements have to be compared to the measurements from all possible reference points. Two methods were proposed to be used in a way to determine position of the user during the calibration measurements. The first method was Bayesian localization with observations from an unknown location and the second method is a comparison method which tries to match the means and standard deviations of the observation with measurements in the radio map.

C Automatic calibration

It is clear that no interaction with the user during the calibration process is a huge advantage of quasi-automatic calibration methods. This is even more obvious in the case that the user is located in the area he is not familiar with. On the other hand, quasi-automatic calibration requires a high number of measurements and use of complex algorithms to calibrate the user device. This was the main reason for development of automatic calibration methods which can calibrate the user device in background during the positioning and navigation process.

The automatic calibration method was proposed in [12]; the authors proposed to compute a log-normalized ratio to reduce the effect of RSS shift between the reference device and the user device. The log-normalized ratio is computed as:

$$lnr(o_i, o_j) = \log(r(o_i, o_j)) - \log\left(\frac{1}{v_{\max}}\right), \tag{8}$$

where $r(o_i,o_j)$ is the ratio of RSS measured from two access points AP_i and AP_j and v_{max} is the maximum signal strength value. The ratio of RSS is calculated for all pairs of AP with constraint $i > j$ for uniqueness. According to [13] this solution approximates only the ratio, but it cannot handle the offset term in a linear shift function. So it is assumed that the approximation error is increased when the offset term is relatively large.

Unsupervised learning approach, which should improve the approximation error for both ratio and offset terms of the linear shift function, was proposed in [13]. The proposed method can automatically learn a signal-pattern transformation function for any unknown device. The learning procedure can be divided into two general steps. In the first step RSS readings from the tracking device are labeled with rough location estimate using the correlation ratio computed from Pearson product-moment correlation coefficient defined by:

$$r = \frac{\sum_{i=1}^{k}\left(\left(s_c^i - \mu(s_c)\right)\left(s_o^i - \mu(s_o)\right)\right)}{\sqrt{\sum_{i=1}^{k}\left(s_c^i - \mu(s_c)\right)^2}\sqrt{\sum_{i=1}^{k}\left(s_o^i - \mu(s_o)\right)^2}}, \tag{9}$$

where k is the number of APs, s_c represents the RSS of the training device from the radio map, μ is the mean or expected value of a random variable, and s_o is the RSS fingerprint from the users device. Pearson correlation is used to measure similarities in the RSS fingerprints. If the value is 0, the vectors are completely linear independent and if the absolute value of correlation is 1, there is the best linear dependency between fingerprints. After labeling the RSS data with rough location estimates, four learning algorithms were applied to train the transformation function.

Koski et al. in [14] proposed a coverage area positioning scheme and calibration method using RSSI histograms. The idea is to create a histogram of the RSS values over a long time interval. The calibration is based on the fact that the shape of histograms for the different mobile devices has similar shapes, thus parameters of distribution such as mean, median or mode are comparable.

In [15] Laoudias et al. proposed an automatic self-calibration method based on the RSS histograms. In this method calibration is performed during the positioning process. In the first step the existing radio map is used to create a histogram of the reference device, from the RSS data stored in the database. Subsequently, when the positioning process starts, the RSS values of currently observed fingerprint are recorded in background in order to create and update the histogram of RSS values for the device. A linear mapping function between histogram from the radio map and positioning process is calculated for the user device. The linear mapping function is then used to transform the measured RSS values to a new fingerprint which is compatible with radio map.

4. Simulation model and scenarios

Simulations were performed in a simulation model created in Matlab environment. In the simulation model the RSS is modelled by two independent parts: path-loss and immediate variations of signal strength. Path-loss is based on a multi-floor-and-wall propagation model (MFW). The MFW model considers the nonlinear relationship between the cumulative penetration loss and the number of penetrated floors and walls. The total loss L_{WMF} in distance d can be computed from equation:

$$L_{MWF} = L_0 + 10n\log(d) + \sum_{i=1}^{I}\sum_{k=1}^{K_{wi}} L_{wik} + \sum_{j=1}^{J}\sum_{k=1}^{K_{fj}} L_{fjk}, \quad (10)$$

where L_0 is the path loss in distance of 1m in dB, n is the power decay index, d is the distance between the transceiver and receiver in meters, I is the number of walls types, K_{wi} is the number of traversed walls of category i, L_{wik} is the attenuation due to wall type i and k-th traversed wall in dB, J stands for the number of floor types, K_{fj} is the number of traversed walls of category j and L_{fjk} represents the attenuation due to wall type i and k-th traversed wall in dB.

Immediate variations of the signal strength could be caused by objects motion at the observed area. These variations influence the RSS measurements and add measurement error. The behavior of the variations was derived from experimental measurements. The measurement error is simulated using random variable with lognormal distribution.

The localization was performed at an area of 512 square meters. Reference points were chosen in grid with 2 m distance between them. The localization area can be seen in Fig. 2. In the figure blue lines represents walls of the building, grey x represents the position of APs and red dots show the position of the reference points. The position of mobile device was randomly chosen from the area.

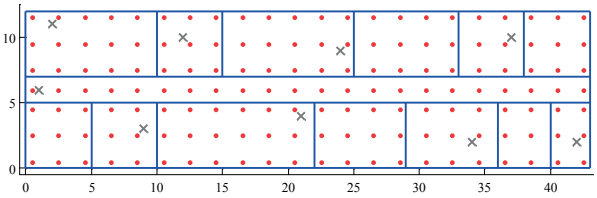

Fig. 2 Localization area

Each fingerprint was created by 20 measurements for a particular AP in very short time on each reference point. The average RSS was calculated from these measurements for every point to eliminate signal fluctuations. Simulations were performed with 1000 independent trials, i.e. for 1000 positions of the mobile device. In the simulations K=4 was used for WKNN algorithm.

In the simulations a change of the mobile device was simulated by four different conditions. In the ideal case the RSS values were computed in the same way in both the offline and online phases. Lists of different mobile changes and formulas used to affect the RSS are shown in Table 1.

Device change parameters in simulations Table 1

Type of signal change	Relationship to RSS_{ref}
Shift	$RSS_x = RSS_{ref} + G$
Scale	$RSS_x = A * RSS_{ref}$
Shift and scale	$RSS_x = A * RSS_{ref} + G$
Nonlinear	$RSS_x = -1\left\lvert \frac{RSS_{ref}^{2.57}}{RSS_{ref} * X} \right\rvert$

In the table RSS_x represents the RSS received by the uncalibrated device, RSS_{ref} stands for the RSS received by the reference device, G is the additional gain of antenna in dB and in simulations was set to 5 dB. Variable A which represents the amplification ratio of the uncalibrated device was set to 0.8 and X is the coefficient which affects nonlinear transformation of the RSS signal and was set to 12.

In simulation two automatic calibration algorithms were used to remove the impact of device change. The first algorithm was proposed in [12] and in simulation was marked as log-normalization, the second used algorithm was proposed in [15] and we will refer to it as CDF calibration.

5. Simulation results

Results of the simulations are shown in this section. In Fig. 3 the results show the impact of different device changes on localization algorithms and calibration techniques.

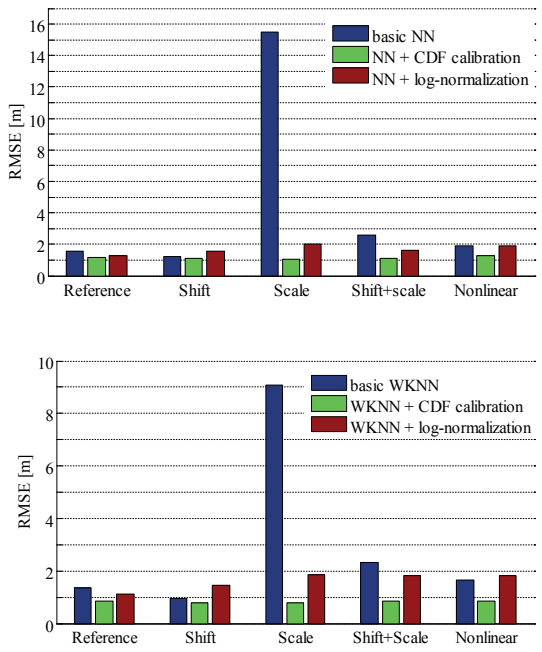

Fig. 3 Impact of device change on calibration and localization accuracy

From the figure it is clear that the worst impact on the positioning accuracy has a scale of device receiver, in other words, differences in antenna gain of different devices. From the results it is also clear that the CDF calibration technique seems to be the most feasible one for a fingerprinting positioning framework. This calibration technique keeps the localization accuracy at the same level in all cases. More detailed results can be seen in Table 2.

From the results it can be seen that the CDF calibration method outperforms calibration via log-normalization in all cases and helps to achieve lower error compared to the fingerprinting positioning without calibration. On the other hand, the log-normalization method achieved the results comparable to the fingerprinting without calibration, but significantly decreased error when the devices have a different scale.

6. Conclusion

In the paper the methods for calibration of a mobile device for positioning using a fingerprinting framework were described and compared. The calibration algorithms can be divided into three main groups. The first group consists of manual calibration algorithms, which can achieve the best results, but they have the huge disadvantage in need to perform a large number of measurements at known positions.

In the second group so-called quasi-automatic methods for device calibration can be found. These methods do not need to perform measurements at known positions, but they require a large number of measurements and high complexity algorithms to find a transformation function for the device calibration.

The last group consists of automatic calibration methods. These are running in background of the positioning process. Their main advantage is that there is no need of additional calibration measurements. On the other hand, some of them may need some time to achieve the performance of manual calibration methods. From the simulation it is clear that the automatic calibration technique proposed in [15] significantly reduces the impact of a device change.

Simulation results

Table 2

		Localization Error [m]							
		Median	STD	Median	STD	Median	STD	Median	STD
Basic	NN	1.0685	0.7755	5.4453	14.9938	2.2882	2.2521	1.7675	0.9950
	KNN	0.9433	0.5544	5.3506	9.8282	1.9573	1.8299	1.6546	0.8580
	WKNN	0.8870	0.5254	5.1950	8.7852	1.9027	1.9213	1.5277	0.9201
CDF calibration	NN	0.9856	0.6441	0.9637	0.6394	0.9805	0.6641	1.1464	0.6930
	KNN	0.8291	0.4642	0.8490	0.4764	0.9112	0.4981	0.8882	0.5177
	WKNN	0.7436	0.4296	0.7472	0.4273	0.7924	0.4592	0.7970	0.4594
Log-normalization	NN	1.2831	1.0080	1.7139	1.5758	2.2116	1.6373	1.7580	1.4022
	KNN	1.3104	0.8800	1.6358	1.5082	2.0608	1.7860	1.7860	1.4086
	WKNN	1.3190	0.8852	1.6090	1.6399	2.0703	1.8118	1.7765	1.3452
Device change type		Shift		Scale		Shift+scale		Nonlinear	

Acknowledgements

This work has been partially supported by the Slovak VEGA grant agency, Project No. 1/0394/13, by

„Broker centre of air transport for transfer of technology and knowledge into transport and transport infrastructure ITMS 26220220156"

We support research activities in Slovakia/Project is co-financed by EU

and by

Centre of excellence for systems and services of intelligent transport II., ITMS 26220120050 supported by the Research & Development Operational Programme funded by the ERDF.

"Podporujeme výskumné aktivity na Slovensku/Projekt je spolufinancovaný zo zdrojov EÚ"

References

[1] SAHA, S., CHAUHURI, K., SANGHI, D., BHAGWAT, P.: Location Determination of a Mobile Device using IEEE 802.11b Access Point Signals, *Wireless Communications and Networking*, WCNC 2003. vol. 3. pp. 1987-1992, ISBN: 0-7803-7700-1, 2003

[2] BRIDA, P., MATULA, M., DUHA, J.: Using Proximity Technology for Localization in Wireless Sensor Networks, *Communications - Scientific Letters of the University of Zilina*, No. 4, vol. 9, 2007, pp. 50-54, ISSN 1335-4205.

[3] KOTZIAN, J., KONECNY, J., KREJCAR, O., LIPPA, T., PROKOP, H., KURUC, M.: *The Indoor Orientation of Autonomous Mobile Devices for Increasing Human Perspective*, Mobilight Workshops 2010, LNCIST. Springer, Heidelberg, ISBN 978-3-642-16643-3, 2010

[4] HAJOVSKY, R., PIES, M.: Complex Measuring System for Longtime Monitoring and Visualization of Temperature and Toxic Gases Concentration, *ELEKTRONIKA IR ELEKTROTECHNIKA,* No. 6, vol. 122, 2012, pp. 129-132. ISSN 1392-1215.

[5] SROVNAL, V., JR., MACHACEK, Z., SROVNAL, V.: *Wireless Communication for Mobile Robotics and Industrial Embedded Devices*, 8th Intern. Conference on Networks ICN, Gosier, France. 2009, pp. 1-6, ISBN 978-1-4244-3470-1

[6] CIPOV, V., DOBOS, L., PAPAJ, J.: Cooperative Trilateration-based Positioning Algorithm for WLAN Nodes Using Round Trip Time Estimation, *J. of Electrical and Electronics Engineering*. No. 1, vol. 4, 2011, pp. 29-34, ISSN 1844-6035, 2011

[7] BRIDA, P., BENIKOVSKY, J.: *Radio Map Framework for GSM Positioning*, *Communications - Scientific Letters of the University of Zilina*, No. 4, vol. 11, 2007, pp. 24-27, ISSN 1335-4205, 2007

[8] HONKAVIRTA, V., PERALA, T., ALI-LOYTTY, S., PICHE, R.: *A Comparative Survey of WLAN Location Fingerprinting Methods,* 6th Workshop on Positioning, Navigation and Communication 2009, WPNC 2009, pp. 243-251, ISBN: 978-1-4244-3292-9, 2009

[9] VAUPEL, T., SEITZ, J., KIEFER, F., HAIMERL, S., THIELECKE, J.: *Wi-Fi Positioning: System Considerations and Device Calibration*, 2010 intern. conference on Indoor Positioning and Indoor Navigation (IPIN), pp.1-7, 2010

[10] HAEBERLEN, A., FLANNERY, E., LADD, A. M., RUDYS, A., WALLACH, D. S., KAVRAKI, L. E.: *Practical Robust Localization over Large-scale 802.11 Wireless Networks*, 10th intern. Conference on Mobile computing and networking (MobiCom), pp. 70-84, 2004

[11] KJAERGAARD, M.: *Automatic Mitigation of Sensor Variations for Signal Strength Based Location Systems*, LoCA'06 Proc. of the 2nd intern. conference on Location- and Context-Awareness pp. 30-47, 2006.

[12] KJAERGAARD, M. B., MUNK, C. V.: *Hyperbolic Location Fingerprinting: A Calibration-free Solution for Handling Differences in Signal Strength,* VI Annual IEEE Intern. Conference on Pervasive Computing and Communications, pp. 110-116, 2008

[13] TSUI, A. W., CHUANG, Y.-H., CHU, H.-H.: *Unsupervised Learning for Solving RSS Hardware Variance Problem in WiFi Localization, Mobile Networks and Applications*, No. 5, vol. 14, 2009, pp. 677-691

[14] KOSKI, L., PERALA, T., PICHE, R.: *Indoor Positioning using WLAN Coverage Area Estimates*, 2010 intern. conference on Indoor Positioning and Indoor Navigation (IPIN), pp.1-7, 2010

[15] LAOUDIAS, C., PICHE, R., PANAYIOTOU, C. G.: *Device Signal Strength Self-calibration using Histograms*, 2012 Intern. Conference on Indoor Positioning and Indoor Navigation (IPIN), pp.1-8, 2012.

https://doi.org/10.26552/com.C.2013.4.54-57

COMMUNICATIONS

Magdalena Mazur - Robert Ulewicz - Frantisek Novy - Pawel Szataniak *

THE STRUCTURE AND MECHANICAL PROPERTIES OF DOMEX 700 MC STEEL

Nowadays fine-grained, quench and tempered steels are more and more used in design of modern semitrailers constructions. High mechanical properties and durability of this type of steel are its advantage. This paper summarizes the results of research together with the data available by the manufacturer SSAB company. The combination of the special features provided by this material enables construction of lighter semitrailer's components, which would result in a semiauto with a lower weight of its own. This paper presents the results of mechanical properties of Domex 700 MC steel.

Keywords: *High strength steels, Domex steel, impact test, impact energy, semitrailers.*

1. Introduction

Increased competition in the market of semitrailers forces manufacturers to design new solutions and use new materials. Analyzing the products of leading manufacturers of semitrailers including products of Wielton S.A., we observe the tendency to use steel characterized by increased resistance to abrasion of easy weldable steels such as steel Hardox. The materials are also used to apply solutions to reduce the weight of the trailer. All these treatments aim to increase the technical objects lifetime.

Based on research realized by Wielton S.A. we can form a list of requirements for materials used for construction of semitrailers with particular emphasis on the requirements posed by the construction of tippers. Such materials must feature: a very high resistance to abrasion, the ability to transfer variable workloads, uniform properties throughout the cross-section of the element as well as susceptibility to create joints with use of standard welding techniques, and easy cold forming.

2. Characteristics of Domex steel

Domex cold forming steels are rolled in a thermomechanical process where the heating, rolling and cooling are carefully controlled. The chemical composition of the steel containing low levels of carbon and manganese is precisely complemented by enriching ingredients such as niobium, titanium and vanadium.

Due to its high mechanical properties and clean structure, the Domex steel is the best alternative for cold formed and welded products. Domex 700 MC steel with designation D and E meet and even exceed the requirements for steel S700 MC according to the standard EN-10149-2 [1]. Domex MC steel can be supplied as wide coil, split coil and cut sheet. The steels are applicable with rolled and pickled as well as oiled surface. Wide coil and sheet are available with milled or cut edge.

Extra high strength steels are used in structures such as truck chassis, cranes and excavators. In these applications, high strength steel is used in order to reduce weight while simultaneously increase load capacity of the structure. These advantages, combined with good formability allow the reduction of total costs. Due to the low content of carbon, phosphorus and sulfur Domex 700 MC steel can be welded by all commonly used methods without requirement of preheating. A narrow heat-affected zone is formed on the border of the weld. This zone is characterized by slightly lower hardness. However, using the normal parameters and methods of welding this zone is of no practical importance. Tested specimens taken across the weld can have the same minimum value of tensile strength, which also characterizes the welded material. If the load of the weld is not high, it can be used to add metal with a lower strength than the weld material. There are a large number of filler metals with the same or higher strength, which can be used for welding of Domex 700 MC steel, while maintaining the same filler metal strength as welded material [2 and 3].

Advantages of using Domex steel:

- reduced weight of steel construction while maintaining loading capacity,
- very good weldability due to low alloy content; resistance to hot and hydrogen cracks,
- good bendability at small radii without risk of cracks,
- good formability facilitating press-forming,
- applicable for shear cutting and plasma cutting,
- smooth and straight edges after laser.

* **Magdalena Mazur[1], Robert Ulewicz[1], Frantisek Novy[2], Pawel Szataniak[3]**
[1] Institute of Production Engineering, Czestochowa University of Technology, Poland
[2] Department of Materials Engineering, University of Zilina, Slovakia
[3] WIELTON S.A., Wielun, Poland
E-mail: mazur.m@zim.pcz.pl

COMMUNICATIONS

Chemical composition and mechanical properties of Domex 700 MC steel Table 1

Chemical composition max. [in weight %]								
C	Si	Mn	P	S	Al	Nb	V	Ti
0.12	0.10	2.10	0.025	0.010	0.015	0.09	0.20	0.015
Mechanical properties								
Re [MPa]			Rm [MPa]			A5 [%]		
700			750 - 950			12		

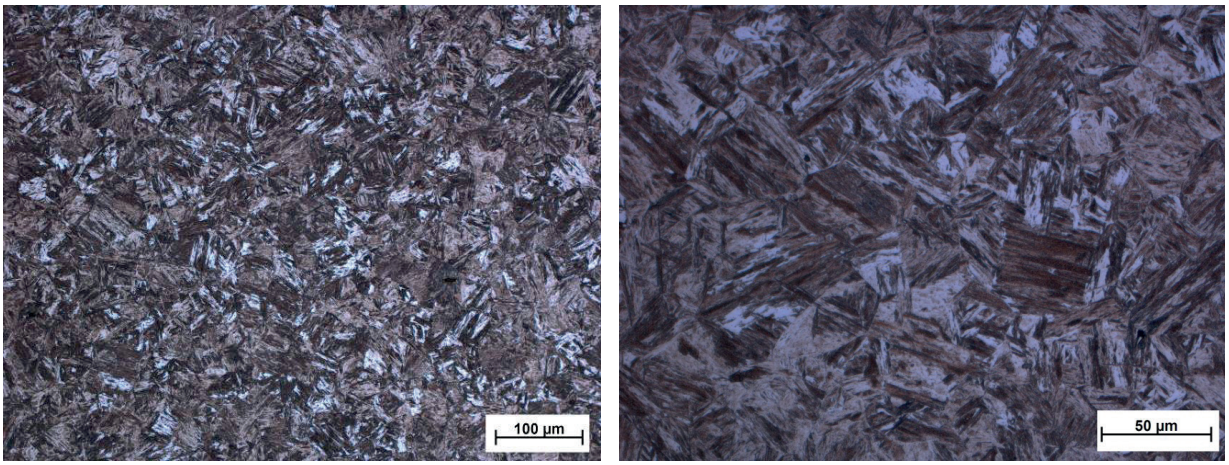

Fig. 1 Microstructure of the Domex 700 MC steel

Domex corrosion resistant steel can be used in products as e.g. containers where high strength and resistance to corrosion reduces the need for maintenance, prolongs life and simplifies production. The material also offers major benefits for industrial chimneys, both externally and in the flue gas passages, since the corrosion-resistant steels can cope well with sulphurous environments. In addition to good resistance to corrosion, Domex corrosion resistant steel is also characterized by good formability, weldability and impact strength. It is produced in two strength levels and the guaranteed minimum yield strengths are 550 MPa and 700 MPa.

3. Mechanical properties of Domex 700 MC steel

Domex is a micro-alloy steel with addition of niobium, titanium and vanadium, which allows for maintaining low level of carbon and manganese content. Advanced technological production processes guarantee the steels' clean structure (Fig. 1). The tested steel had a martensitic structure, with clear needles arranged in cells [4 and 5]. Table 1 shows the chemical composition and mechanical properties of Domex 700 MC steel.

4. Impact test of Domex 700 MC steel

Construction elements are very often exposed to dynamic loads. For this reason, there is a need to know the properties that characterize the behavior of the material in case of sudden changes in load. Mainly fatigue and impact tests are used to determining these properties. Impact tests allow exploring the impact toughness and, at the same time, they allow checking the quality of heat treatment, in regard to tendency of the material to aging and defining the resistance against to the brittle fracture. In practice, the most common is the Charpy impact test [6 and 7].

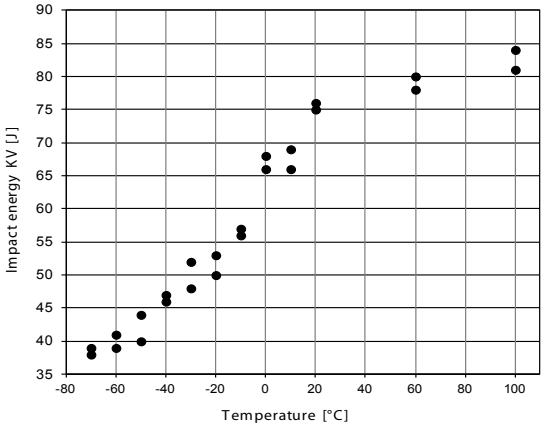

Fig. 2 Impact energy v/s temperature for Domex 700 MC steel

COMMUNICATIONS

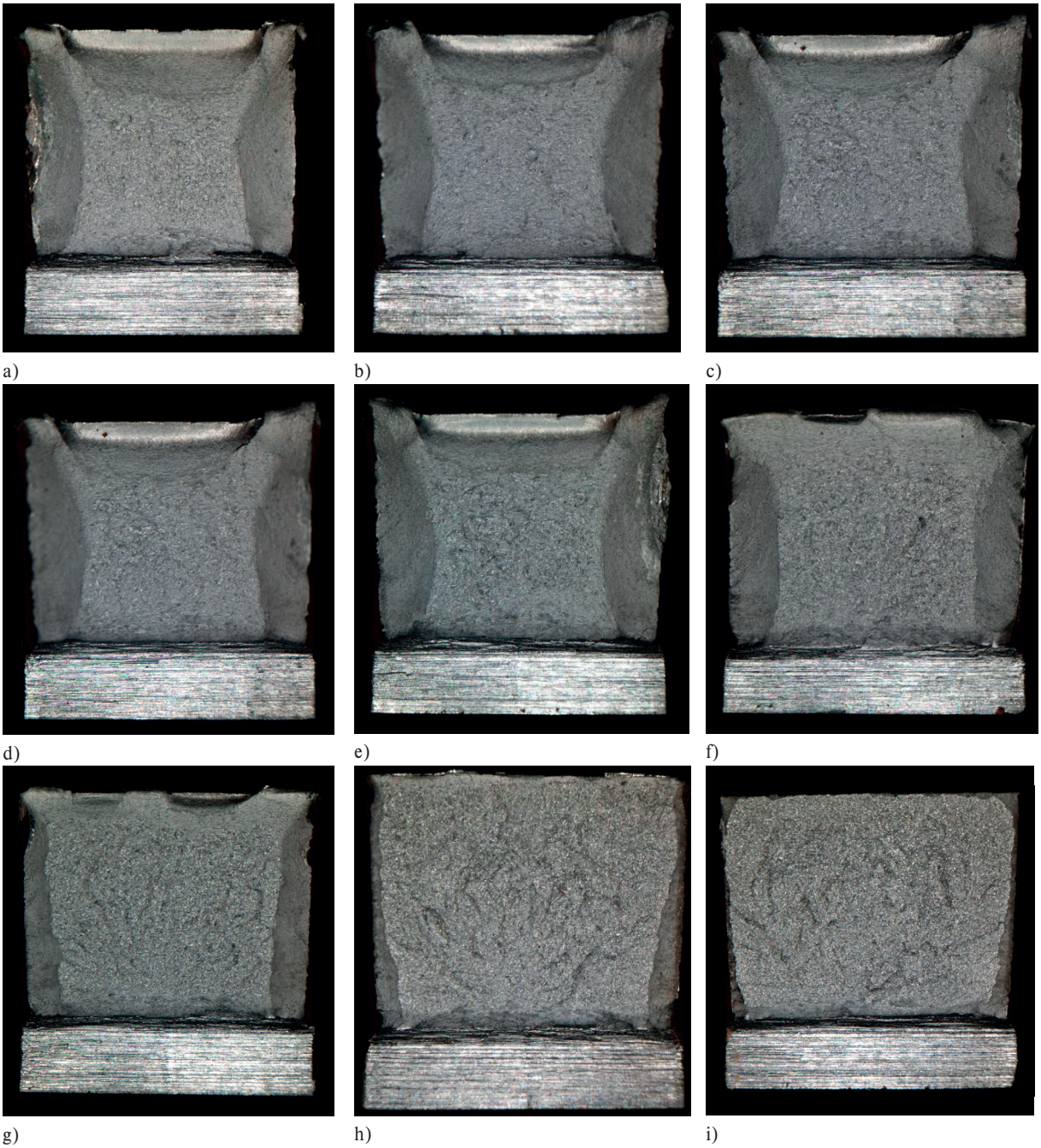

Fig. 3 Fracture morphology of the specimens broken at temperature: a) +100°C, b) +20°C, c) +15°C, d) +10°C, e)0°C, f) -10°C, g) -30°C, h) -50°C, i) -70°C

Impact tests were performed in order to assess behavior of the material under conditions leading to brittle fracture. Semitrailers are commonly working in a wide temperature range. In general, lower temperature increases the material tendency to brittle fracture and this is the reason why impact test were performed in temperature range from -70 °C up to + 100 °C with use of 24 specimens. For testing at different temperatures, the specimens were immersed in a cooling medium or heated in the oven for a time necessary to obtain required temperature in the whole volume of the specimen. Standard specimens for Charpy impact test (a length of 55 mm and a square cross-section of 10 mm side length) were used. In the centre of specimens was made a V-shaped notch, with an angle of 45 °, a depth of 2 mm and the rounding radius of the bottom of 0.25 mm. The impact tests were done using the Standard Charpy impact equipment, swinging with

COMMUNICATIONS

a constant energy resource potential. The results obtained during the experiment are shown in Fig. 2.

5. Summary

The determination of the temperature effect on material properties, mainly the tendency to brittle fracture at low temperatures is very important for safety design of components working at temperatures below 0 °C. Impact tests greatly reflect the material behavior under different temperatures and after systematic analysis it is possible to find the threshold, where material rapidly loses its ductility. The results obtained for Domex 700 MC steel show that the impact energy KV = 75 J obtained at the temperature of 20 °C drops down to KV = 38 J at the temperature of – 70 °C. Comparing the obtained results with the material data specified by the manufacturer can be said that in the temperature range from -20 °C to -40 °C were obtained higher values of impact energy than are listed in the material datasheet. Based on the fracture morphology (Fig. 3) it can be observed that with decreasing temperature, the fracture mechanism changes from ductile to quasi cleavage manner [8]. As the temperature decreases, the ratio between the ductile and brittle fracture changes and bigger part of the fracture surface is formed by brittle fracture.

Increase of production and optimization of operating costs is the main interest of every manufacturer. This is why they pay great attention to obtain the highest level of components durability and safety. In the search for new design solutions, there is a great requirement for new materials with higher mechanical properties than the conventional ones [9 and 10]. Later in research, the obtained steel characteristics will be the basis for determination of other material properties and specification of components which can be produced from this steel in WIELTON S.A semitrailers [11].

Acknowledgement

This research was supported by the grant program „DoktoRIS - Scholarship program for innovative Silesia“ co-financed by the European Union under the European Social Fund and partially by the Scientific Grant Agency of the Ministry of Education, Science and Sports of the Slovak Republic and Slovak Academy of Sciences, grant No. 1/0743/12 and by APVV, project SK-RO-00088-12.

References

[1] WIELTON, S. A.: *Company Information Data (in Polish)*, Wielun 2011.
[2] MAZUR M., ULEWICZ, R., BORKOWSKI, S., NOVY F. *Properties of Steel Used in the Production of Semi-Trailers Car.* W: SEMDOK 2012. 17th Intern. of PhD. Students‘ Seminar, 2012, Zilina - Terchova, 2012.
[3] SZATANIAK P., ULEWICZ, R., NOVY, F., MAZUR M., TOROKOVA, A.: *New Materials and Requirements for Construction Materials Applied to Car Semitrailers*. W: Advanced Manufacturing and Repair Technologies in Vehicle Industry, 29th Intern. Colloquium, Zilina - Terchova, Slovakia. EDIS – University of Zilina, 2012
[4] TILLOVA, E., CHALUPOVA, M.: Solution Treatment Effect on Microstructure and Mechanical Properties of Automotive Cast Alloy. *Materials Engineering/Materialove inzinierstvo*, vol. 19, No. 2, 2012, pp. 39-46.
[5] MIKOVA, K., NOVY, F., TRSKO, L., BOKUVKA O.: *Fatigue Life of Micro-alloyed Steels for Pipelines Intended to Transport Natural Gas (in Slovak)*, SEMDOK 2012, 17th Intern. of PhD. Students‘ Seminar, Zilina - Terchova, pp. 193-196, EDIS - University of Zilina, 2012.
[6] WYRZYKOWSKI, J. W., PLESZAKOW, E., SIENIAWSKI, J.: *Deformation and Cracking of Metal (in Polish)*. Wydawnictwo Naukowo-Techniczne, 1999.
[7] SKOCOVSKY, P., BOKUVKA, O., KONECNA, R., TILLOVA, E.: *Theory of Materials Science for Departments of Mechanical Engineering (in Slovak)*, EDIS – University of Zilina, 2001.
[8] ZEMANDL, M.: Fractography of Fatigue Fracture and its Practical Use in the Analysis of the Causes Machine Elements Failure *(in Czech)*, Summer school of fatigue ‘2006, EDIS – University of Zilina, 2006.
[9] KONSTANCIAK, M.: *Analysis of Technological Strategies on the Example of the Production of the Tramway Wheels*, Archives of Materials Science and Engineering, No. 2, vol. 57, 2012, pp. 69-74.
[10] DIMA, I. C., GRZYBOWSKI, A., GRABARA, J.: Statistical Modeling of the Mechanical Properties of the Heavy Steel Plates - Dealing with the Ill Conditioned Data. *Metalurgia International*, No. 1, vol. 18, pp. 11-14, ISSN: 1582-2214
[11] ULEWICZ, R., MAZUR, M., NOVY, F., SZATANIAK, P. *Fatigue Properties of Selected Grades of Steel Used for Main Components of Semitrailers and Agricultural Machines*. W: Advanced Manufacturing and Repair Technologies in Vehicle Industry, 29th Intern. Colloquium, 2012, Zilina - Terchova, pp. 64-70, EDIS - University of Zilina, 2012.

https://doi.org/10.26552/com.C.2013.4.58-62

Michal Titko - Adam Zagorecki *

MODELLING VULNERABILITY OF TRANSPORTATION NETWORK USING INFLUENCE DIAGRAMS

The transportation network (TN) is important to serve the national priorities such as economic sustainability and growth, but it as well plays important role in disaster management and is subject to hazards. The understanding of the TN resilience and vulnerabilities is important for the national security. In this work we focus on the notion of TN vulnerability. We propose the use of a decision-theoretic approach based on Influence Diagrams (IDs). We argue that the use of IDs (1) provides an improved framework for risk assessment through more elaborate combining probabilities and consequences, and (2) facilitates knowledge elicitation from human experts through a structured approach to the problem. The proposed methodology is intended to be applied to the critical infrastructure.

***Keywords**: Vulnerability, transportation, critical infrastructure, influence diagrams.*

1. Introduction

The recent years have witnessed several examples of the transportation infrastructure being affected by extreme natural hazards such as the earthquake in Kobe (1995) and hurricane Katrina (2005) as well as man-made threats such as terrorist attacks (Madrid 2004, London 2005) or industrial accidents [1]. Even, if the transportation infrastructure is not directly affected during such incidents, it plays critical role in providing security for public as it plays key role in delivering disaster relief, or facilitating mass evacuations. Some parts of the transportation network are more important than the others, resulting in identification of the notion of critical infrastructure – a subset of the transportation infrastructure that is of the particular importance and interest.

The transportation network (TN) is important to serve the national priorities such as economic sustainability and growth, social development, providing security and public order, operational capability of the armed forces, etc. Analysis of TN should always be viewed in a broader context – with relation to geo-spatial, industrial, social context, etc. Reliability and performance of TN have significant influence on services which are provided by the other sectors, and in many instances TN spans these sectors. Therefore, the understanding of the TN weak points and its resilience to disasters is important in general, and in particular critical for the national security.

In this work we focus on the notion of TN vulnerability. Understanding vulnerability is not only essential to disaster management, but also important in transportation planning, development, and management. Berdica [2] argues that reducing vulnerability can hence be regarded as reducing risks involved in various incidents. We can interpret vulnerability as the measurement of the degradation or loss of TN's functions, but as we will discuss it, the exact definition is a subject of active academic debates.

In this paper we use a decision-theoretic approach based on Influence Diagrams (IDs) as a tool for model vulnerability. We argue that the use of IDs can address two important aspects of vulnerability modelling: (1) provide an improved framework for risk assessment through more elaborate combining probabilities and measures of consequences than it is the case in current approaches, and (2) facilitate knowledge elicitation from human experts through a structured approach to the problem.

2. Relevant work

The key function of a TN is to provide means to move people and goods between the origin and destination, usually by optimizing the transport costs. Typically transportation network infrastructure is modelled as a graph where links represent connections between two points and nodes represent hubs.

The elements of the graph have typically some attributes associated with them that are intended to represent properties of the elements of the TN such the number of lanes, average number of vehicles per day, etc. Such models can be used to simulate different disruptions and predict how the TN would respond to those conditions. Consequences resulting from the disruption of the transport element can vary depending on many factors such as network topology, properties of particular network element, the population characteristics around it, likelihood of disruptive events, etc. In ordinary cases TN has certain capacity to absorb some degree of disruptions. When larger scale events such as natural disasters are considered, there is possibility of more extreme effects on network infrastructure, including its partial

* [1]Michal Titko, [2]Adam Zagorecki
[1]Department of Crisis Management, Faculty of Special Engineering, University of Zilina, Slovakia, E-mail: Michal.Titko@fsi.uniza.sk
[2]Cranfield University, Department of Informatics and Systems Engineering, Defence Academy of the United Kingdom, United Kingdom

failure. In recent years it has been of interest of academic and practitioners' communities to quantify these effects. Eventually, the concept of *vulnerability* has been introduced.

There is no consensus on the definition of vulnerability in the context of TN. One can define the vulnerability as overall susceptibility to a specific hazardous event. It is also the magnitude of the damage given the occurrence of that event [3]. Some authors [4 and 5] argue that a system might be vulnerable to certain events but be resilient to others; therefore, it is important to account for the specific risk and threat profiles to the area under analysis.

There is common agreement that the vulnerability in the context of TN represents a measure of loss of the TN's capabilities to perform its functions [2 and 6 - 9]. However, there are individual interpretations. According to Taylor and D'Este's a vulnerable network node is such a node for which a loss (or substantial degradation) of a small number of links significantly diminishes the accessibility of the node. Their model described in [6] is used as the basis for the probabilistic algorithm for the choice of certain section by a passenger (carrier). Model is based on the definition of the vulnerability which can be simplified as: in case the "best" route is not available, how much worse (more expensive) would the second best option be than the third one and so on. Berdica [2] defines vulnerability as susceptibility of TN to incidents that can result in considerable reduction in TN serviceability. Yang, Qian developed a method for the assessment of TN vulnerability using the users' final lost time as measurement [7]. Jenelius et al. [8] focused on the socio-economic impacts of transport network dysfunction. This approach represents an effort to express the vulnerability of the transport network using the measure of satisfaction of the demand for transport services at the time when a section of the network is unavailable. Husdal [9] defined vulnerability as the consequential cost of the lack of reliability, and this consequential cost must compromise not only the immediate toll on the network-users, but the overall socio-economic costs on the community that this vulnerability would entail.

One of the interpretations of vulnerability in the transportation context is closely related to reliability. Linking these two concepts should give the means to define vulnerabilities as costs resulting from a lack of reliability [2, 6, 8 and [9] and in our work we follow this trend. In wider interpretation, reliability can be regarded as a complement of vulnerability. Berdica [2] proposed the following definition: vulnerability in road transportation system is reliability, meaning adequate serviceability under the operating conditions encountered during a given time period. Between vulnerability and reliability are certain differences which could be expressed as follows: appropriate measures to improve reliability may not have to be suitable to reduce the vulnerability. Vulnerable does not have to imply unreliable and vice-versa.

The concept of vulnerability is more often understood as the consequences of link failure, irrespective of the probability of the failure. In some cases, link failure may be unlikely but the resulting impact on the community may be devastating [6]. Slivone [10] claims that ignoring the probability of failure is justified, as in some instances producing probabilities for some events are virtually impossible (warfare, sabotage, terrorist attack, etc.). However, as was argued, vulnerability must be related to specific hazardous events and, therefore, ignoring the event's probability deprives the definition from an important element, as it is the likelihood of events that often differentiates more vulnerable areas from those less vulnerable.

The aim of vulnerability assessment is not to provide overall value of the vulnerability measure of the TN as a whole but to identify the weak points (most vulnerable) of the network. If one wants to analyse vulnerability of the TN it is necessary to divide the network into atomic elements – links and nodes for which the vulnerability scores would be determined. The patterns of connectivity for the TN are also important for modelling of the TN. Simple example of TN is shown in Fig. 1.

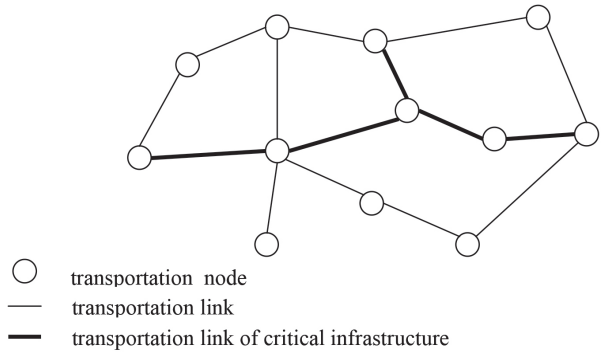

Fig. 1 Simple example of transportation network

To provide practical value of the vulnerability analysis it is important to identify to what type of events or threats TN's element is vulnerable. In general, the TN can be vulnerable to a wide range of influences and disruptions that can lead to an operational degradation. They can be the results of changes in environmental conditions or qualities pertaining to the network characteristics. One applicable categorisation of influences to TN is offered by Brathen and Laegran [11]: *structure*, *nature*, *traffic*, and *malevolence*.

Structure-related influences pertain to the way the infrastructure is built, and attributes of the network itself - in terms of topology, and connectivity. It also captures factors such as the physical body of the road, geometry, width, curvature, gradient, tunnels, bridges, access restrictions for certain vehicle types, etc. Nature-related influences relate to adverse natural processes, such as flash floods, avalanches, falling rocks, snow and ice, fog, earthquakes, tsunamis, etc. Traffic-related influences pertain to attributes describing the generic flow of traffic such as traffic accidents, maintenance operations, construction works and civil emergencies [11]. Malevolence related influences pertain to the intentional man-induced disruption of the traffic – examples include terrorist attacks and acts of sabotage.

To undertake a risks assessment (even if it is limited to geophysical aspect only) throughout the whole TN is not practical and cost-effective, according to Taylor and D´Este [6]. It is simply because the cost of such thorough assessment that would result in any practically useful results for the whole spectrum of risks would be too high. However, the vulnerability analysis provides a different approach to this problem. It could be used to find

structural weaknesses which make the network more sensitive to the consequences of any failures or degradation of its parts without the need to perform a complete thorough risk assessment for the whole TN. This is why we argue to focus the analysis on a subset of TN, namely the critical infrastructure, which can be identified by the experts or through simulations. The process should start with identification of key threats and corresponding probabilities as well as specifying the elements of TN for which serviceability could be affected. Then the collected information would be used for suggesting or realising appropriate strategies to reduce risk of occurring of the identified threats and means to enhance resilience of the elements of TN. In this way we could combine vulnerability, risk, hazardous events and serviceability. Understanding of relation between them could result in improved framework for risk and vulnerability assessment as well as of vulnerability modelling. Relation of these terms is shown in Fig. 2. According to Berdica [2] reducing vulnerability can result in reducing risk of various events, which can enhance serviceability of the TN.

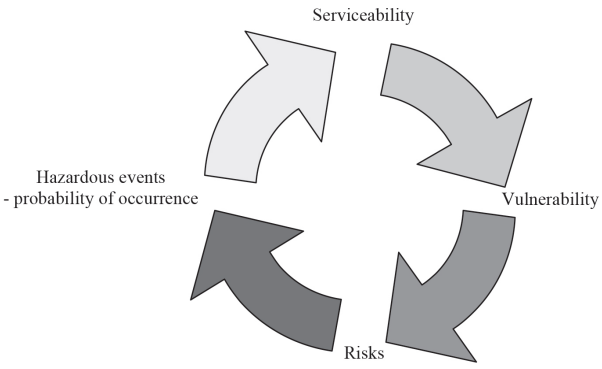

Fig. 2 Vulnerability of transportation network in wheel of concepts (by Berdica)

There are several possible strategies for the identifying threats and perceived risk that can lead to vulnerability reduction. One option is to make the transportation infrastructure more resilient. It can be achieved, for instance, by raising it above expected maximum flood levels. Another strategy would be to introduce additional links to the network – in such a way that the resulting TN would become more robust. Normally, such links may be redundant but in the cases of emergency provide alternative routes for traffic. These examples of strategies could make the TN more resilient (less vulnerable) in the context of specific risks and threats. But before one decides to adopt appropriate measures he or she needs to understand vulnerability. In this work we propose an outline of a simple methodology to quantify vulnerability by means for IDs.

Modelling Vulnerability using Influence Diagrams

In this work we are concerned with defining a vulnerability index (VI) for a single element of the transportation network – either a link or a node. Earlier we argued that in practical context this would be done only for a part of whole transportation network, specifically the critical part of the infrastructure. The purpose is to produce a numeric measure that would quantify the notion of vulnerability.

The influence diagram [12] is a probabilistic decision model that is a more compact representation of a decision problem than decision tree. Unlike the probability or decision trees, the ID does not explicitly specify every single path through the problem; instead, it captures dependencies between variables in the modelled domain. This property allows for more compact and efficient (especially in terms of knowledge elicitation) representation of the problem, implying that it is suitable for larger scale decision problems. There are three types of variables in ID: (1) *chance nodes* that capture unknown events and relevant probabilities including probabilistic dependencies (by means of conditional probabilities), (2) *utility nodes* that encode utilities (which can be costs, profits, etc.) that define user's preferences over the set of outcomes, and (3) *decision nodes* that define elements of the domain over which the decision maker has complete control.

To model vulnerability we propose to define a measure of vulnerability which we further call *vulnerability* index (VI). In order to define VI we propose a structured approach based on IDs: in the first step we would ask subject matter experts (SMEs) familiar with given TN to produce a list of possible threats to a particular network element. The SMEs are expected to be practicing mid-level managers from institutions that are involved in TN maintenance and should be familiar with the concept of risk assessment. The elicitation process can be done using specialized computer-based elicitation tool, where the SMEs would identify relevant threats from a pre-defined list of possible threats. For each of the relevant threats, the SME would need to specify if the threat has a potential to affect the capacity of the network element (i.e. to block, damage or destroy road surface) and provide corresponding probabilities which are expected to be subjective or in less likely scenario based on risk assessment studies). Next, the SME would need to define if the threat has potential to result in decreased or increased traffic, or to cause a mass evacuation – in other words, if it can affect demand on the network element, and again provide corresponding probabilities.

We assume a fixed three-layer network structure of an ID. In the top layer nodes that correspond to threats are placed. They are assumed to be binary (threat can be *present* or *absent*) and quantified by asking the SME to provide probability of the threat occurring – we propose to use two scales, depending on frequency: for likely threats such as traffic incidents, snow storms, floods, etc. we propose to use the average number of days per year. For less likely threats, such as hazardous chemical releases, terrorist attacks, etc., the qualitative scale would be used such as *unlikely, highly unlikely, and extremely unlikely*. These would be translated into specific probabilities. We argue that as long as the scale is used consistently for all threats (and all network nodes) the actual values of probabilities do not matter that much, as the VI is intended to rank different elements of the transportation network relatively to each other rather than to provide interpretation of particular values of VI. The middle layer of the network always includes two nodes: *Demand* and *Capacity*. They are intended to model two factors: each threat can produce demand on network (cause people to use transportation network) and/or affect the capacity of the TN. The states of the nodes would be: *Lowered*,

Normal, *Increased*, *Mass Evacuation* for the *Demand* node and *Nominal*, *Decreased,* and *Critical* for the *Capacity* node. In the lowest layer a single utility node would be placed that would combine the effects of *Demand* and *Capacity*. An example of definition for the *Vulnerability* node is shown in Fig. 3. A simple example of the ID model is shown in Fig. 4.

Demand	Capacity		
	Nominal	Affected	Critical
Lowered	0	0.1	0.25
Normal	0	0.25	0.75
Increased	0.25	0.75	0.9
MassEvac	0.75	0.9	1

Fig. 3 An example of definition for the Vulnerability node

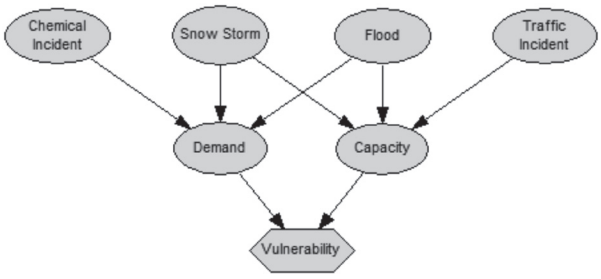

Fig. 4 A simple example of the ID model

For the sake of example, we assumed only 4 threats: *Traffic Incident*, *Snow Storm*, *Flood*, and *Chemical Release*, with the corresponding probabilities of occurrence: 0.01, 0.005, 0.0002, 10^{-6}. In order to understand the working of the approach we analyze the HAZMAT scenario. The HAZMAT scenario would be denoted in the model as *Chemical Release* and it would produce demand on network – it is because a HAZMAT incident is likely to be followed by some form of evacuation and resulting with people forced to leave the threatened area and incur heavy load on the network. On the other hand, *Chemical Release* has no direct impact on capacity of the TN, as we assume that the infrastructure is able to withstand the HAZMAT incident effects with no noticeable effects. A *Traffic Incident* does not directly produce demand on the system, but it has a potential to affect capacity of network element (i.e. to totally block traffic). In the cases when the threats such as *Snow Storm* or *Flood* are occurring they can produce demand on network and affect the capacity of TN because there is a chance that a mass evacuation could be required and also some transportation links could be impossible to use or damaged.

One of particular limitations of IDs is the number of numerical probabilities required to quantify a model. In particular nodes with large numbers of incoming links (often referred and nodes with a large number of parent nodes) should be quantified with a number of probability distributions that is exponential in the number of parent nodes in the graphical part. This implies that if there are 10 incoming links to a node and assuming that all variables are binary (have two states), an SME would be required to provide $2^{10} = 1024$ probability distributions, which would be unrealistic in practice.

In order to reduce the number of parameters required to specify the ID model, we decided to use the noisy-average model [13] for local probability distributions that is available in GeNIe software. The noisy-average model shown in Fig. 5 is suitable for the modelled interactions between variables where there are following conditions required: (1) both the parent variables have a state that describes the 'normal' state of the world (no snowstorm, no flood, etc.), (2) the child variable has as well the 'normal' state (corresponding to typical traffic patterns or the level of traffic flow for which the road was designed), (3) for the child variable the deviation from the 'normal' state can be in both increased and decreased values, and (4) the way the influences are combined is achieved by averaging (hence the name of the model), which means that no single parent variable is assumed to have stronger influence on the state of the child variable than the other parent variables. We believe the noisy-average model is suitable for the task we want to achieve with creating the VI index. Finally, the application of the noisy-average allows to substantially reduce the elicitation task on the SME – it allows reducing the number of parameters required to quantify the model from exponential to linear in the number of parent nodes.

The defined VI ranges from 0 to 1, with increasing values indicating increasing vulnerability. Its values have no strict interpretation, but if the model definition and elicitation process are used consistently for all the network elements, the values for different network elements can be interpreted in the context of all VIs produced from the network. This approach allows for identifying vulnerability areas. There is additional benefit resulting from using IDs – this approach allows for dynamic calculation of VI, under assumption that some of the events are observed (we say that some nodes are instantiated in ID) – for example, if there is snow storm in some area, the model can result with increased VI for some nodes, allowing for implementing tools that would provide situational awareness based on the proposed VI.

Parent (Weight)	Snow Storm (1)		Flood (1)		Chemical Incident (1)		LEAK (1)
State	Present	**Absent**	Present	**Absent**	Present	**Absent**	
Lowered	0.25	0	0.45	0	0	0	0
Normal	0.75	1	0.25	1	0.25	1	1
Increased	0	0	0.3	0	0.25	0	0
MassEvac	0	0	0	0	0.5	0	0

Fig. 5 An example of model definition for the node Demand using the noisy-averege model

4. Conclusions

The concept of vulnerability in the context of TN is a subject of active interest from both practitioners' and academic communities. In particular, the understanding of distribution of vulnerabilities in the TN may help to identify critical components of transportation infrastructure. As discussed, the proposed methodology is intended to be applied to this critical infrastructure element, rather than to the TN as whole. This is dictated by practical considerations – to define models is necessary knowledge of experts on which should be placed the limited burden of elicitation.

In this paper we proposed a method for the assessment of TN's vulnerability using the concepts of "demand" and "capacity" that are consequently combined to produce a numeric vulnerability index. We provided a simple example to illustrate the proposed approach and to demonstrate the way how to model TN's vulnerability using IDs. We presented how the noisy-average model is used to take advantage of independence of causal influences in order to reduce the knowledge elicitation effort and to make the proposed method more practical. Our approach to vulnerability modelling does not take into consideration socio-economic impacts of TN's link failure – it is focused on capturing TN's sensitivity to combination of the specific adverse events directly related to transportation functions.

We believe that the contribution of the paper is two-fold: (1) we proposed to develop a method of vulnerability assessment based on a decision-theoretic framework of IDs, which allows for exploiting well established body of experience with creating this type of models in a new application, (2) we proposed use of the noisy-average model for local probability distributions as a tool to improve and streamline knowledge elicitation processes.

Determining actual TN's vulnerability is important to identify weak links in the network. It can be used to identify and implement appropriate risk reduction strategies for the identified threats. If once can develop a useful way to quantify vulnerability it can potentially be used to improve TN safety. It can be useful not only in the crisis management context, but as well in planning and as a tool to inform future developments and expansion.

We want to emphasise that the proposed approach is at an early stage of development and that this paper only outlines the proposed approach. Further work is needed to validate the approach on an actual example of transportation network, and this is our intention to do so.

Acknowledgements

This work was supported by the Slovak Research and Development Agency under the contract No. APVV-0471-10.

References

[1] ZANICKA-HOLLA, K., RISTVEJ, J., SIMAK, L.: *Systematic Method of Risk Assessment in Industrial Processes*, Risk analysis VII: simulation and hazard mitigation - Southampton : WIT Press, 2010. ISBN 9781845644747 - WIT transaction on information and communication technologies; v. 43. ISSN 1746-4463. DOI: 10.2495/RISK100111

[2] BERDICA, K.: An Introduction to Road Vulnerability: What has been Done, is Done and should be Done. *Transport Policy*, vol. 9, No. 2, 2002, pp. 117-127.

[3] JONSSON, H., JOHANSSON, J., JOHANSSON, H.: Identifying Critical Components in Technical Infrastructure Networks. Proc. of the Institution of Mechanical Engineers, Part O: *J. of Risk and Reliability*. vol. 222, No. 2, 2008. pp. 235-243.

[4] DILLEY, M., BOUDREAU, T. E.: *Coming to Terms with Vulnerability: A Critique of the Food Security Definition*. Food Policy, 2001, 26, pp. 229-247.

[5] WISNER, B., BLAIKIE, P., CANNON, T., DAVIS, I.: *At Risk: Natural Hazards, People's Vulnerability and Disasters.* 2nd ed. Routledge, London, 2004.

[6] TAYLOR, M. A. P., D'ESTE, G. M.: *Concepts of Network Vulnerability and Applications to the Identification of Critical Elements of Transport Infrastructure.* 26th Australasian Transport Research Forum Wellington New Zeland, 2003.

[7] YANG, L., QIAN, D.: Vulnerability Analysis of Road Networks. *J. of Transportation Systems Engineering and Information Technology*, vol. 12, No. 1, 2012, pp. 105-110.

[8] JENELIUS, E., PETEMEN, T., MATTSSON, L. G.: Importance and Exposure in Road Network Vulnerability Analysis. *Transportation Research Part A: Policy and Practice*, vol. 40, No.7, 2006, pp. 537-560.

[9] HUSDAL, J.: *Reliability and Vulnerability Versus Cost and Benefits*. The 2nd Intern. Symposium on Transportation Network Reliability. Queenstown and Christchurch, New Zealand, 2004, pp. 180-186.

[10] SLIVONE, M.: Several Approaches to Identification of Critical Links in Transport Network. *Perner's Contacts*, vol. 3, No. 5, 2008, pp. 261-275.

[11] BRATHEN, S., LAEGRAN, S.: *Bottlenecks in Cargo Transport in Norway.* Molde Research Institute/SWECO Groner, Norway, 2004.

[12] HOWARD, R. A., MATHESON, J. E.: *Influence Diagrams.* Howard and Matheson (eds.) The Principles and Applications of Decision Analysis, vol. II., Strategic Decisions Group, Menlo Park, CA pp. 721-762.

[13] ZAGORECKI, A. DRUZDZEL, M. *The Noisy-average Model for Local Probability Distributions*. Technical report, Decision Systems Laboratory, University of Pittsburgh.

https://doi.org/10.26552/com.C.2013.4.63-67

Josef Vodak - Jakub Soviar - Viliam Lendel *

IDENTIFICATION OF THE MAIN PROBLEMS IN USING COOPERATIVE MANAGEMENT IN SLOVAK ENTERPRISES AND THE PROPOSAL OF CONVENIENT RECOMMENDATIONS

The main purpose of the article is to present some knowledge in cooperative management focused on the area of management and marketing and to show possibility to use the cooperation in a company practice effectively. The article contains drafts for successful functioning of the cooperation in practice. There are also identified the main fields of potential problems which should be discussed by responsible participants within cooperation to achieve effective functioning. The solution of the questions researched within the article needs to use several methods depending on the character of particular parts of the solution.

Keywords: *Cooperative management, research of cooperation potential, cooperation towards competitiveness.*

1. Introduction

Nowadays the area of cooperative management is not fully elaborated, contrarily; it is the core interest for theoretical specialists and practitioners. Their main effort is to create a model of successful use of cooperative management in a company, which would secure their competitiveness. Cooperative management creation in a company often fails. The reason is that mostly there is no clear activities plan, there is an absence of competence division for implementation, and strategy of an enterprise is not oriented towards creation and improvement of the cooperation. In the company's practice there are some mistakes within the loss of managers in this field. Mainly it is an incorrect understanding of the term cooperative management and insufficient use of cooperation potential in the enterprise. The suitable recommendation draft within this field can considerably contribute to increase the success of cooperative management use in the enterprise [1, 2, 3, 4, 5, 6, 7 and 8].

Cooperative management offers effective direction of cooperative processes in an enterprise. Its aim is to permanently improve activities of enterprise and provide flexibility in order to satisfy growing demands of customers and partners of enterprise. A result of its effort is the security of competitiveness. However, it is important to create strategy for using cooperative management in enterprise based on a conveniently implemented informative system, developing enterprise culture supporting cooperation, providing financial and human resources.

The purpose of the article is, on the base of a detailed analysis of literary sources in the field of strategic management, cooperative management, marketing and realized research, to gain a picture of the use of cooperative management in Slovak companies and to subsequently apply the gathered knowledge into a recommendation draft for effective cooperation control in a company's practice.

2. Objective and Methodology

The main aim of this work is to gain new knowledge in enterprise management focused on the areas of management and marketing and to point out possibility of the effective use of the cooperation in the enterprise practice. The article contains recommendations for successful functioning of cooperation in an enterprise practice. The recommendations should serve mainly to individual participants of the cooperation as a valuable tool of its successful management. The article identifies the main fields of potential problems which should be observed by responsible participants within the cooperation in order to reach its effective functioning. Solving the examined tasks within the article needs the use of several methods depending on the character of individual parts of the solution.

To gain and gather the information we used the methods of document analysis (analyzing current and historical data referring to the topic), a questionnaire and the method of semi-structural interview (data collection in empirical research), observation method (visit to particular enterprises).

In the process of information elaboration we mainly used the method of quantitative assessment (creation of statistical averages, statistical tests application and other statistical methods) and comparative method (when comparing the data gained through the empirical research and the data from the analysis of secondary sources).

The companies acting in all branches of the national economy in Slovakia were the subject of the research. In fact they are the companies included in medium-sized and big businesses depending on the number of employees according to the Statistical office of the Slovak Republic.

The sample size was 367 respondents for a 95% confidence interval required at a 5% maximum permissible mistake. With regard to the fact that 273 respondents participated in the

* **Josef Vodak, Jakub Soviar, Viliam Lendel**
Faculty of Management Science and Informatics, University of Zilina, Slovakia
E-mail: josef.vodak@fri.uniza.sk

research, the mistake that occurred was 5.83%. The data were collected only by personal interviewing. 497 companies were interviewed, of which 273 managers filled in the questionnaire, which means 54.93% return.

To solve the problem observed we used the methods of induction, deduction, synthesis (when creating the recommendations for successful functioning of the cooperation in the enterprise practice), abstraction and simulation.

3. Current state of dealing with the issue

Nowadays there is a debate on a definition of cooperative management and allocation of the areas of its operation among the professional public. There are a few definitions of cooperative management published, however, each of these covers only a section of the overall role of cooperative management. Table 1 summarizes the definitions of the term *cooperative management*.

Definitions of the term *cooperative management* Table 1

Author(s)	Definition
Ray (2002)	Cooperative management is a framework for the integrated management of enterprise networks.
Staatz (1983)	Cooperative management is a cooperative decision making in the context of heterogeneous preferences, there is a need to develop models which address the issue explicitly and in so doing suggest alternative ways of structuring cooperatives to deal with a group choice.
Brown (1998)	Cooperative management is a partnership between government and industry.
Lafleur (2005)	Cooperative management is the way the management and development of a cooperative are conducted in a competitive setting.
Zhang (2011)	Cooperative management is the core of all management problems. Conditions of constructing a cooperation system are analysed which are the motivation of resource dependence, objective of effect enhancement, constraints of encouraging cooperation and possession of technology of cooperation.
Mendoza	Cooperative management might be defined as the efficient and effective utilization of the resources of a cooperative as a business organization for the purpose of serving the needs of its members within the context of the accepted cooperative principles.
Watzlawick	Cooperative management should be understood as a complex decision making process within the three levels of management pyramid which aims at achieving a proper balance of success of cooperative enterprise as a business unit as well as a social institution.

The definitions mentioned above bring to fore the following features of cooperative management [9, 10, 11, 12, 13 and 14]:

- Cooperative management is a complex decision making process, and decisions are made at all the three levels of management pyramid.
- The overriding objective of cooperative management is to serve the needs of members.
- The conduct of all the activities must be governed jointly by the two sets of principles namely, a) principles of management and b) principles of cooperation.
- The creation of proper balance between efforts aiming at commercial success and those aimed at maintaining the institutional goals of the cooperative association.
- Like any other management, it seeks to achieve its aim by means of effective and efficient use of resources.

Based on a thorough analysis of domestic and foreign literature, we can proceed to the following definition: *Cooperative management is effective and purposeful relationship management in the meaning of cooperation between individual, relatively independent organisations or individuals with the aim to increase their competitiveness* [15].

4. Situation in Slovak enterprises – results of empirical research

A research was carried out from September 2012 to February 2013 the task of which was to acquire and interpret the information related to the level of cooperation use in the conditions of Slovak enterprises. The main purpose of the research was an attempt to identify key elements of the effective managing (functioning) of cooperation, problems, satisfaction with enterprises' cooperation and possibilities to improve functioning cooperation. The data gained brought a complete picture of Slovak enterprises' preparedness to use cooperative management.

273 managers of middle-sized and big enterprises acting in the Slovak Republic took part in the research. All respondents were addressed through personal asking. In the processing of the information χ^2 independence tests of qualitative features and a cluster analysis were used.

A lack of literature referring to the issue of cooperative management use (specification of terms, structure and methods of use) reflects the reality that just a few managers had the processes documented and understood the issue.

The ascertainment that almost half of the respondents (48 %) are planning to cooperate with another enterprise or organization intensively in the near future (within 1 year time), can be taken positively.

The fact that even 46 % of the managers interviewed would decide to cooperate with their most important partner repeatedly may be evaluated the same way. It proves their tough relationship which can be considered as the basic prerequisite for a successful cooperation.

The intensity rate of cooperation of a certain enterprise with other enterprises on the rating scale from 1 up to 10, where 1 means "almost none" and 10 means "very intensive", was found out in the research. Interesting findings:

- Enterprises cooperate most intensively with commercial enterprises; high intensity of cooperation (level 8, 9 and 10) was confirmed by 64.4 % of the managers asked,
- Enterprises do not almost cooperate (the level 1) with non-profit organizations, this possibility was pointed by 55.2 % of the respondents asked,
- Really weak intensity of enterprises cooperation is with the European Union, 49.7 % managers asked affirmed that they do not almost cooperate with the EU,
- Similar situation is within the enterprises cooperation with a local self-government and regional self-government (Senior Territorial Unit).

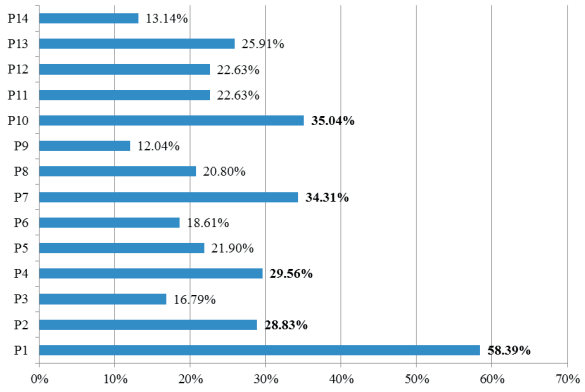

Legend:

P1 Insufficient fulfilment of terms of contract within cooperation
P2 Unwillingness to provide internal information referring to a cooperative enterprise (fear of providing internal information of an enterprise)
P3 Unwillingness to cooperate from the side of a cooperative enterprise (a partner)
P4 Low efficiency of the cooperation, i.e. expenses for the cooperation are always higher than resulting effects
P5 Insufficient unison and adopting of the informative systems with the partner IS
P6 Unwillingness of the communication among cooperative enterprises
P7 Informative distortions (incorrectness, insufficiency, etc.)
P8 Low willingness of the customers to keep and support the cooperation (their negative relation towards the cooperation)
P9 Low willingness of the enterprise management or organisation towards the cooperation
P10 Financial demands
P11 Time busyness of the management
P12 Questionable quality of cooperation (unclear cooperation contributions)
P13 Results not corresponding with the effort expended
P14 Distrust of cooperative enterprises

Fig. 1 Problems arising when cooperating with other enterprises and organisations Source: Own research

χ^2 independence test of qualitative features proved that there is a kind of dependency between satisfaction of enterprises with the level of the current cooperation (satisfaction index) and largeness of enterprises.

The following were considered to be the main problems which occurred during cooperation of an enterprise with other enterprises and organizations: insufficient fulfillment of terms of contract (58.39%), financial demands (35.04%), information distortions (34.31%), low efficacy of cooperation (29.56%) and unwillingness to provide internal information from the side of a co-operational enterprise, i. e. concern about providing internal information of an enterprise (28.83%). For more information see Fig. 1.

5. Identification of the main problems and formulating recommendations

Using the cooperative management in enterprise is a difficult process which needs detailed knowledge of the business environment. Enterprise managers should be ready for risks that the using of the cooperative management brings. Otherwise, the initiative doomed to failure. The fundamental for success in this field is an early identification of risk fields and acceptance of appropriate decisions to increase possibility of the success connected with the cooperative management in enterprise.

The following part deals with the identifications of possible risk fields and recommendations, which should help to decrease the risks. Prevention is a necessary prerequisite for successful functioning of the cooperative management in enterprise.

An unemployed cooperation potential of an enterprise is the most common problem. The enterprise either does not know its cooperation potential or there are none conditions in an enterprise for its improvement and use. Displays of these problems differ. First of all it is connected with the appearance of misunderstandings, expenses and realization of inefficient cooperation processes (recurring many times).

Managers of the enterprise should be interested in a detailed analysis of cooperation capacity of the enterprise. The enterprise must have a view of their knowledge, experience, sources, property and managerial abilities and skills which they have at their disposal and they can use them to the full when creating and managing cooperation. To do so, it is important that the top management of the enterprise have an exact conception referring to cooperation creation and their management which must be stated in the enterprise strategy supported by responsible human and financial sources. Managers must communicate with potential partners and their employees actively and join them into the cooperation creation. The top management should create a kind of motivational scheme, which will stimulate their employees to join the cooperation processes.

Another risk area is *absence of information system* supporting effective exchange of information among partners within cooperation. The information coming from partners is not often registered in the form which could be used later on or it is not accessible to all responsible people. This leads to the situations when managers and employees react insufficiently towards the information replies within the cooperation.

Managers of an enterprise should create certain databases connected with an information system of the enterprise. In the case of impulse everyone in the enterprise must exactly know how to react. This ensures effective work within the cooperation. The information system must take into consideration requirements and a current situation in the field of information technologies of individual partners within the cooperation.

A lack of appropriate conditions supporting cooperation creation is considered to be a serious problem. Managers of the enterprise should focus on creation of the enterprise culture with an appropriate motivational scheme. Except for the above mentioned recommendations whose application causes improvement of the cooperation conditions, it is needed to focus on the employees of the enterprise. The top management should try to encourage their activity and to create appropriate conditions, which will secure open communication, discussion on cooperation possibilities and team works. Employees of enterprise should bring their enthusiasm into the development of a new cooperation.

Cooperative programme incorrectly prepared is a frequent problem when using cooperative management in enterprise. Enterprise managers tend to focus only on providing the technological side of the cooperation. Yet, the enterprise must have enough information on cooperative processes, cooperative ability and cooperative sources at its disposal. If the enterprise is not interested enough in this field and starts to implement cooperative management on the base of insufficient documentation, then the using of cooperative management in enterprise is doomed to failure. The following might be recommended to the managers of an enterprise:

- realize a detailed analysis of a current situation in the enterprise,
- correctly understand the role of technology when using the cooperative management,
- map a potential for cooperation comprehensively and specify demands for cooperation,
- set the assessment system of cooperative efficiency of the enterprise including its rules in a correct way.

Problems might also occur *when defining cooperative goals*, which the enterprise wants to achieve considering the cooperation planned. Very often the enterprise does not know how the cooperation will be provided and realization of what activities will be necessary. In such a situation it is necessary that the enterprise understands its cooperative possibilities and these are reflected into its strategic goals. The following proceedings might be recommended to the managers of the enterprise:

- Understand the principles of cooperation correctly (good knowledge of the issues gained through the literature studies or through appropriate professional education),
- Clarify the situation where the enterprise wants to get using the cooperative management,
- Understand the expected cooperation contribution and ways leading to their achievement,
- Work out a common vision with the partners.

Exclusion of a human factor from the process of using the cooperative management is also a serious problem. The employees who do not take part in creating necessary documentation referring to the future cooperation, process of cooperative potential identification and setting the cooperation requirements, so they do not have enough information about cooperative management goals. This causes the situations when they do particular activities passively, with no interest because they are not informed about the enterprise intensions in this field. The following might be recommended to enterprise managers to minimalize this problem:

- Secure a regular communication with the employees in order to create the environment suitable for origin and development of the cooperation,
- Enable the employees to take part in the development of the cooperative programme and subsequently use the cooperative management in the enterprise,
- Accept and take into consideration the employees' ideas on creating the cooperative programme,
- Explain to the employees a meaning of the cooperation for further directing of the enterprise,
- Provide the employees with necessary information about each step of using of the cooperative management in the enterprise.

In the process of securing the cooperative processes there might be a danger of *automation of the previous wrongly set (faulty) processes*. To minimalize the origin of such a situation we can recommend to the managers of the enterprise to:

- Identify and regularly update cooperative processes,
- Emphasize mainly the processes which are directly connected with the work in the field of cooperation,
- Pay attention to the current state of the cooperative process analysis,
- Create a separate process model of the cooperation realised.

Using the cooperative management in the enterprise can be successful just in case that the enterprise accepts the initial conditions which include limits of a different character. In the case of *ignoring the initial conditions* a lot of serious problems occur. In order to prevent them we can recommend to the managers of the enterprise to:

- Set the key indicators of cooperative management application in the enterprise,
- Set control points within cooperative management application in the enterprise,
- Take into consideration restrictions (extent of the use of the cooperative potential, risk of the failure, cooperative capacity level, etc.).

Only in the case of setting the measured goals the top management can judge and evaluate contributions of the cooperation. *Absence of feedback*, which is intended for the leading of the process, is a frequent mistake in the process of cooperative management application. It is necessary to observe and assess the whole process of using the cooperative management (from the analyses up to the realisation).

That is why we can recommend to the managers of the enterprise to secure the continuing assessment of cooperative management application in the enterprise. This requires setting the goals of cooperative management application on the base of

measurable indicators clearly. The enterprise managers should limit and set the metrics so that they can through better set measurable goals faster and more effective lead particular fields in the enterprise, the ones which influence the cooperation. Yet, it is necessary to create a group of metrics on the base of the main priorities in leading of the cooperative activities in the enterprise.

6. Conclusion

The analysis of special literature and the carried out research proved the fact that mutual reliance, fulfillment of the terms of contract, the level of communication and information system enabling effective work with the information referring to the cooperation have the key role in the issue. It is possible to say that:

- Effective cooperation has a significant impact on competitiveness.
- Experience and mutual trust are important factors for cooperation development.
- Cooperation between independent companies could be managed in order to gain competitive advantage.
- Cooperation with R&D could improve an innovation process.

Managers of the enterprise should make a plan connected with the creation and improvement of cooperation including a method how to achieve it; remake an enterprise strategy so that it contains creation and improvement of cooperation relationships; earmark sufficient sources (human and financial) for cooperation and their searching; make appropriate conditions for creating and improvement of cooperation relationships. "Business strategies which do not recognize the presence of complexity and uncertainty with related and future changes will be inflexible and unlikely to be correct" [8].

The article dealt with the field of cooperating and its effective leading of the enterprise. The results are definitions of the main problems occurring in the process of cooperative management application in the enterprise. Some recommendations have been prepared to run this process without any problems, which are considered to be a valuable tool for managers when creating a conception and a subsequent use of cooperative management in the enterprise. The recommendations do not only help to decrease probability of creating problematic fields, they are also a kind of prevention and a tool to improve cooperative processes in the enterprise.

Acknowledgement

This paper was supported by the Slovak scientific grant VEGA 1/0992/11 2011-2013.

References

[1] AXELROD, R.: *The Evolution of Cooperation*. New York, Basic Books, 1984. ISBN 0-465-02121-2.
[2] BOYD, R., RICHERSON, P. J.: Culture and the Evolution of Human Cooperation. *Philosophical Transactions of the Royal Society B-Biological Sciences*, No. 1533, vol. 364, 2009, pp. 3281-3288.
[3] DORCAK, P., POLLAK, F.: Marketing & E-business: *How to Familiarize with the Main Terminology and Processes of New Marketing (in Slovak)*, Presov: EZO.sk, s.r.o. 2010. ISBN 978-80-970564-0-7.
[4] ROBBINS, P, S., COULTER, M.: *Management*. Grada: Prague, 2004. ISBN 80-247-0495-1.
[5] SETHI, R., SOMANATHAN, E.: Understanding Reciprocity. *J. of Economic Behaviour & Organization*, No. 1, vol. 50, 2003, 1-27. ISSN 0167-2681.
[6] SOLVELL, O., GORAN, L., KETELS, Ch.: *The Cluster Initiative Greenbook*. Stockholm: Brommatryck AB. [online]: http://www.cluster-research.org/greenbook.htm, 2003.
[7] SOVIAR, J., VODAK, J.: Value Network as Part of New Trends in Communication. *Communications – Scientific Letters of the University of Zilina*, No. 2, vol. 14, 2012. ISSN 1335-4205.
[8] VARMUS, M.: *Comparison of Selected Concepts Strategies.* Theory of Management - part 1, EDIS: University of Zilina, 2009. ISBN978-80-554-0147-8.
[9] BROWN, R. C.: Community-based Cooperative management: Renewed Interest in an Old Paradigm. *Reinventing Fisheries Management*, vol. 23, 1998, pp. 185-194.
[10] LAFLEUR, M.: A Model for Cooperative Challenges. *Cooperative Grocer Network*, No. 116, [online]: http://www.cooperativegrocer.coop/articles/2009-01-21/model-cooperative-challenges.
[11] STAATZ, J. M.: The Cooperative as a Coalition: A Game-Theoretic Approach. *American J. of Agricultural Economics,* No. 5, vol. 65, 1983, pp. 1084-1089.
[12] VEERAKUMARAN, G.: COCM 511 - *Management of Cooperatives and Legal Systems*, Faculty of Dryland Agriculture and Natural Resources, Mekelle University, 2006.
[13] ZHANG, W.: *Cooperation System Constructing and Model of its Operation Mechanism.* Intern. Conference on Business Management and Electronic Information (BMEI), vol. 3, 2011, pp. 784-787.
[14] RAY, P. K.: *Cooperative Management of Enterprise Networks*. Kluwer Academic Publishers, 2002. ISBN 0-306-46972-3.
[15] SOVIAR, J.: *From Cooperation to Management – Cooperative Management*. Habilitation thesis. University of Zilina, Faculty of Management Science and Informatics, 2012.

https://doi.org/10.26552/com.C.2013.4.68-72

Magdalena Brezaniova *

USE OF CORRELATION ANALYSIS TO EXAMINE RELATIONSHIP BETWEEN TAX BURDEN AND BUSINESS ENVIRONMENT IN SELECTED EU COUNTRIES

The aim of the article is to examine the relationship between tax burden and business environment in Slovakia, Czech Republic and Germany. The examination is carried out using correlation analysis to identify the level of dependence between selected indicators of tax burden and number of business entities in selected countries. The article contains also analysis and comparison of found facts.

Keywords: *Tax burden, corporate income tax, tax rate, CIT-to-GDP-ratio, tax-to-GDP-ratio, direct taxes-to-GDP-ratio, implicit tax rate on corporate income, business entities, correlation analysis, correlation coefficient.*

1. Introduction

In general, tax burden is considered an important factor in decision making about the business activity of enterprises in particular country. Taxes affect many areas of the business sector, particularly economic behaviour and subsequent financial decisions of business units. Among the applicable taxes, direct taxes have more impact on cost-effectiveness or profits of enterprises as indirect ones. In the paper the relationship between tax burden and business environment in Slovakia, Czech Republic and Germany is examined using correlation analysis. These three countries were chosen to compare Slovakia with the country that has similar history, tradition and economic and tax system and is of comparable level of development (Czech Republic) and with more developed country with different history, tradition and economic and tax system (Germany). Thanks to the differences found out through the research we can compare the effectiveness of different tax systems in relationship with business environment.

2. Data and methodology

For the purpose of examining the relationship between tax burden and business environment we selected specific indicators representing tax burden on the macroeconomic level, namely nominal tax rate on corporate income (CIT rate), tax-to-GDP-ratio, implicit tax rate (ITR) on corporate income, share of direct taxes to GDP (direct taxes-to-GDP-ratio) and share of corporate income taxes to GDP (CIT-to-GDP-ratio). Tax rate is used to determine the actual level of business taxes from the tax base. Tax-to-GDP-ratio (namely the aggregate tax-to-GDP-ratio) is commonly used for international comparison of tax burden and is defined as a share of all taxes, levies, duties and non-tax payments to the GDP of a country. Implicit tax rate on corporate income is defined as a share of taxes on income or profits of businesses on their total income. The share of direct taxes to GDP and the share of corporate income tax to GDP is an expression of the tax burden of these taxes. These indicators were selected because of their expected impact on the business environment, as well as their availability on international statistics, in particular on Eurostat, the statistical office of the European Union. The business environment is represented by number of business entities, particularly entities that are potential taxpayers of corporate income tax. In this analysis we abstract away from other influences affecting the business environment, and the attention is focused only on the impact of tax burden.

Number of business entities – legal persons, was considered the variable y and the individual indicators of tax burden were identified as x_1 (tax rate on corporate income), x_2 (tax-to-GDP-ratio), x_3 (implicit tax rate), x_4 (share of direct taxes to GDP) and x_5 (share of corporate income taxes to GDP). Gradually, we investigated linear dependence between the variable y and x_1, x_2, x_3, x_4 and x_5 using the method of correlation analysis, and therefore the correlation coefficients reflecting the degree of the dependence, were calculated [1].

The input data are values of selected indicators for the years 2003 to 2010 in Slovakia, Czech Republic and Germany.

3. Relationship between indicators of tax burden and business environment in Slovakia

Table 1 contains the input data for Slovakia used in correlation analysis.

* **Magdalena Brezaniova**
Department of Communications, Faculty of Operation and Economics of Transport and Communications, University of Zilina, Slovakia
E-mail: magdalenabrez@gmail.com

COMMUNICATIONS

Values of selected indicators of business environment and tax burden in Slovakia for the years 2003 to 2010 Table 1

Indicator/year	2003	2004	2005	2006	2007	2008	2009	2010
Number of business entities (y)	101412	114285	126777	139240	149772	169960	179352	197089
CIT rate [%] (x_1)	25	19	19	19	19	19	19	19
Tax-to-GDP-ratio [%] (x_2)	33	31.7	31.5	29.4	29.5	29.4	29.1	28.3
ITR on corporate income [%] (x_3)	34.8	22.6	23.3	20.3	19.8	21.7	22.5	19.2
Direct taxes-to-GDP-ratio [%] (x_4)	7.1	6.1	6.0	6.1	6.2	6.5	5.5	5.4
CIT-to-GDP-ratio [%] (x_5)	2.8	2.6	2.7	2.9	3.0	3.1	2.5	2.5

(Source: Own elaboration by using data from Slovak Statistical Office and Eurostat) [2], [3]

Number of business entities in Slovakia during the examined period of time is shown in Fig. 1.

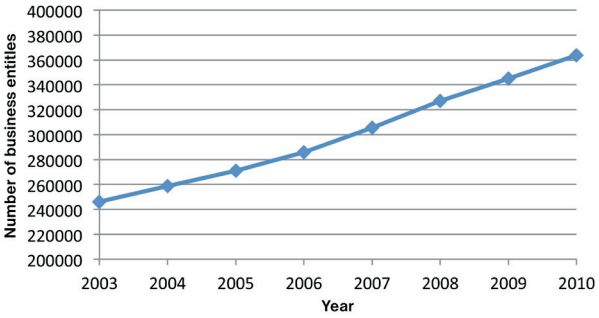

Fig. 1 Number of business entities in Slovakia between 2003 and 2010. (Source: own elaboration by using data from Slovak Statistical Office) [2]

In Fig. 2 we can see time characteristic of selected indicators of tax burden for Slovakia in 2003 – 2010.

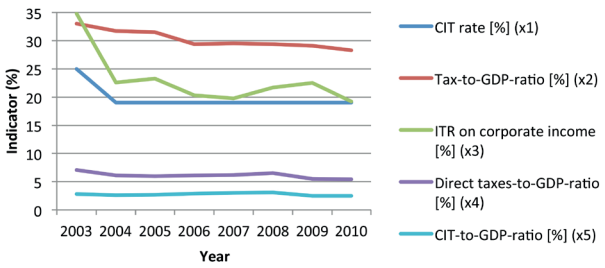

Fig. 2 Time characteristic of selected indicators of tax burden in Slovakia in 2003 – 2010 (Source: Own elaboration by using data from Eurostat) [3]

The values of correlation coefficients of selected indicators for Slovakia are shown in Table 2.

Correlation coefficients for the examination of dependence between selected indicators in Slovakia Table 2

Indicators	Correlation Coefficients
y, x_1	-0.558
y, x_2	-0.925
y, x_3	-0.653
y, x_4	-0.709
y, x_5	-0.179

where y is the number of business entities (legal persons), x_1 is tax rate on corporate income tax, x_2 is Tax-to-GDP-ratio, x_3 is Implicit tax rate on corporate income, x_4 is Direct taxes-to-GDP ratio, x_5 is CIT-to-GDP ratio *(Source: author's calculation)*

The values of correlation coefficients in Table 2 show that in Slovakia the strongest dependence is between number of business entities and the overall tax burden, measured by tax-to-GDP-ratio. The correlation coefficient in this case has the value of -0.925, and thus it is a negative linear correlation. Between the other examined indicators and number of business entities is only medium or low dependence. Therefore, we can conclude that in Slovakia among the selected indicators the most important for business activity is tax-to-GDP-ratio and the reduction of its level is accompanied by an increase in number of business entities.

As seen from the data in Table 1 and Figs. 1 and 2, during the monitored period the number of business entities in Slovakia was increasing, with the largest increase in 2008 (20 188 companies more than in 2007). Conversely, the lowest increase in number of business entities was recorded in 2009 (by 9 392), which should be considered a result of the financial crisis. Tax-to-GDP-ratio was decreasing during the period, except for 2007, when a slight increase by 0.10% was recorded. Its most significant decrease was in 2006 (by -2.10%). This can be considered the effect of the tax reform adopted in previous two years, in which

besides the introduction of the flat tax rate for income tax and VAT, the method of income taxation in Slovakia had changed (including increased basic personal allowance to 19.2 x minimum subsistence level), the preferential treatment of taxation of business activities of legal persons applying the linear tax rate compared to natural persons had been abolished, the terms of quantifying the income tax base, which was obtained from the activities of the same nature (in particular, income of business) had been unified, and the application of deductible expenses from taxable income and the application of business losses from previous years had been introduced. In 2006, the reduced VAT rate of 10% was introduced for selected commodities. Other examined indicators of tax burden were developing variously and their values had not significant influence on number of business entities. Worthy of notice is corporate income tax rate, which declined markedly in 2004 (by 6%) after the above mentioned tax reform related with the introduction of flat tax rate of 19%, which was also reflected in considerable decrease of implicit tax rate on corporate income (by 12.19%) [4].

4. Relationship between indicators of tax burden and business environment in Czech Republic

Table 3 shows the input data for the Czech Republic used in correlation analysis.

Number of business entities in the Czech Republic during the examined period of time can be seen in Fig. 3.

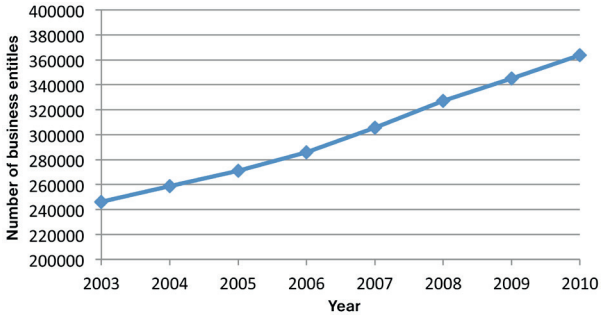

Fig. 3 Number of business entities in Czech Republic between 2003 and 2010 (Source: own elaboration by using data from Czech Statistical Office) [5]

In Fig. 4 there is time characteristic of selected indicators of tax burden for the Czech Republic in 2003 – 2010.

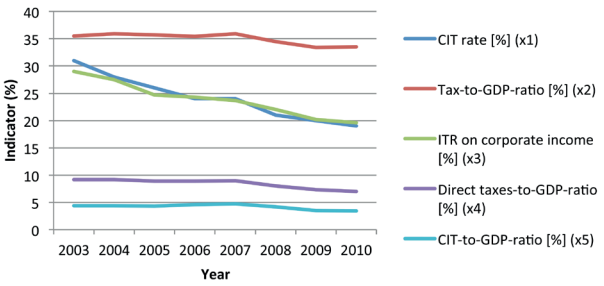

Fig. 4 Time characteristic of selected indicators of tax burden in Czech Republic in 2003 - 2010
(Source: own elaboration by using data from Eurostat) [3]

The values of correlation coefficients of selected indicators for Czech Republic are shown in Table 4.

Correlation coefficients for the examination of dependence between selected indicators in Czech Republic Table 4

Indicators	Correlation Coefficients
y, x_1	-0.969
y, x_2	-0.865
y, x_3	-0.972
y, x_4	-0.934
y, x_5	-0.752

where y is the number of business entities (legal persons), x_1 is tax rate on corporate income tax, x_2 is Tax-to-GDP-ratio, x_3 is Implicit tax rate on corporate income, x_4 is Direct taxes-to-GDP ratio, x_5 is CIT-to-GDP ratio *(Source: author's calculation)*

In Czech Republic four indicators of tax burden have strong correlation with number of business entities (Table 4). The strongest dependence is between number of business entities and implicit tax rate on corporate income. In this case the value of the correlation coefficient is -0.972. Due to its minus sign the decrease of implicit tax rate on corporate income reflects an

Values of selected indicators of business environment and tax burden in the Czech Republic for the years 2003 to 2010 Table 3

Indicator/year	2003	2004	2005	2006	2007	2008	2009	2010
Number of business entities (y)	246181	258674	271242	285943	305707	327173	345156	363801
CIT rate [%] (x_1)	31	28	26	24	24	21	20	19
Tax-to-GDP-ratio [%] (x_2)	35.5	35.9	35.7	35.4	35.9	34.5	33.4	33.5
ITR on corporate income [%] (x_3)	29.0	27.5	24.7	24.3	23.7	22.0	20.2	19.6
Direct taxes-to-GDP-ratio [%] (x_4)	9.2	9.2	8.9	8.9	9.0	8.0	7.3	7.0
CIT-to-GDP-ratio [%] (x_5)	4.4	4.4	4.3	4.6	4.7	4.2	3.5	3.4

(Source: Own elaboration by using data from Czech Statistical Office and Eurostat) [3], [5]

increase in number of business entities. Similar situation is in the case of corporate income tax rate (the correlation coefficient is equal to -0.969), and the share of direct taxes to GDP (-0.934). Slightly smaller, but still strong dependence is between number of business entities and overall tax-to-GDP-ratio. Between number of business entities and share of income tax to GDP is only medium correlation, so we could conclude that the effect of this variable to number of business entities – legal persons in the country is the least.

Throughout the monitored period tax rate on corporate income, as well as implicit tax rate on corporate income, decreased or remained unchanged, while the downward trend of these two parameters was among monitored indicators the most notable (Table 3, Figs. 3 and 4). The course of values of the other studied indicators was variable and there were only slight changes in values. Number of business entities was increasing every year. The largest increase in number of business entities was in 2008 (by 21 466), at the same year as there was the greatest reduction in corporate income tax rate (by 3%, as well as in 2004) and the second largest decrease in implicit tax rate on corporate income (by 1.75%, the largest decrease of the indicator was in 2005, by 2.50%). These decreases in values of the indicators were due to implementation of tax reforms in the Czech tax system in 2004 and 2008.

5. Relationship between indicators of tax burden and business environment in Germany

Table 5 contains the input data for Germany used in correlation analysis. In the case of Germany, we examined the dependence using four indicators of the tax burden, whereas data on implicit tax rate on corporate income for the examined period was not available. Number of business entities (in this case all enterprises regardless of their legal status) is for the years 2006-2010, data for previous years was not available.

Number of business entities in Germany during the examined period of time is shown in Fig. 5.

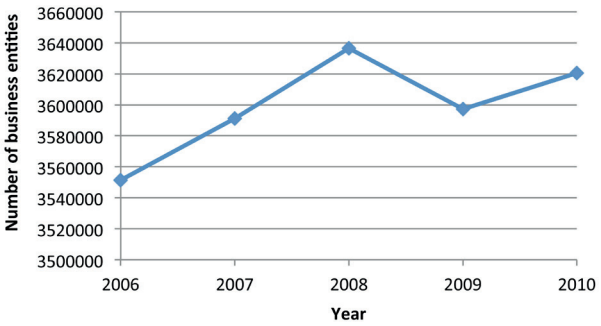

Fig. 5 Number of business entities in Germany between 2006 and 2010 (Source: own elaboration by using data from German Statistical Office) [6]

In Fig. 6 time characteristic of selected indicators of tax burden for Germany in 2003 – 2010 is shown.

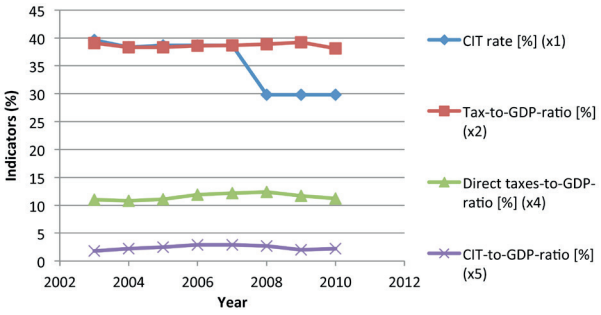

Fig. 6 Time characteristic of selected indicators of tax burden in Germany in 2003 - 2010 (Source: own elaboration by using data from Eurostat) [3]

Values of selected indicators of business environment and tax burden in Germany for the years 2003 to 2010 Table 5

Indicator/year	2003	2004	2005	2006	2007	2008	2009	2010
Number of business entities (y)*	-	-	-	3551240	3591265	3636495	3597248	3620576
CIT rate [%] (x_1)**	39.6	38.3	38.7	38.7	38.7	29.8	29.8	29.8
Tax-to-GDP-ratio [%] (x_2)	39.1	38.3	38.3	38.6	38.7	38.9	39.2	38.1
ITR on corporate income [%] (x_3)	24.0	25.4	24.3	30.0	27.7	25.9	14.7	21.6
Direct taxes-to-GDP-ratio [%] (x_4)	11.0	10.8	11.1	11.9	12.2	12.4	11.7	11.2
CIT-to-GDP-ratio [%] (x_5)	1.8	2.2	2.5	2.9	2.9	2.7	2.0	2.2

** number of business entities includes all companies in Germany, data on the number of enterprises - legal persons separately was not available*
*** it is total tax rate, i.e. statutory tax rate + solidarity surcharge + local trade tax*
(Source: Own elaboration by using data from German Statistical Office and Eurostat) [3], [6]

The values of correlation coefficients of selected indicators for Germany are shown in Table 6.

Correlation coefficients for the examination of dependence between selected indicators in Germany Table 6

Indicators	Correlation Coefficients
y, x_1	-0.791
y, x_2	-0.029
y, x_3	-
y, x_4	0.028
y, x_5	-0.377

where y is the number of business entities (legal persons),
x_1 is tax rate on corporate income tax, x_2 is Tax-to-GDP-ratio,
x_3 is Implicit tax rate on corporate income,
x_4 is Direct taxes-to-GDP ratio, x_5 is CIT-to-GDP ratio
(Source: author's calculation)

As for Germany, we can see that the most of the selected indicators of tax burden has no significant impact on the evolution of number of business entities, since the most values of correlation coefficients indicate only low dependence between monitored indicators. An exception is the tax rate on corporate income, which has nearly strong dependence with number of business entities (correlation coefficient = -0.791, Table 6). This indirect dependence was reflected in the most significant increase in the number of business entities in 2008 (about 45,230 more than in 2007), when was the most significant reduction in the total tax rate on corporate income (+8.9%) to 29.8% of previous 38.7% (due to a reduction in the statutory tax rate to 15%) - Fig. 6. It is worth noting also marked reduction of the number of business entities in 2009 – there were 39,247 less companies registered than in 2008 - Fig. 5. It is therefore clear that business activity in Germany was negatively influenced by the financial crisis that erupted in autumn 2008. In the development of the values of the other studied variables of tax burden, there were no significant fluctuations [7].

As we can see from the used data, the values of selected indicators of tax burden are the highest in Germany. On the other hand also the number of business entities in this country is really high. Based on these findings, we can conclude that the business environment in Germany is affected more by factors different from tax burden. Germany is a developed country with a developed infrastructure, high levels of health care and education system, with a good legal system and advanced use of modern technologies, so business entities are willing to do business in this country in spite of higher tax burden.

6. Conclusion

Comparing the three chosen countries we can find differences in relationship between tax burden and business environment. From the values of correlation coefficients follow that most significantly influenced by tax burden is business environment in Czech Republic, where four indicators of tax burden have strong correlation with number of business entities (corporate income tax rate, overall tax-to-GDP-ratio, implicit tax rate on corporate income, share of direct taxes to GDP). In Slovakia we found strong dependence of one indicator of tax burden to business environment - the overall tax burden, measured by tax-to-GDP-ratio. In Germany the results showed that no of the selected indicators of tax burden has significant impact on the evolution of number of business entities.

Based on the findings from the analysis we can conclude that in creating favourable conditions for business activity in Slovakia, attention should be focused primarily on reducing the overall tax burden, so various measures in tax policy to reduce the tax burden should be implemented. In the Czech Republic business entities have responded favourably primarily on decrease of corporate income tax rates, as well as implicit tax rate on corporate income, so it is appropriate to focus on other items affecting the tax base, too. One possibility to make business environment more attractive is to support small and medium enterprises with preferential taxation.

Acknowledgements

The contribution is processed as a part of the research projects VEGA 1/1321/12 Research of new trends in management in the era of globalization and KEGA 070ZU-4/2011 Management and network entrepreneurship in knowledge economics and VEGA 1/0895/13 Research on strategic business management as promoting competitiveness in a dynamic business environment.

References

[1] CHAJDIAK, J.: *Statistical exercises and their solutions in Excel (in Slovak)*, Bratislava, STATIS, 2005. ISBN 80-85659-39-5
[2] *Statistical Office of the Slovak Republic,* [online] Available on Internet: http://www.statistics.sk/pls/elisw/casovy_Rad.procDlg
[3] *Taxation Trends in the European Union. Data for the EU Member States, Iceland and Norway*. Eurostat Statistical Books. European Union, 2012. ISBN 978-92-79-21209-3. Available on Internet: http://ec.europa.eu/taxation_customs/resources/documents/taxation/gen_info/economic_analysis/tax_structures/2012/report.pdf
[4] STOFKOVA, J. et al.: *Finance and Financial Management (in Slovak)*, EDIS – University of Zilina, 2012. ISBN 978-80-554-0169-0
[5] *Statistical Yearbook of the Czech Republic 2012*. Czech Statistical Office, [online] Available on Internet: http://www.czso.cz/csu/2012edicniplan.nsf/engkapitola/0001-12-eng_r_2012-1200
[6] *Genesis – Online Datenbank*. Destatis Statistisches Bundesamt. [online] [cit. 2013-02-02]. Available on Internet: https://www-genesis.destatis.de/genesis/online;jsessionid=CD98F78766583267A12D742C09F61CA0.tomcat_GO_1_1?operation=previous&levelindex=3&levelid=1365452777436&step=3
[7] *Monitoring Revenue Trends and Tax Reforms in Member States 2008, 2009.*

https://doi.org/10.26552/com.C.2013.4.73-79

Pavol Stastniak - Jozef Harusinec *

COMPUTER AIDED SIMULATION ANALYSIS FOR COMPUTATION OF MODAL ANALYSIS OF THE FREIGHT WAGON

This paper deals with theoretical and practical aspects of modal analysis, which belongs to the tests for design of new rail wagons. The paper describes the process for calculating the eigenfrequencies of the wagon with non-standard design and dimensions and strength analysis of the modified construction of bogie type Y25. This computer aided simulation analysis significantly reduces the time to verify the static and dynamic evaluation of rail vehicles.

Keywords: *Modal analysis, eigenfrequencies, design, wagon frame.*

1. Introduction

Modal analysis is a relatively young field of dynamics and in industry started to be used in the 80s of the last century. Late inclusion into practice is associated with the development of software and hardware for finite element method. Modal analysis can be applied in theory, such as computational method or at practical level, such as real experimental measurements of mechanical structures. The modal parameters obtained from experimental analysis in engineering practice are often compared with the modal parameters obtained from computational methods [1]. The resulting modal parameter analysis include:

- eigenfrequencies of the construction,
- mode shapes,
- modal damping of the construction.

The great advantage of the mentioned simulations is that the entire development process of rolling stock is so accelerated, leading to a reduction in overall costs. Simulations and subsequent optimization of the vehicle structure is made before production of the vehicle itself. This leads to minimizing the number of unsatisfactory results conducted on a real vehicle. This may, in such a stage of development lead to delays and increased costs [2].

Computational models of vehicles and their components are more or less simplified compared with the actual ones. This simplification is seen when comparing the results from real tests.

2. Application of modal analysis

Modal analysis method can solve many technical problems encountered in the design, manufacture and operation of mechanical systems or parts. It is also used in the analysis of adverse events of mechanical systems, such as excessive noise, deformation, vibration, damage and so on.

Ride properties significantly influence vehicles mechanical systems [3, 4, 5] dynamic behaviour. We can theoretically predict the movement of the wheelset in the track by means of the wheelset and track geometric characteristics [6] analysis. Geometric characteristics define the rail / wheel profiles contact couple geometrical relationship. The shape of the contact couple crucial influences the size of the contact patch and contact stress between wheel and rail [7] value. This creates loading and excitation forces acting inside vehicle and track systems [8, 9]. The analysis of the mechanical systems dynamics may be analyzed by means of various methods [10].

Reasons for using modal analysis:

- Comparison of data obtained from experimental measurement on the prototype with the corresponding data obtained from finite element method. Optimization of the analytical model, which will be used for further calculations and simulations. This optimized model is free of errors, which were caused by poor application of boundary conditions.
- With the resulting eigenfrequencies unsafe operating conditions can be determined, which are not allowed. If the eigenfrequencies and frequency of excitation are equal, the resonance occurs. This reduces operating life, increases noise and could damage the construction.
- With the resulting mode shapes of vibrations we can determine the places of maximum errors. Subsequently, it is possible to make structural modifications (editing geometry, adding additional elements, changing material characteristics, etc.), which eliminate dangerous vibration.

* **Pavol Stastniak, Jozef Harusinec**
University of Zilina, Faculty of Mechanical Engineering, Department of Transport and Handling Machines, Zilina, Slovakia,
E-mail: pavol.stastniak@fstroj.uniza.sk

- The resulting modal parameters are used to diagnose faults and places of operation.

3. Modal analysis solved by finite element method

The most common type of the dynamic calculation is modal analysis, which determined mode shapes, eigenfrequencies and modal damping of mechanical systems [11]. These parameters provide us with basic information on the dynamic behaviour of mechanical systems.

At present, the modal analysis of mechanical systems is performed in computer programs that operate on the principle of finite element method. The most commonly used programs include ANSYS, ADINA, COMSOL and others.

Using modal analysis by finite element proceeds as follows:

1. Create geometry of the analysed construction.
2. Define material properties (density materials, Poisson's ratio, Young's modulus of elasticity of material).
3. Define the boundary conditions for the creation of computational model.
4. Create a mesh of finite elements (Fig. 1), which consists of a suitably chosen element and its final size (smaller mesh, longer calculation).

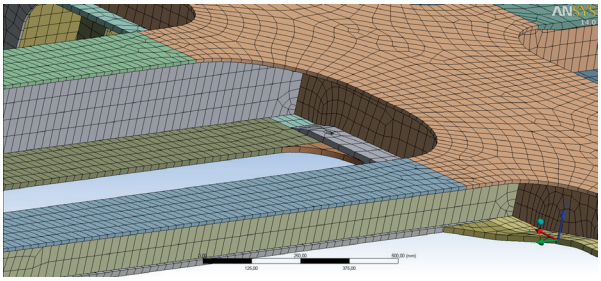

Fig. 1 The mesh of finite elements in the model of wagon

5. Set the solver which contains a suitable computational algorithm. Select the frequency range and number of wanted modes of vibrations in mechanical constructions.
6. Export modal parameters of the analysed construction.

4. Model eigenfrequencies computations

4.1. Model description

- CAD model – freight wagon for intermodal transport in Europe – WEL-WAGON [12, 13, 14],
- the dimensions of FEM model and CAD model – 1:1,
- spatial 3D elements (automatic meshing) – (15 – 30) mm [12, 13, 14],
- standard gravity in axis z – g = 9.8066 m/s^2.

4.2. Material model

- engineering steel S355J2C+N,
- minimum yield value 355 MPa (323 MPa in an immediate close distance of the weld),
- material – homogenous, isotropic, linear and elastic,
- mechanical properties – Young modulus of elasticity E = 210 000 MPa, Poisson`s ratio μ = 0.3.

4.3. Utilised software

ANSYS software allows engineers to construct computer models of structures, machine components or systems, apply operating loads and other design criteria and study physical responses, such as stress levels, pressure, etc. [15].

4.4. Boundary conditions

a) boundary condition in the place of A–D (4 slides),
(The coordinate system is oriented in accordance with Fig. 2. The wagon is supported in the spots of slides. The knots in the slides spots are interconnected with spring elements having stiffness of 0.57 N/m),

b) boundary condition in the places E and F (2 hemispherical bogie pivots) - Table 1.

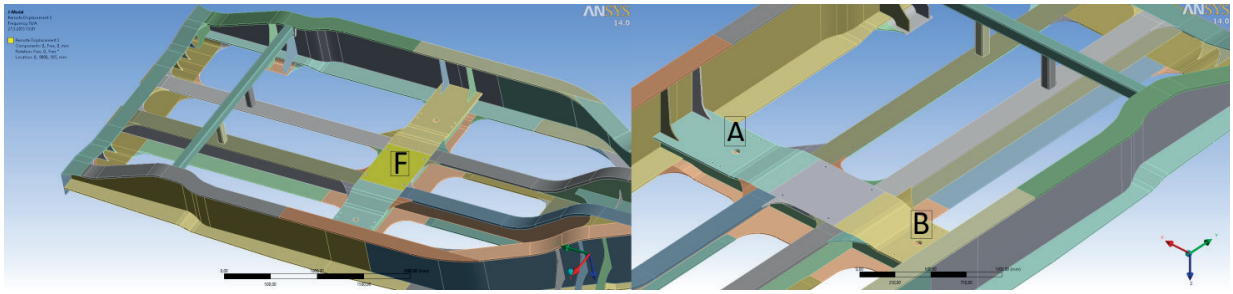

Fig. 2 The places for hemispherical bogie pivots and slides in the model of wagon (the figure shows only 1/2 of wagon, because the model is symmetric)

Boundary condition in the hemispherical bogie pivot Table 1

Ball point No. 1	Condition	Ball point No. 2	Condition
Fx	LOCK	Fx	LOCK
Fw	LOCK	Fw	LOCK
Fv	LOCK	Fv	FREE
Rx	FREE	Rx	FREE
Rw	FREE	Rw	FREE
Rv	FREE	Rv	FREE

LOCK – fixed, FREE – free to the directions of movement or rotation. F_x - displacement in the x direction, F_v – in the v direction, F_w – in the w direction. R_x - rotation in the x axis, R_v – in the v axis, R_w – in the w axis. The program ANSYS used to determine the direction of the symbols x, v, w instead of x, y, z) [16, 17].

4.5. Computation

The bogie for wagon design is the same as the Y25 Lsd1 wagon design and the used suspension has the kinked characteristic curve in the point of 6.63 t/axle [2 and 3]. Spring rigidity: outer spring 0.5076 N/m, inner spring 0.8244 N/m [18].

Wagon spring stiffness up to 6.63 t/axle.
(acts the outer spring only) c = 8121827 N/m

Wagon springs stiffness over to 6.63 t/axle.
(act both of springs) c = 21312264 N/m

Unsprung mass of 1 axle:

$$m_R = m_{wheelset} + m_{axlebox} + m_{springs} \quad (1)$$

$$m_R = 1072 + 240 + (7.2 + 15.45) * 4 = 1402.6\,kg$$

$$m_a = TARA - 4 * m_R = 22000 - 4 * 1402.6 = 16390\,kg \quad (2)$$

The natural angular frequency can be computed by:

$$\omega = \frac{1}{2\pi} \cdot \sqrt{\frac{c}{m_a}} \quad (3)$$

Input parameters for the calculation are given in Table 2.

4.6. Results

It is clear from the analysis that the third loaded wagon eigenfrequency (Fig. 3) is close to the third loaded wagon suspension eigenfrequency (the difference is 0.95 Hz). For further development of the wagon, its ride tests in operation performance are needed. The structural design modification for 3-rd eigenfrequency from the loaded wagon suspension is also needed. Modification can be done by using structural parts respectively assemblies and subassemblies (shape, material thickness, etc.).

5. Strength analysis of the modified construction of bogie type Y25

Bogie Y25 is equipped with a single suspension with duplex coil springs with kinked characteristic curve, a wheel guiding device of axle guard without clearances and with friction dampers with a special construction [19]. Transverse suspension is partially achieved through flexi-coil spring effect (clearance 2 x 10 mm). The frame of the wagon is usually associated with a bogie through the hemispherical bogie pivot (radius 190 mm) and its centre of 925 mm above the track at a weight of 20 t. The bogie

Input parameters for computation Table 2

State of load	Mass [kg]	Suspension stiffness [N/m]	Eigenfrequency [Hz]
Empty -1t	15390	8121827	3.66
Empty	16390	8121827	3.54
Empty +1t	17390	8121827	3.44
Loaded	80390	21312264	2.59

Comparison of the calculated value of eigenfrequency and eigenfrequency of suspension is presented in Table 3.

Comparison of the results for empty and loaded wagons Table 3

Eigenfrequency - number	Calculated value of eigenfrequency [Hz]	Eigenfrequency of suspension [Hz]
Empty wagon		
1	5.01	3.54
2	5.59	3.54
3	9.08	3.54
Loaded wagon (2x40´ containers)		
1	1.52	2.59
2	1.87	2.59
3	2.1	2.59

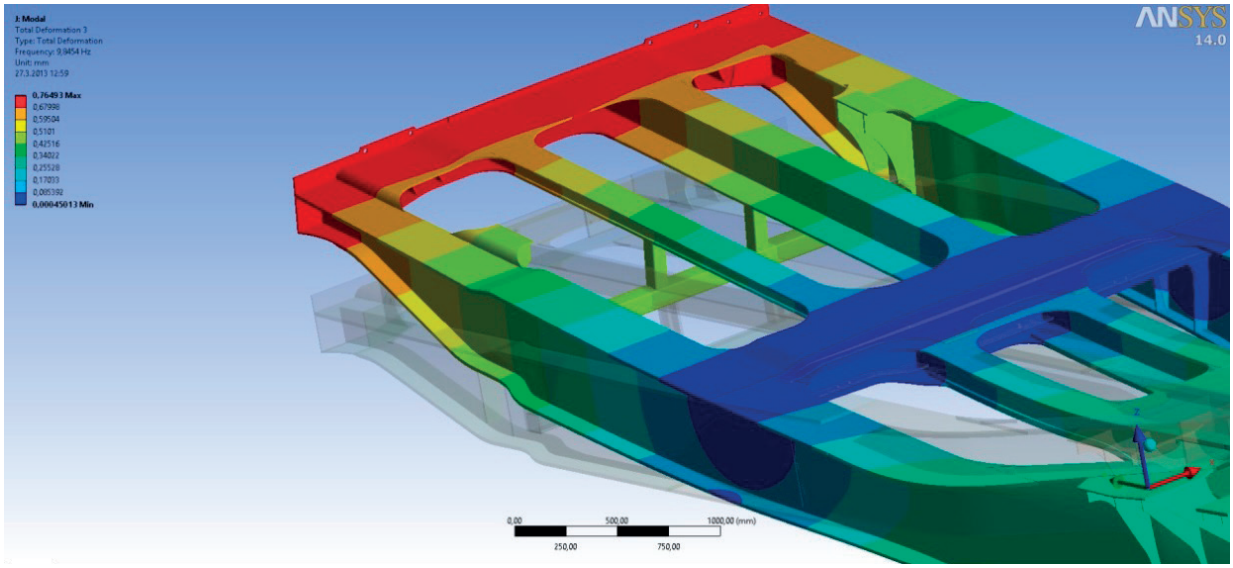

Fig. 3 Visual display of shape shifting in the third eigenfrequency in program ANSYS

was originally designed for the load of 20 t/axle and maximum speed of 100 km/h with a wheel base of 1800 mm [20]. During the development these parameters were upgraded.

At present most bogies are designed for 22.5 t axle load and the maximum speed increased to 120 km/h. Bogies weight is usually from 4.5 to 5 t. Wheel diameter is 920 mm and the wheelbase is 1800 mm. The overall width of the bogie frame is 2440 mm, width at the centre of the axle boxes is 2000 mm for 1435 mm track gauge. 3D model of said bogie frame is shown in Fig. 4.

The modification brought about expansion of the bogie frame Y25 to 1520 mm (Russian gauge) in such a way that the geometry of the frame was changed in the cross-section (+36 mm). The width in the middle of the axle box after modification is 2036 mm. Axle dimensions are given in Table 4.

The diameter of the wheel on the axle is 957 mm. The axle load also increased from 22.5 t to 23.5 t. Due to the rougher climate it is intended with material labelled S 355J2 + N (11523) which has a yield point of 355 MPa and tensile strength 490/630 MPa. It is believed that the weight of the bogie with the adjustments is raised to about 5 t.

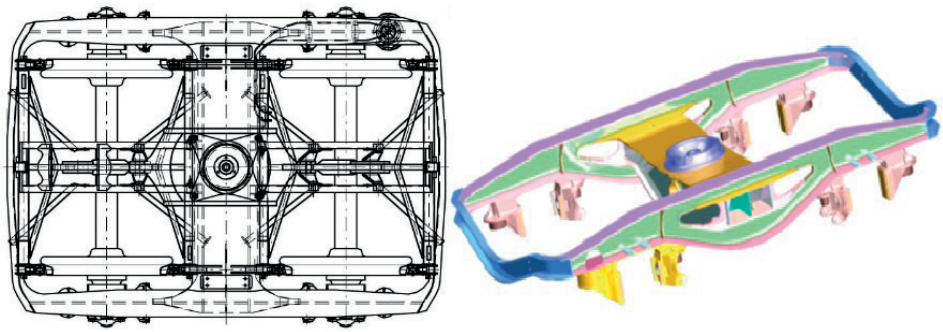

Fig. 4 2D and 3D model of frame bogie in program ProEngineer

Dimensions of PM3 axle

Table 4

Dimensions in mm									
Type of axis	**d1**	**d2**	**d3**	**d4**	**d4**	**d5**	**d5**	**R1**	**R2**
	+0.052	+0.2	+2.0	Nominal value	Tolerance	Nominal value	Tolerance		
	+0.025	+0.12	-0.5						
PM3	130	165	197	180	-1.0	200	+0.045	100	25
							+0.015		

Boundary conditions – hemispherical bogie pivot Table 5

Hemispherical bogie pivot	Displacement	Rotation
The direction of the longitudinal axis of the bogie (global axis x)	ux = R	ϕx = R
The direction of the transverse axis of the bogie (global axis y)	uv = F	ϕv = F
The direction of the vertical axis of the bogie (global axis z)	uw = R	ϕw = F

Boundary conditions – axle guard Table 6

Axle guard	Displacement	Rotation
The direction of the longitudinal axis of the bogie (global axis x)	ux = F	ϕx = F
The direction of the transverse axis of the bogie (global axis y)	uv = R	ϕv = F
The direction of the vertical axis of the bogie (global axis z)	uw = F	ϕw = F

5.1. Computation

The object of the calculation is the strength test of freight bogie frame through FEM analysis. For the calculation of the analyzed parts of the bogie through finite element the program ANSYS was used. They are used as rectangular, four-node "shell" elements. The size of elements in the area under consideration is 5 to 10 mm. The frame is stored in a cylindrical tube with the stiffness equivalent to the stiffness of the suspension. Boundary conditions are created so as to be applicable to all burdensome conditions. Analysis is performed in the linear region. Distortion analysis results due to the simplification mentioned in the introduction are practically negligible [21, 22]. Consideration is being given to the fact that the material is linearly elastic and isotropic.

5.2. Boundary conditions

Reactions in the longitudinal direction (x-axis) are captured in the nodes lying inside the hemispherical bogie pivot (Table 5).

Reactions in the transverse direction (y-axis) are captured in nodes of slides (Table 6).

5.3. Elements

SHELL181 Element

SHELL181 (Fig. 5) is suitable for the analysis of thin and medium thick shell structures. This is a four-node element with six degrees of freedom at each node: in the direction of axis x, y, z and rotation x, y, z. SHELL181 is suitable for large rotation or high stress. Changes in the shell are counted in nonlinear analysis [15].

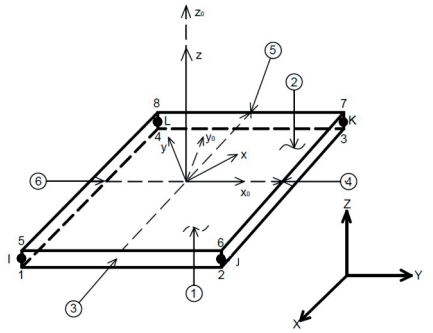

Fig. 5 Four-node element with six degrees of freedom at each node

5.4. Load conditions

Load conditions are as follows:

- **Load condition 1** - consists of vertical force in a hemispherical bogie pivot - 824 kN.
- **Load condition 2** - consists of vertical force in a hemispherical bogie pivot - 429 kN, vertical force on the slides - 107 kN and transverse forces on the hemispherical bogie pivot - 90 kN.

Schematic view of the load condition is shown in Fig. 6. Each component of the solid model was exported as a separate part. Contact links were created among the components (type "bonded"), which simulate the welded joints.

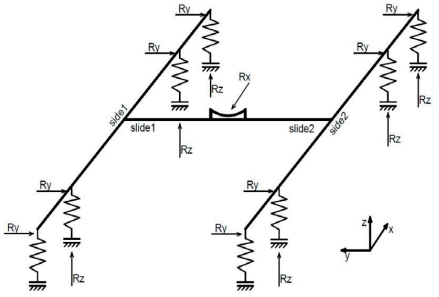

Fig. 6 Schematic view of load condition

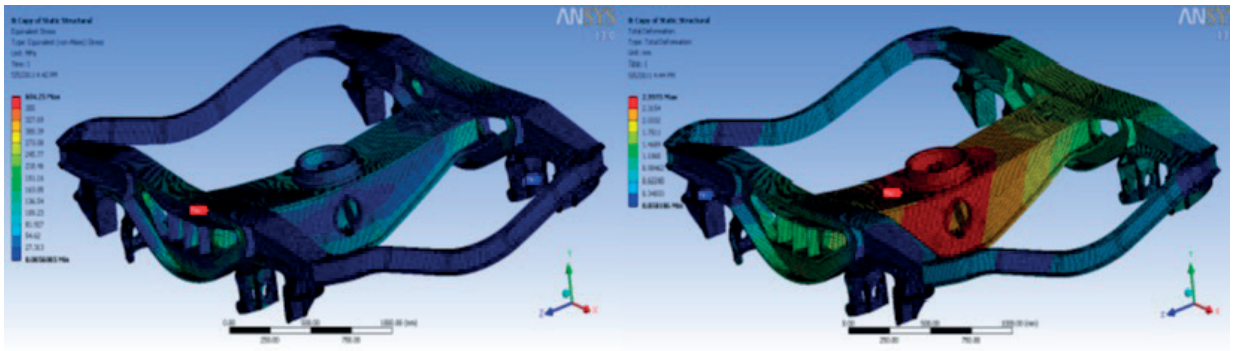

Fig. 7 The behaviour of stress and deformation in program ANSYS

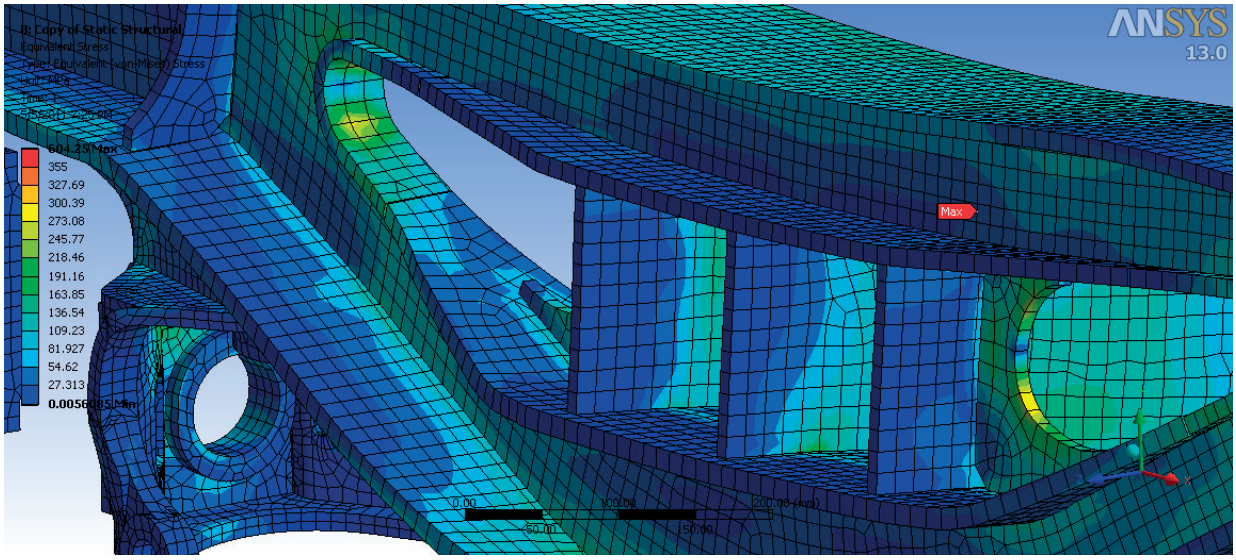

Fig. 8 Location on the model with greatest stress

5.5. Results

Due to the limited scope of this paper, only the results to the load condition 2 are presented. As mentioned, in this case vertical and transverse forces operated in the hemispherical bogie pivot and the slides as well. After the loading of construction in certain places the peaks incurred of stress. These deficiencies can be remedied in several ways. For example, the shape or thickness reinforcements are modified or another type of material is used.

The behaviour of stress and deformation (displacement) is shown in Fig. 7.

Figure 8 shows the location of the greatest stress.

6. Conclusion

Computational simulations are now an integral part of the development process of rolling stock. They allow a more detailed analysis of the behaviour of the vehicle as a whole or its individual parts. Therefore, it is possible to better optimize the design of rail vehicles and prevent potential problems in the operation, which would require increased costs.

Research-Educational Centre of Rail Vehicles (VVCKV)

Acknowledgement

This paper was created during the processing of the project No. APVV-0842-11: "Equivalent railway operation load simulator on the roller rig". The work is also supported by the Scientific Grant Agency of the Ministry of Education of the Slovak Republic and the Slovak Academy of Sciences in project No. 1/0347/12: "Railway wheel tread profile wear research under the rail vehicle in operation conditions simulation on the test bench.", project No. 1/0383/12: "The rail vehicle running properties research with the help of a computer simulation." and No. 1/1098/11: "Stress Distribution in a Braked Railway Wheel".

References

[1] ZMINDAK, M., GRAJCIAR, I., NOZDROVICKY, J.: *Modelling and Computations in Finite Element Method*, Zilina, ISBN 80-968823-5, 2004.

[2] STASTNIAK, P., HARUSINEC, J., GERLICI, J., LACK, T.: *Containers Transport Wagons Design (in Slovak).* Dynamics of Rigid and Deformable Bodies, Usti nad Labem : University J. E. Purkyne. ISBN 978-80-7414-510-0. p. 7, 2012.

[3] NANGOLO, F., N., SOUKUP, J., SVOBODA, M.: Modelling of Vertical Dynamic Response of Railway Vehicle System with Experimental Validation. *Machine Modelling and Simulation*, pp. 295-302, Polytechnika Poznanska : Rokosovo, ISBN 978-83-923315-2-0, 2012.

[4] SKOCILAS, J., SKOCILASOVA, B., SOUKUP, J.: *Determination of the Rheological Properties of Thin Plate under Transient Vibration.* Latin American J. of Solids and Structures. Brasil Society for Mechanics and Engineering. ISSN 1679-7817 (print), 1679-7825 (online).

[5] SOUKUP, J., VALES, F., VOLEK, J., SKOCILAS, J.: Transient Vibration of Thin Viscoelastic Orthotropic Plates. *Acta Mechanica Sinica*, vol. 27, No. 1, pp. 98 - 107. The Chinese Society of Theoretical and Applied Mechanics; Institute of Mechanics, Chinese Academy of Sciences, co-published with Springer, ISSN 0567-7718 (Print), 1614-3116 (online).

[6] GERLICI, J., LACK, T.: Railway Wheel and Rail Head Profiles Development Based on the Geometric Characteristics Shapes. *Wear: An International J. on the Science and Technology of Friction, Lubrication and Wear*. ISSN 0043-1648, vol. 271, No. 1-2 Sp., pp. 246-258, 2011.

[7] GERLICI, J., LACK, T.: Contact Geometry Influence on the Rail / Wheel Surface Stress Distribution. *Procedia Engineering.* ISSN 1877-7058, No. 1, pp. 2249-2257, 2010.

[8] LACK, T., GERLICI, J.: *Tangential Stresses for Non-elliptical Contact Patch Computation by Means of Modified FASTSIM Method.* IAVSD 2013, 23rd Intern. Symposium on Dynamics of Vehicles on Roads and Tracks, Qingdao, Southwest Jiaotong University Chengdu, USB key, p. 6, 2013.

[9] LACK, T., GERLICI, J.: Wheel/Rail Contact Stress Evaluation by Means of the Modified Strip Method. *Communications - Scientific Letters of the University of Zilina,* ISSN 1335-4205, vol. 15, No. 3, pp. 126-132, EDIS – Publishers of the University of Zilina, 2013.

[10] GERLICI, J., LACK, T.: Methods for Vehicle Vibration Analysis in Time Domain. *Prace naukowe Politechniki Warszawskiej,* Z. 63, Transport, pp. 71-81, 2007, 2007.

[11] HARUSINEC, J., STASTNIAK, P., DIZO, J.: *Calculations and Simulations in the Rail Vehicle Constructions Development (in Slovak).* Technolog, University of Zilina: EDIS Zilina, ISBN 1337-8996, pp. 239-244, 2013.

[12] FABIAN, P., GERLICI, J., MASEK, J., MARTON, P.: Versatile, Efficient and Long Wagon for Intermodal Transport in Europe. *Communications - Scientific Letters of the University of Zilina.* ISSN 1335-4205, vol. 15, No. 2, pp. 118-123, 2013.

[13] VEL-WAGON: http://www.vel-wagon.eu/index.php/description. [online], 2010.

[14] FABIAN, P., GERLICI, J., MASEK, J., MARTON, P.: *Development of a New Wagon for Intermodal Freight Transport*. EURO-ZEL 2013. Proc. of the 21st Intern. Symposium Recent Challenges for European Railways, Zilina – Brno : Tribun EU. ISBN 978-80-263-0380-0. - CD-ROM, pp. 298-306, 2013.

[15] ANSYS, *user guide* (part of the program package).

[16] ERRI B12/RP17, No. 8, *Programme of Stresses to be carried out on Wagons with Steel Underframe and Body Structure*. European Rail Research Institute, 1993.

[17] STASTNIAK, P., GERLICI, J., LACK, T., HARUSINEC, J.: *Computer Aided Simulation Analysis for Computation of Modal Analysis of the Freight Wagon*. Transcom 2013, Proc. of the 10th European Conference of Young Researchers and Scientists, Zilina: University of Zilina, ISBN 978-80-554-0695-4, pp. 297.

[18] EN 13749/2005 - Railway Applications - Wheelsets and Bogies - Method of Specifying the Structural Requirements of Bogie Frames.

[19] STASTNIAK, P., HARUSINEC, J., GERLICI, J., LACK, T.: *Stress Analysis of the Modified Bogie Frame of Type Y25 (in Slovak).* Dynamics of Rigid and Deformable Bodies, Usti nad Labem: University J. E. Purkyne. ISBN 978-80-7414-607-7. p. 8, 2013.

[20] DIZO, J., GERLICI, J., LACK, T.: *The Goods Wagon Equipped by Y25 Bogies Computer Simulation Analysis.* Transcom 2013, Proc. of the 10th European Conference of Young Researchers and Scientists, Zilina: University of Zilina, ISBN 978-80-554-0695-4. - pp. 63-66.

[21] EN 12663-2/2010 – *Strength Requests on the Railway Vehicles Bodies Design*.

[22] HARUSINEC, J., DIZO, J., STASTNIAK, P.: *The Computer Simulation of the Goods Wagon Equipped by Y25 Bogies (in Slovak).* Technolog, University of Zilina – EDIS Zilina, ISBN 1337-8996, pp. 245-250, 2013.

https://doi.org/10.26552/com.C.2013.4.80-84

Jana Izvoltova - Peter Pisca - Vladimir Kotka - Marian Mancovic *

3D LASER SCANNING OF RAILWAY LINE

3D laser scanning is very useful method to reach digital terrain model as the common output of map making. The paper deals with an application of 3D laser scanning in railway track measurements, which belong to the field of engineering surveying. Experimental measurements were carried out on the ballast-less railway construction with the purpose to determine its track geometry by the combination of terrestrial and laser scanning methods. Measurements were carried out in conformity with conditions involved in corresponding technical standards. Surveyors used a variety of firmware, CAD and mathematical software for laser scanning processing to reach the expected outputs in adequate volume, accuracy and reliability.

Keywords: *Laser scanning, terrestrial measurements, digital terrain model, ballast-less track construction.*

1. Introduction

Laser scanning belongs to the non contact, fast and accurate methods, which bring highly detailed information about the observed object. It is a type of a surveying procedure with the wide application in the field of civil engineering, industry and architectural surveying, urban topography, reverse engineering, archaeology, mechanical dimensional inspection and many other fields of human activities. 3D laser scanning provides high quality surface modelling, 3D digitizing of mobile and portable objects, inspection and diagnostics in the process of reconstruction of various situations, product development, which means digital reproduction via CAD modelling of some assemblies and other procedures.

The article is focused just on the application of 3D laser scanning in engineering surveying. Up to now, surveyors have reached great experience with laser scanning by slope stability monitoring, bridge deformation measurement, mining and tunnelling, roadway and highway inspection to predict any deteriorations, plant and power station monitoring and observations of cities and historical buildings needed in the process of their reconstruction or documentation.

As classical photogrammetry, surveyors use both ground and aerial laser scanning (LIDAR). Its selection depends on how detailed and accurate data are required to be and what the range of monitored objects is.

The aim of the article is to describe the application of 3D laser scanning in the process of monitoring a railway track construction to find the optimal conditions and real measured accuracy that depends also on the instrument performance: accuracy, range and scan resolution. However, the selection of the optimal mathematical procedure reliable for surface modelling is also very important. Despite the fact that there has not been great experience with the scanning of the railway track construction, because of concern about possible surface reflexion of such a steel construction, the basic aim of this experiment was to reach the real track geometry resulted from the digital model obtained from a point cloud processing.

2. Railway structure specification

Railway modernisation in the Slovak Republic has brought reconstruction of the north route of railway line from west to east Slovakia with the aim to involve high-speed trains. The reconstruction is related to building the new unconventional type of railway structure, ballast-less track RHEDA 2000 [1], based on continuous reinforced concrete slab, which has been situated in the tunnel part of this railway route between towns **Trencin** and **Nove Mesto n/Vahom**. For this fact, the experimental measurements of the representative parts of such a railway

Fig. 1 Ballast-less track structure in the tunnel

* **Jana Izvoltova[1], Peter Pisca[1], Vladimir Kotka[1], Marian Mancovic[2]**
[1]Department of Geodesy, Faculty of Civil Engineering, University of Zilina, Slovakia
[2]The Institute of Foreign Languages, University of Zilina, Slovakia,
E-mail: jana.izvoltova@fstav.uniza.sk

construction were carried out. The experimental location is situated in the railway tunnel (Fig. 1), railway bridge (Fig. 2) and transient sections between the ballast-less track and traditional track structure (Fig. 3) to verify the possible track geometry changes caused by traffic loading.

Fig. 2 Ballast-less track above the railway bridge

Fig. 3 Transient part between ballast-less track and traditional foundation

Railway needs a regular maintenance to keep its deformation and straining, caused by traffic, within elastic limits, otherwise the permanent deformations occur which bring track geometry changes and, consequently, increase the traffic loading efficiency. Now, the track inspection and maintenance is done in the competence of Slovak Railways and it is facilitated by a variety of specialised railway machines. Common maintenance jobs include surfacing and lining track to keep straight lines gauge and curves within maintenance limits [2].

For the purpose to define the track in the absolute position within the national positional reference system, additional geodetic measurements are required. Besides the precise digital levels, which bring absolute heights of railroad, also total stations, GNSS systems or 3D laser scanners can be used to determine absolute three dimensional position of the track layout.

3. Technical requirements for measurements

Generally, the process of control measurements of building objects is carried out in conformity with the complex of technical standards STN 73 0202 – 73 0280, which define the general requirements, purpose, conditions, accuracy and tolerances needed for their measurement and evaluation. Notably, Technical Standard STN 73 0275 [3] is oriented to the accuracy control of three dimensional geometry of the line building objects including their horizontal and vertical layout, longitudinal elevation, transverse elevation and control of the mutual distances between line objects in crossroads. In Slovakia, the Direction SR 103-8 [4] designates special conditions for measurement of the ballast-less high speed track, built from continuous reinforced concrete slab, which links to the direction SZDC S9 [5] valid in the Czech Republic.

Technical standard [3] defines accuracy of the control measurements of building objects by the value of standard deviation:

$$\sigma_{meth.} = 0.5\,\delta_{meth.}\,, \tag{1}$$

where maximal value of control measurements $\delta_{meth.}$ depends on a prescribed tolerance value Δx of a particular measured parameter of track (f. e. track gauge, elevation, curvature, etc.):

$$\delta_{meth.} = 0.2\,\Delta x\,. \tag{2}$$

4. 3D laser scanning of railway track

Recently, 3D laser scanning has become a very useful method for acquiring the accurate three-dimensional detail of a complex observed object or facility, but its application in engineering surveying has some limitations resulting from the uniqueness of the measured structure. Railway track belongs to the long line ground objects and so the technology of its laser scanning has to be conformed to this fact.

For the scanning procedure of rail track, we used a pulsed dual-axis compensated laser scanner Leica ScanStation C10 with the prescribed accuracy of single measurement in position ±6 mm and in distance ±4 mm and angular accuracy is ±12". These specifications designate standard deviation for target acquisition 2 mm. The scanning system is based on 3R green laser of wavelength 532 nm with the scanning range 300 meters [6].

Scanner stations were situated on both sides of the railway lines and their 3D position was determined by the resection method in dependence of the railway benchmarks position. A point cloud was gathered in scan resolution 3 cm at a range of 30 meters while keeping the prescribed accuracy in position ±6 mm. The scan area was limited by the horizontal field of view from 0° to 180° and vertical field of view from -45° to +90°.

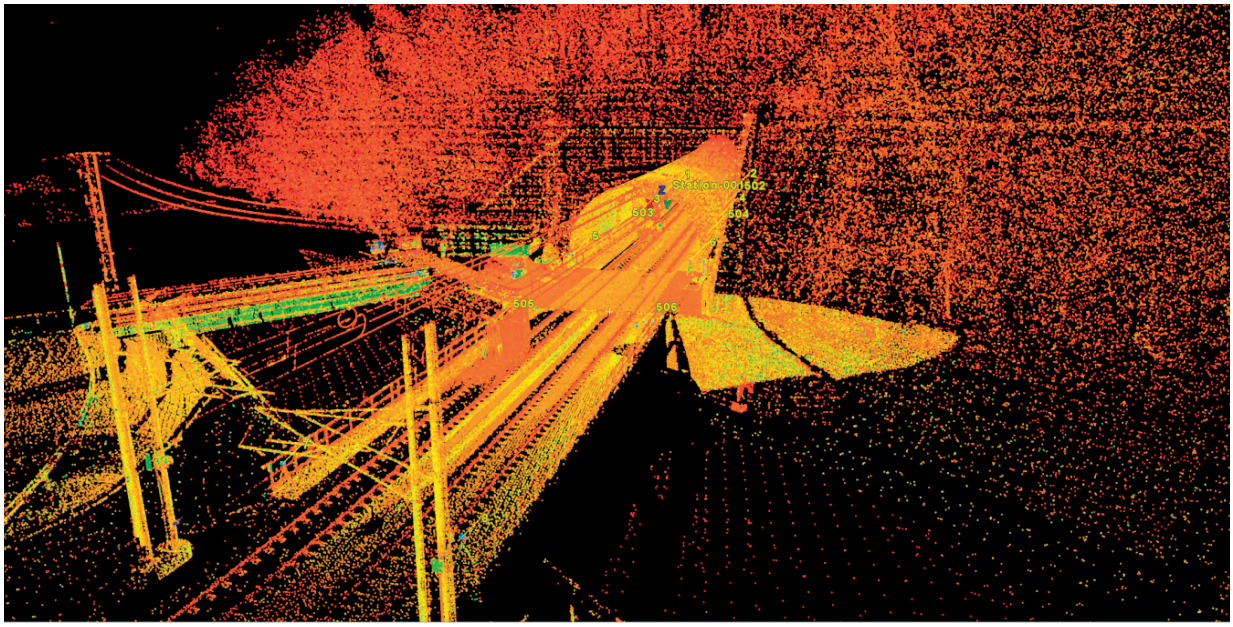

Fig 4 Point cloud of the northern part of the tunnel

Specifically, the experimental location is situated at the railway section 102.360 – 102.535 km in the southern part of the railway tunnel called **Turecky vrch** and at the section 104.200 – 104.840 km in the northern part of the tunnel built in the railway route **Bratislava - Zilina**. The scanning process produces about 9 million points organized in a point cloud, each with their own unique x, y, z, which occupies about 277 MBytes of a computer memory.

5. Point cloud processing

The great volume of raw data gathered by laser scanning, so called point cloud, is utilized by the Cyclone firmware of Leica Geosystems (see Fig. 4) and by CAD software. The point cloud processing belongs to the most time-consuming and a very important part of data utilization.

Each point in the point cloud is measured with the respect to the scanner position, and so the parameter transformation from a local to global national system is necessary to fit the point cloud to the global coordinate system. For this fact, the connection between laser scanning and terrestrial measurement is necessary, which is based on the 3D position of identical points of the both systems. The combination of the both measurement methods also helps to verify the positional data, which are utilized in the post processing procedures [7]. The positional control of observed point cloud is also realized by the photogrammetric method which enables the overlapping of digital photos made by video camera, with corresponding scans [8].

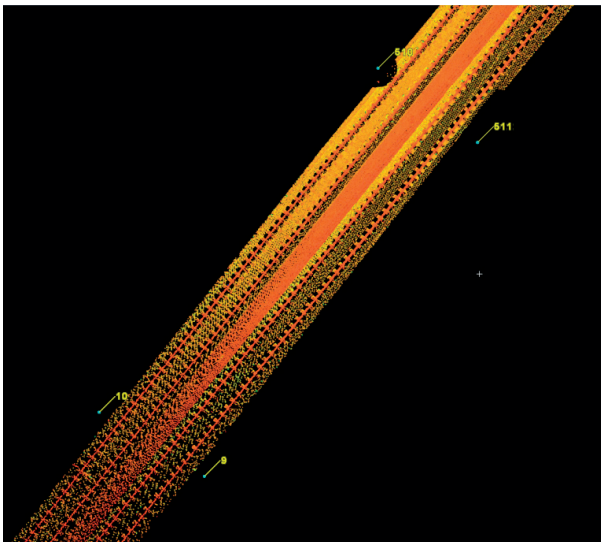

Fig. 5 Point cloud with noise removing in cyclone

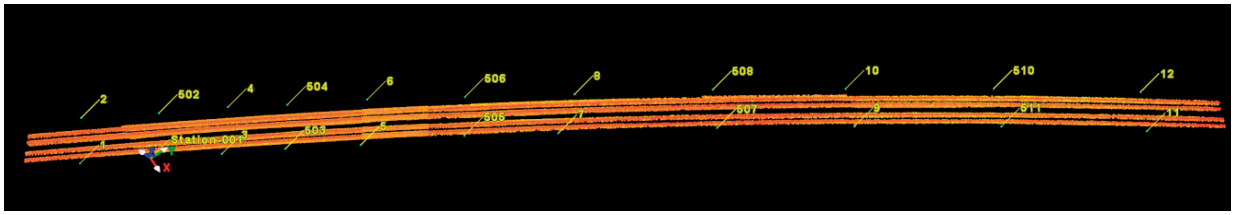

Fig. 6 Railway with two rail tracks in cyclone

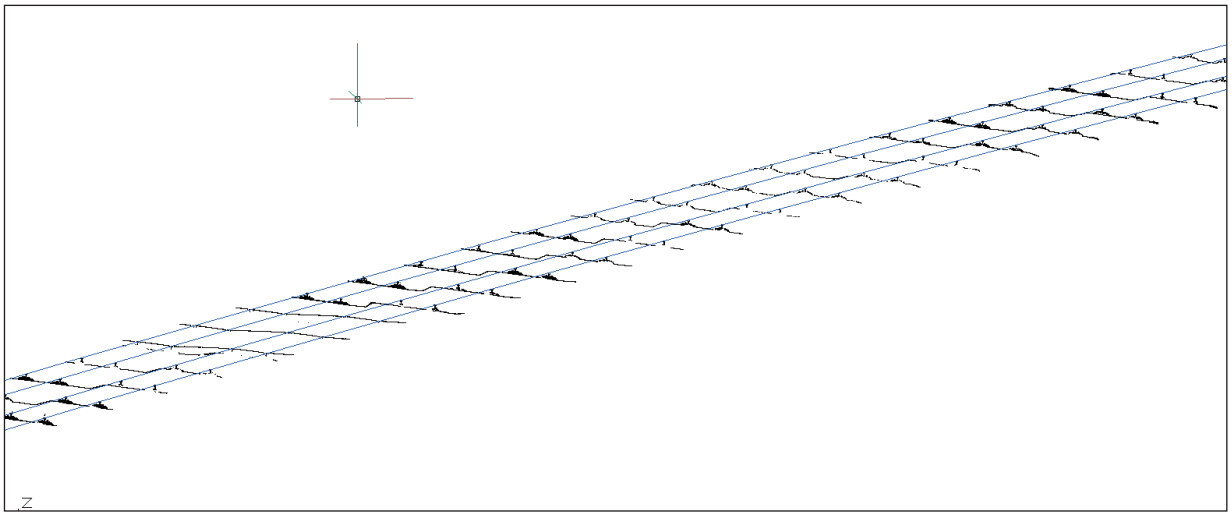

Fig.7 Railway tracks in AutoCAD

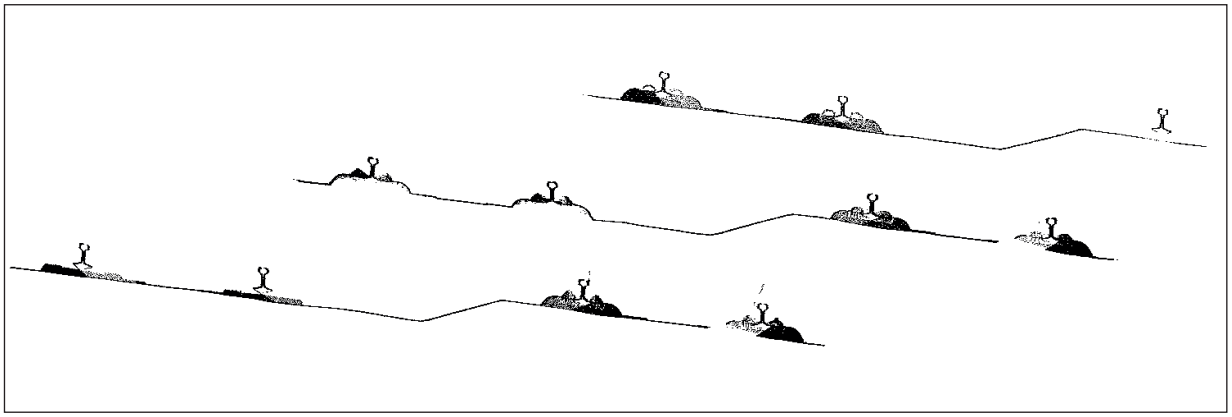

Fig. 8 The scan detail of track shape UIC60

The point cloud processing continues with the feature codes extraction directly from the point cloud and their export to feature code processing software. While scanning a site, the scanner captures everything in the selected field of view. Objects which are not relevant to the surveyor have to be removed from the scan. This removal process is an interactive process and a skilled operator needs only few minutes for extracting and deleting the useless objects. Figs. 5 and 6 show a successive objects extraction of scans which were processed by Cyclone software.

After process removing, the operator creates a digital terrain model, generates contours and measures among any points to calculate elevation differences, slope, axis position and the mutual distance between the railway tracks. This phase of laser scanning processing consists mostly of applying mathematical procedures especially to the regression analysis and mathematical modelling to receive the faithful model of reality [9]. The received mathematical model was finally used to reconstruct the railway track geometry (Figs. 7 and 8).

6. Conclusion

The application of the laser scanning brings to surveyors a great possibility to display the real world in many more details as it was in the past, and it also brings new approaches to utilization of scanning outputs by variety of software. For civil engineering, the most common output from laser scanning is the digital terrain model which can be applied in map making, designing, deformations diagnostics, construction inspection or reconstruction of the historical objects.

The article focuses on the description of the 3D laser scanning method in the process of railway track measurement to define railway layout in the national coordination system and, consequently, to determine the railway track geometry. The connection of terrestrial measurements and laser scanning is very important to define the point cloud in the global reference system, control 3D position of a point and, finally, assure accuracy and reliability of the whole digital terrain model. Measured accuracy depends especially on the used laser system and therefore, the

surveyor has to conform the technology of measurement to its technical performance.

Acknowledgement

This article is the result of the implementation of the project: "Innovation and internationalization of education – the means to increase the quality of the University of Zilina in the European educational space (ITMS: 26110230079) supported by the Research & Development Operational Programme funded by the ERDF.

References

[1] IZVOLT, L., HODAS, S.: *Modernisation of Railway Infrastructure in the Slovak Republic*. COMPRAIL XIII. Intern. Conference on Design and Operation in Railway Engineering. WIT Press Southampton, Boston, ISBN 978-1-84564-616-5

[2] VILLIM, A., MUZIK, J.: *Railway Line Route Trstena - Nowy Targ, the Possibilities of Maintenance*. 15. Science Conference of PhD. study, VUT Faculty of Civil Engineering, Brno, 2013, ISBN 978-80-214-4669-4.

[3] STN 73 0275 Control Measurements of Line Building Objects. Slovak Technical Standard, Bratislava 1985

[4] Direction SR 103-8 (S) General Demands on Designing, Building, Maintenance and Work Acceptance on Ballast-less Structure of Railway Line. Direction of Slovak Railways, Bratislava

[5] Direction SZDC S9 Continuous Railroad, Railroad Administration, Czech Republic, Prague, 2012

[6] HDS Training Manual. Leica Geosystems HDS LLC European Office. Geotech Bratislava

[7] SIMA, J., SEIDLOVA, A.: *Utilization Reflector-loss Distance Meter Leica for Measurement of Rock Walls*. XXI Russian–Slovak–Polish seminar, Moscow: Archangelsk, 2012 ISBN 978-83-7814-021-4

[8] COINER, CH., BRUN, A. P.: 3D *Laser Scanning for Common Surveying Applications Cyra technologies*, Inc. A Leica Geosystems Company: San Ramon, CA, 2006

[9] MUZIK, J., KOVARIK, K., SITANYOVA, D.: Meshless Analysis of an Embankment Using Local Galerkin Radial Point Interpolation Method (LGRPIM), *Communications - Scientific Letters of the University of Zilina*, No. 2, 2013, ISSN 1335-4205, p. 34-40.

https://doi.org/10.26552/com.C.2013.4.85-90

Vladimir Mozer *

MODELLING FIRE SEVERITY AND EVACUATION IN TUNNELS

Adequate design methods and tools are vital to any construction project, especially when its complexity and value are high. Tunnels, road or railway, are a good example of such structures. This paper deals with the topic of computer modelling utilization in the design and evaluation of fire safety in tunnels. The capabilities of selected software – Fire dynamics simulator + Evac – are demonstrated on a practical example – Tunnel Lucivna in the Slovak Republic. In this example case, both fire and evacuation modelling is used in conjunction to assess the overall fire safety of the tunnel. The results show the effects of fire on the tunnel structure as well as the persons inside the tunnel trying to evacuate.

Keywords: *Fire severity, computer fire modeling, evacuation, tunnel fires, smoke movement.*

1. Introduction

This paper is the third one in a series of papers dealing with computer modelling of fires in tunnels. The first paper [1] is an introduction to the topic and deals with a simplified scenario to demonstrate computer modelling capabilities in this area. In the second paper [2] full detailed scenario is modelled and further parameters evaluated. Current work goes even further and incorporates evacuation modelling and evaluates the effect of the boundary conditions at the tunnel's portals.

Tunnel fires are very different from fires within 'standard' buildings due to their specific construction. This, in combination with potentially large fire loads, such as fully laden lorries, creates conditions for very severe fires of tens of megawatts. It is therefore necessary that every tunnel is designed to withstand a realistic worst case fire and allows for safe evacuation and effective fire-fighting.

Computer fire modelling is a very suitable tool for this purpose. After over three decades of application of computer based information systems to the crisis management, these systems are getting wider acceptance by the community of the emergency managers and designers [3].

1.1. Fire as a major hazard and threat to tunnels

It was stated previously that tunnels are quite vulnerable to fire, be it accidentally or deliberately started, which is primarily due to their specific construction and the ease of access.

A recent study entitled *Making transportation tunnels safe and secure* [4] evaluated the various hazards and threats that may adversely affect transportation tunnels. To give a concise overview of the hazards and threats, they are tabulated, together with their potential to damage the normal operation of a transportation system, including specific tunnel components (Table 1).

Major hazards and threats to transportation tunnels and associated features [4] Table 1

Hazard or threat	Vulnerable tunnel feature									
	Tunnel construction and engineering feature						Tunnel system feature			
	Immersed tube	Cut-and -cover	Bored or mined	Vent shaft	Portal	Station	Distribution channel	Control center	Substation	Utility building
Hazard										
Fire (unintentional)	✓	✓	✓	✓	✓	✓	✓	✓	✓	✓
Structural integrity loss by natural causes	✓	✓	✓	✓	✓	✓	✓	✓	✓	
Introduction of hazardous materials	✓	✓	✓	✓	✓	✓				
Threat										
Small IEDs	✓	✓	✓	✓	✓		✓	✓	✓	✓
Medium-sized IEDs	✓	✓	✓	✓	✓	✓	✓	✓	✓	✓
Large IEDs	✓	✓	✓	✓	✓	✓	✓	✓	✓	✓
Chemical agents				✓		✓				
Biological agents				✓		✓				
Radiological agents	✓	✓	✓		✓	✓				
Cyber attack								✓		
Maritime Incident	✓		✓							
Fire (arson)	✓	✓	✓	✓	✓	✓	✓	✓	✓	✓
Sabotage of MEC systems	✓	✓	✓	✓		✓	✓	✓	✓	✓

IED – Improvised explosive device
MEC- mechanical, electrical and communication

* **Vladimir Mozer**
Department of Fire Engineering, Faculty of Special Engineering, University of Zilina, Slovakia, Email: vladimir.mozer@fsi.uniza.sk

It is clear that fire has the most destructive potential, along with medium and large improvised explosive devices (which can lead to a fire too) The table lists the various types of tunnels, as well as their engineering and system features that may be affected. Thus, there is a possibility that a fire may take the tunnel out of service. The duration of the service disruption, of course, depends on the extent of damage caused. Nonetheless, it is not just the tunnel itself that is affected, but also the transportation network the tunnel forms a vital part of. This is particularly the case of tunnels forming part of critical infrastructure and tunnels located in urban areas.

It is therefore necessary that these tunnels are designed to withstand a predictable and reasonable worst case scenario, taking into account their specific construction and engineering features. Since there is no universal approach to fire safety in tunnel design, the design team should exercise all due diligence and employ appropriate tools.

2. Tunnel fire and evacuation model

Fire dynamics simulator incorporating sub model Evac was selected for modelling of the tunnel fire and evacuation scenario. It is a CFD modelling software developed by the National Institute of Standards and Technology (NIST, USA) and VTT Technical Research Centre of Finland.

The tunnel in which the fire was modelled is Lucivna tunnel located on the D1 motorway near Strba, Slovak Republic.

2.1. Fire dynamics simulator

FDS is a computational fluid dynamics field computer model. FDS solves numerically a form of the Navier-Stokes equations appropriate for low-speed flow with an emphasis on smoke and heat transport from fires [5]. The second part of the package is Smokeview, a computer program for visualization of the results computed by FDS.

FDS uses rectangular geometry and divides the computational domain into a number of cells that compose a rectangular grid. All basic geometry is to fit within these cells; each cell represents uniform conditions. Besides the geometry one needs to set the fuel properties (chemical and physical), combustion reaction properties, ventilation and ambient conditions etc, known also as boundary conditions. FDS allows the user to work with logical devices that can undertake a specified action for a set condition.

This way, it is possible to model various detectors (smoke, heat, ionization), measure temperature, visibility obscuration and so on. Activation impulses from these devices then can trigger either some desired action (e.g. turn on ventilation) or activate sprinklers or start the discharge of a gaseous suppressant into the protected space. Results, point or planar, can be represented in numerical form or visually in Smokeview for planar results.

FDS version 6.0 RC 3 was used to model the case for this paper.

2.2. FDS + Evac

FDS+Evac is a combined agent-based egress calculation model and a Computational Fluid Dynamics (CFD) model of fire-driven fluid flow, where the fire and egress parts are interacting. FDS+Evac models the egress of the agents using continuous space and time, but the building geometry is fitted to the underlying rectilinear mesh. FDS+Evac uses simple rules and artificial intelligence to model the exit selection processes of the evacuees [6]. Evac is embedded in the FDS executable and is invoked automatically when an FDS input file contains Evac commands.

FDS+Evac version 2.5.0 included with FDS version 6.0 RC was used to model the case for this paper.

In FDS-Evac, there are two main parts of an evacuation scenario. Firstly, one needs to specify the geometry of the modelled case and assign specific boundary conditions. Secondly, the number and characteristics of the evacuees are required.

As part of the geometry of an evacuation case, a dedicated evacuation mesh is required. This is essentially a two-dimensional mesh as it has only one cell in the z direction. Specific exit boundary conditions have to be assigned to areas which are to be used as egress points (removal of agents from the calculation). Any part of the fire geometry that is to form an obstruction must extend itself through the evacuation mesh.

To define the response and behaviour of the evacuees (agents) a wide range of properties is available. This includes the dimensions of the agents, their response and speed, social force parameters etc.

2.3. Modelled tunnel

As mentioned above, the modelled tunnel is an existing road tunnel in the Slovak Republic. It was selected as its geometry is nearly rectangular and the length of the tube is 250m. Due to its length ventilation is natural via the portals. Each tube has a width of approx 12m and a height of approximately 6m. The walls of the tunnel are constructed of reinforced concrete approximately 1m thick. Only one of the two tunnel tubes was modelled as they are identical and completely separated. A fire in one of the tubes would therefore not affect the other tube, unless a structural failure occurred.

In order to achieve reasonable accuracy and computational times three, partially-overlapping, computational grids (meshes) were employed.

The main fire mesh had cells with dimensions 0.25m×0.25m×0.25m and was used to model the central section of the tunnel, where the fire source was located. This section covered a length of 30m, 15m in each direction from the fire centreline.

A coarser mesh, with a cell of 0.5m×0.5m×0.5m, covers the rest of the tunnel tube on each end of the fire mesh. These meshes have a 2.5m overlap with the fire mesh, to allow for uninterrupted flow.

This mesh setup resulted in a total of 267840 cells in the computational domain.

The boundaries of the computational domain corresponded with the tunnel walls, floor and ceiling. To simulate the discharge of smoke from the tunnel portals the computational domain was extended by 3m from each portal. This part of the computational domain was assigned an open boundary condition, meaning that smoke and air could flow freely from and into the tunnel.

Apart from lighting and signage, there is no further equipment installed in the tunnel. It represents a base modelling scenario, in which the fire is the primary driving force for all flows within the tunnel.

2.4. Fire scenario

A fully-laden van fire was simulated. The footprint of the fire was 10m^2 (5m×2m) and its growth was simulated using the t-squared 'ultrafast' fire [7], which is the recommended design fire for tunnel scenarios [8]. The fire was set up in the following phases:

Growth phase	0 – 330s	0 20MW
Fully-developed phase	330 – 2130s	20MW constant
Decay phase	2130 – 2700s	20 0MW

The development of the fire and rate of burning is depicted in Fig. 1. After integration, the total mass of fuel burned during the simulation equals approximately to 1125kg of fuel which is a very realistic assumption for a fully-laden van including its interior materials.

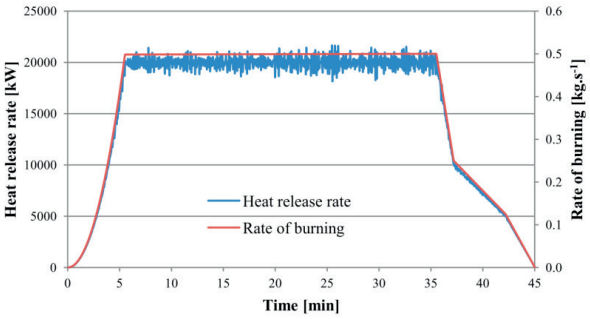

Fig. 1 Development of heat release and burning rates

The type of fuel was selected a mixture of plastics, namely polyethylene, polypropylene and polycarbonate. This way, it reflects the nature of the transported goods as well as interior materials.

Although of a significant size, the above fire represents a less severe tunnel fire, which according to the literature [9] can achieve 100MW and more.

2.5. Evacuation scenario

An evacuation scenario was specified in addition to the fire scenario described above. 60 evacuees (estimate based on the number of vehicles in the tunnel) were placed in one half of the tunnel length. One half of the tunnel length was assumed due to the fact that the vehicles after the fire (in the direction of travel) would continue to drive, leaving the second half of the tunnel length empty.

There were a total of 24 vehicles placed in the tunnel, representing obstructions for the evacuees. The initial distribution of the vehicles and evacuees (random) is shown in Fig. 2. The evacuation computational grid had 75 000 cell (1250×60) and covered the same geometrical area (X- and Y-axis-wise) as the fire meshes.

The start of the evacuation was set to 180s from the ignition of the fire. At this time the smoke travels approximately ¾ of the length from the fire to a portal, i.e. the presence of fire would be apparent. This was based on the outcomes of the model in [2]. Where smoke density exceeded prescribed levels, the evacuees started egress before the preset 180s start point.

2.6. Measured quantities

Measurements of various quantities were taken during the simulation. These measurements were taken at the fire centre point (0m), 5m, 10m, 20m, 50m and 100m away. At each of these locations, there was a tree of thermocouples, located at 1m, 2m, 3m, 4m, 5m and 6m above floor level.

Temperatures of the ceiling were recorded to establish the destructive potential of the fire. Other temperature measurements were taken at 2m above floor level to assess tenability levels and potential danger to evacuating persons.

To further assess tenability and impact on the evacuees, the levels of carbon dioxide–CO, and smoke movement were monitored; the first in the form of point measurements at 2m above floor level, the latter visually through Smokeview.

Additional data were available from the evacuation calculations.

3. Results

As mentioned above, the first measured quantity was the temperature of the ceiling, the development of which is shown in Fig. 3.

The temperatures measured directly above the fire, increased sharply during the first five minutes, following the trend of the heat release rate. The concrete spalling temperature of around 300°C is therefore quickly exceeded; dangerous explosive

Fig. 2 Top view of tunnel with vehicles (white), fire (red), exits (yellow) and evacuees

deterioration of the concrete structure is expected to occur at this rate of temperature increase and the temperature achieved.

Another conclusion that may be drawn from the ceiling temperatures is the effect on steel pre-stressing or reinforcing members inside the concrete structure. The critical temperature of steel (around 400–450°C) may be achieved, depending on the location—depth, which leads to a loss of strength and potentially structural integrity.

On the other hand, the temperature sharply decreases with the increasing distance from the fire. Even 5m away from the fire the temperature drops below critical values (around 200–250°C), meaning that any structural damage to the tunnel would be most likely of a local character. This is of course subject to the fire not spreading to further vehicles in its vicinity, in which case the damage would be of a greater extent.

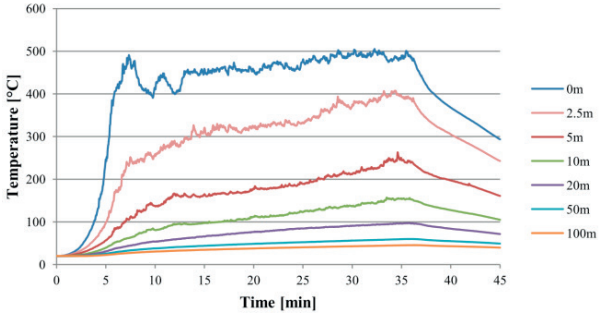

Fig. 3 Ceiling temperatures at various distances from fire

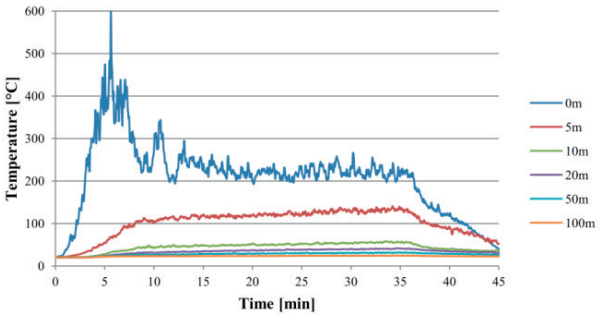

Fig. 4 Temperatures at 2m above floor at various distances from fire

Temperatures at 2m above floor level (Fig. 4) show, that except for the fire itself, tenability limits are exceeded only in the location 5m away from fire. In this location, the maximum temperature is peaking at around 130°C. Further away from the fire, the temperatures decrease to levels which are not life threatening (50°C and less). This is caused by the current of fresh air, which is being drawn from the portals towards the fire.

To establish whether radiative fire spread would take place the intensity of radiative heat flux was monitored in the vicinity of the fire. The results of these measurements are shown in Fig. 5. The critical value of radiative heat flux (shown in dashed line), below which fire spread should not occur is 10 $kW.m^{-2}$ [10].

It is clear from the above figure that there is a significant potential for fire spread via radiation to the vehicles in the vicinity of the fire. The critical value of 10 $kW.m^{-2}$ is exceeded on the entire front face of the first vehicle located 3m away from the fire; even higher intensities are recorded on the vehicle to the side of the fire. It is therefore likely that the fire would spread to these vehicles and grow beyond 20MW. This highlights the importance

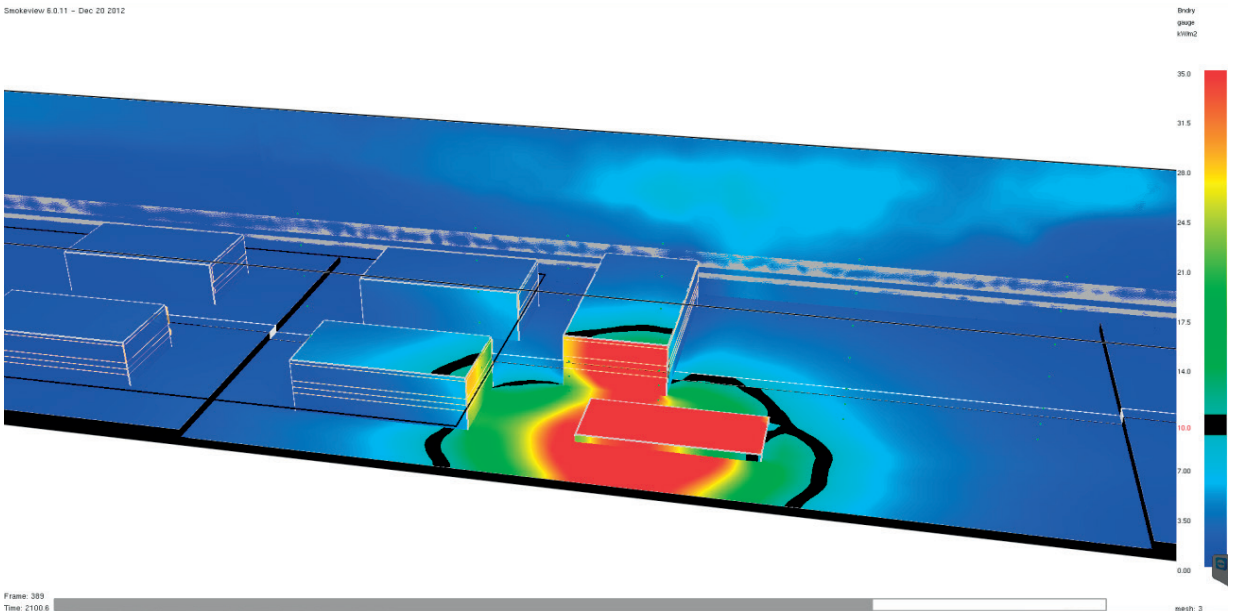

Fig. 5 Radiative heat flux intensity on surfaces (limit shown in black) at 35min

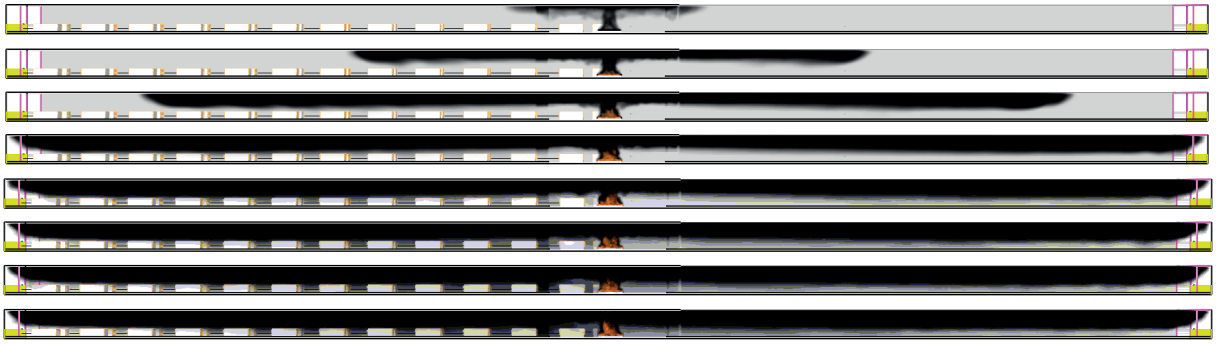

Fig. 6 Smoke movement inside the tunnel 60-480s (60s intervals)

of adequate fire scenario selection – isolated accident vs accident involving a number of vehicles.

With the exception of the fire area and its very close proximity (2m), the CO levels monitored at 2m above floor level did not exceed 11ppm during the simulation. Such levels pose no threat to the evacuees and there is no danger of their incapacitation. Again, this is caused by the fresh air current flowing towards the fire.

The visualisation of the simulation shows that there would be some smoke present in the lower layer of incoming air. This is caused by the turbulent mixing on the boundary between hot (smoke) and cold (fresh air) layers. In Fig. 6 a sequence of images illustrates how smoke is being drawn from the upper layer by the incoming air current. This is particularly obvious at the portals. The presence of smoke may of course negatively affect orientation and evacuation.

The evacuation simulation indicates that for this particular scenario (size of fire, geometry of tunnel, number of evacuees and their distribution) all the evacuees (also referred to as agents in FDS+Evac) were able to leave the tunnel safely.

Figure 7 shows the progress of the evacuation in time from the start of the fire. The evacuees commenced evacuation after 180s (see Section 2.5 for details) and the ones located near the tunnel entrance portal left almost immediately. Then the number of the evacuees decreased steadily with time indicating that the widths of the evacuation routes were sufficient. The evacuation time was therefore a function of the distribution and travel speed of the evacuees. Apart from two, all the evacuees had chosen to egress via the tunnel entrance portal, i.e. away from the fire, which is logical and expected behaviour.

To establish the level of evacuees' exposure to toxic combustion products FDS+Evac calculates so-called fractional effective dose (FED) which is a cumulative rate of all the toxic combustion products. When this rate reaches the value of 1, the affected agent is 'dead', i.e. it has been exposed to a lethal dose of noxious substances. Fig. 8 shows that none of the evacuees experienced a lethal or near-lethal exposure. The FED increases with the duration of exposure and concentration of noxious gases which is directly dependent on the size of the fire. When the graph in Fig. 8 is compared with the smoke distribution in Fig. 6, the growing smoke layer corresponds with the increase in FED. The sharp decrease of the FED curve is caused by the fact that all the evacuees left the tunnel safely and are no longer included in the calculation.

The visualization of the evacuation (via Smokeview) is also available, however, its format is not adequate for paper presentation; it shows the movement of the individual agents.

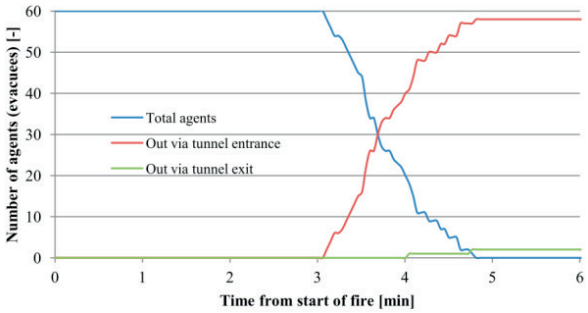

Fig. 7 Evacuation progress and usage of tunnel entrance and exit

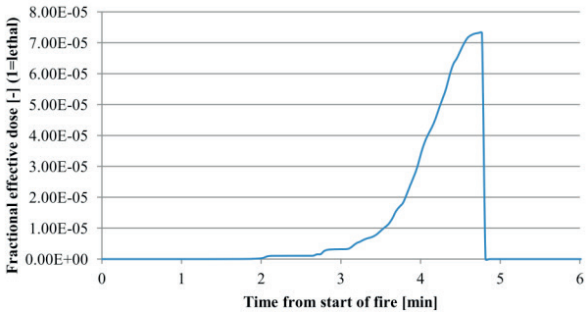

Fig. 8 Maximum fractional effective dose of toxic combustion products

4. Conclusion

Computer fire and modelling, namely Fire dynamics simulator + Evac, has been applied to a simple realistic scenario. The aim of the model was to demonstrate the capabilities of computer modelling in this area as well as evaluate the fire safety of an

existing tunnel. The modelled fire was a fire of a van carrying plastic goods.

The results show that even a relatively small (on this scale) initial fire has the potential to grow significantly larger if other vehicles are sufficiently close. Radiative heat transfer plays a major role in this.

As regards structural integrity, the modelled fire would most likely cause some damage to the structure of the tunnel. The extent of the damage would be limited to the actual area of fire and its immediate vicinity.

The evacuation model results indicate that all persons inside the tunnel should be able to evacuate safely and reasonably fast. There should be no dangerous concentrations of combustion products, only some smoke in the lower layer, due to the turbulent nature of the air and smoke currents.

Overall, the fire scenario used as a basis for this paper should not pose a significant threat to the tunnel construction and persons located inside during the accident.

References

[1] MOZER, V.: *Predicting Fire Severity in Tunnels*, Proc. of conrefence Transcom 2013, Zilina, University of Zilina: Edis, 2013.
[2] MOZER, V., et al.: *Fire Safety in Tunnels Forming Part of Critical Infrastructure, Proc. of conference* ICCST 2013, Medellin, University of Antioquia, 2013. (to be published)
[3] RISTVEJ, J., ZAGORECKI, A.: Information Systems for Crisis Management - Current Applications and Future Directions, *Communications: Scientific Letters of the University of Zilina*, No. 2, vol. 13, 2011, p. 59-63, ISSN: 1335-4205.
[4] Transportation Research Board, *Making Transportation Tunnels Aafe and Secure*, NCHPRP Report 525, vol.12 Washington DC, Transportation Research Board, 2007.
[5] MC GRATTAN, K. et al.: *Fire Dynamics Simulator (Version 6) - User's guide*, Maryland, NIST, 2012.
[6] KORHONEN, T., HOSTIKKA, S.: *Fire Dynamics Simulator with Evacuation: FDS+Evac Technical reference & User's guide*, Finland: VTT, 2010.
[7] DI NENO, P. J.: *SFPE Handbook of Fire Protection Engineering*, 3rd ed. Maryland, SFPE, 2002
[8] BROOKS, R., et al.: *Design of Smoke Ventilation Systems for Loading Bays & Coach Parks – a Guide for System Designers*, Reading, Smoke control association, 2010
[9] MAEVSKI, Y. I.: *Design Fires in Road Tunnels*, Washington DC, NCHRP, 2011
[10] NFPA 92B *Standard for Smoke Management Systems in Malls, Atria, and Large Spaces*, 2009 ed. Massachusetts, 2009.

https://doi.org/10.26552/com.C.2013.4.91-95

Jan Fischer *

SUSTAINABLE MOBILITY IN THE CITY OF BRATISLAVA – TRAM PRIORITY

United Nations Development Programme (UNDP), acting as an implementing agency of the Global Environment Facility (GEF) implemented the project "Sustainable Mobility in the City of Bratislava". One component of the project deals with a higher level of priority to Bratislava's trams.

Driving time information from the ITCS of Bratislava public transport operator was evaluated with Hamburg-Consults software "planfahrt" in order to find obstacles responsible for slowing down tram operation. Thereafter measures based on best practice solutions were introduced for a fast and reliable tram operation: "The tram stops at stations only".

Integral part was the simulation of public transport priority at three signalized intersections using transport modelling software "ptv VISSIM". The results prove the effectiveness of the priority. Public transport waiting times are reduced; the reliability of public transport operations improves.

Keywords: *Public transport, tram, transport planning, ITCS, driving times, public transport priority.*

1. Introduction

The transport sector is the third largest polluting sector in the Slovak Republic with respect to the emissions of greenhouse gases, after Energy and Manufacturing. CO2 emissions from transport represented 14.5 % of the total national GHG emissions in the Slovak Republic in 2010 [1]. The United Nations Development Programme (UNDP), acting as an implementing agency of the Global Environment Facility (GEF), is implementing the project "Sustainable Mobility in the City of Bratislava" financed by GEF within the umbrella of its Operational Program 11 and Strategic Program 5 Promoting Sustainable Innovative Systems for Urban Transport [2].

This part of the project deals with a higher level of priority to Bratislava's trams at signalized intersection in order to increase the service speeds. Additionally to the project title the focus was extended to all components of a modern tram system.

Exemplarily two out of four tram branches were surveyed in order to find obstacles responsible for slowing down tram operation. Both Racianska and Vajnorska branches have a widely separated alignment from the individual transport. Therefore, priority measures can be realised comparatively easily. Multiple tram lines serve each corridor with headways up to 4 minutes together [3].

The project was realized between June 2011 and February 2012. First, it was evaluated whether the selected tram corridors comply with design principles and system parameters of modern tram operations. By detailed analyses of ITCS (Intermodal Transport Control System) data main bottlenecks were located. Afterwards in-depth analyses of three intersections were carried out. The effectiveness of priority measures was checked by a micro-simulation model.

Stakeholders in this project were:

- UNDP as the implementing agency represented by UNDP Bratislava Regional Centre,
- Energy Centre Bratislava as the central project manager,
- Hamburg-Consult (HC) providing international expertise together with VerkehrsConsult Dresden-Berlin responsible for the modelling, and
- DIC Bratislava as a local counterpart.

At all stages, the local municipality (namely the Main Transport Engineer of Bratislava) and the local public transport operator Dopravny Podnik Bratislava (DPB) participated and supported the project.

2. Survey of current situation

Besides a comprehensive field survey, main bottlenecks and shortcomings should be assessed in a quantitative way. Therefore, the realised driving times of Bratislava trams were evaluated. Bratislava public transport company DPB provided us with performing data from their operation control system. Nearly 20,000 trips representing the traffic situation in March 2011 were transferred to Hamburg-Consult´s software "planfahrt". This software used by more than 100 public transport operators and authorities in Europe is designed for analysing data from Automatic Passenger Counting systems as well as driving time surveys [4].

* **Jan Fischer**
Hamburg-Consult GmbH, Transport Planning and Public Transport Operations, Hamburg, Germany, E-mail: j.fischer@hamburg-consult.de

Driving times on Racianska corridor Table 1

Station	Distance (m)	Theoretical (shortest) driving time (s)	Realised average driving time (s)	Deviation (s)	Deviation (%)	Average dwell time (s)
Racianske myto						
Ursinyho	502	49	69	21	42%	14
Pionierska	836	73	139	67	91%	15
Riazanska	552	52	84	32	61%	16
Mlada garda	396	41	63	21	52%	16
Nam. Biely kriz	548	52	77	25	48%	13
ZST Vinohrady	456	45	113	68	150%	17
Vozovna Krasnany	349	38	81	43	114%	13
Novy zahon	347	38	51	14	36%	11
Pekna cesta	639	59	91	32	54%	15
Cernockeho	529	51	67	17	33%	13
Heckova	375	40	61	22	54%	17
Hybesova	567	53	80	26	50%	13
Detvianska	516	50	77	27	55%	16
Zahumenice	404	42	95	54	128%	13
Pri vinohradoch	530	51	77	26	52%	10
Komisarky	164	24	28	4	15%	
Total	**7.710**	**757**	**1.254**	**497**	**66%**	**213**

Main bottlenecks are located at following sections
- Nam. Biely kriz – ZST Vinohrady: 68 s / 150 %
- Ursinyho – Pionierska: 67 s / 91 %
- Detvianska – Zahumenice: 54 s / 128 %

The performance data indicate e.g. for Racianska branch an average journey time of 24.5 minutes. As the timetable states a driving time of 20 minutes, an average delay of 4.5 minutes shows the unreliability of tram operations [5]. Additionally, a theoretical minimum driving time consisting of the vehicle performance and station spacing distance was calculated with 12.6 minutes (+3.5 minutes total dwell time at the stations). The gap between the theoretical and realised driving times represents the potential for tram priority. A total utilization of this potential would increase the attractiveness of the tram system and would additionally save 3 vehicles under the conditions of the current timetable. Table 1 shows the results for Racianska branch.

The combination of the driving time evaluation with the field survey demonstrates the bottlenecks in a very obvious way and allows for creating applicable improvements. The following Fig. 1 shows an extract of Racianska branch.

After the analyses of current situation, measures were introduced in order to realize the mentioned potential and to ensure the fast and reliable tram operation: "The tram stops at stations only". All recommendations are based on best practice solutions from the state of the art tram systems consisting of following components:
- Alignment separated from other means of transport,
- Alignment with low level of constraints because of track conditions, curve radii or switches,
- Attractive station design with a focus on safe access and waiting areas,
- Attractive public transport transfer hubs,
- Priority at unsignalized intersections,
- Priority at pedestrian crossings, and
- Priority at signalized intersections.

Outside the Central Business District, Bratislava trams operate almost exclusively on separated alignments but multiple constraints causing severe speed limits can be found. The constraints result from an alignment with tight curve radii, outdated technology of point locks and insufficient maintenance of the track superstructure. Examples are shown in Fig. 2.

The station design has a high importance for the passengers. Stations are the first and last contact points within the public transport system. Therefore, a high amenity embodied in proper waiting areas, barrier-free elevated platforms and easy-accessible entrances at both ends of the platform is crucial for attractiveness of the whole system. Easy-accessible stops with clear passenger routing provide a higher level of safety as well (see Fig. 3). This ensures a fluent and fast operation with minimized interferences.

At unsignalized intersections and pedestrian crossings trams should have the right of way similar to railway crossings. This can be realised by red-dark signals based on train detection as shown in Fig. 4. Individual traffic is only affected if a tram is arriving,

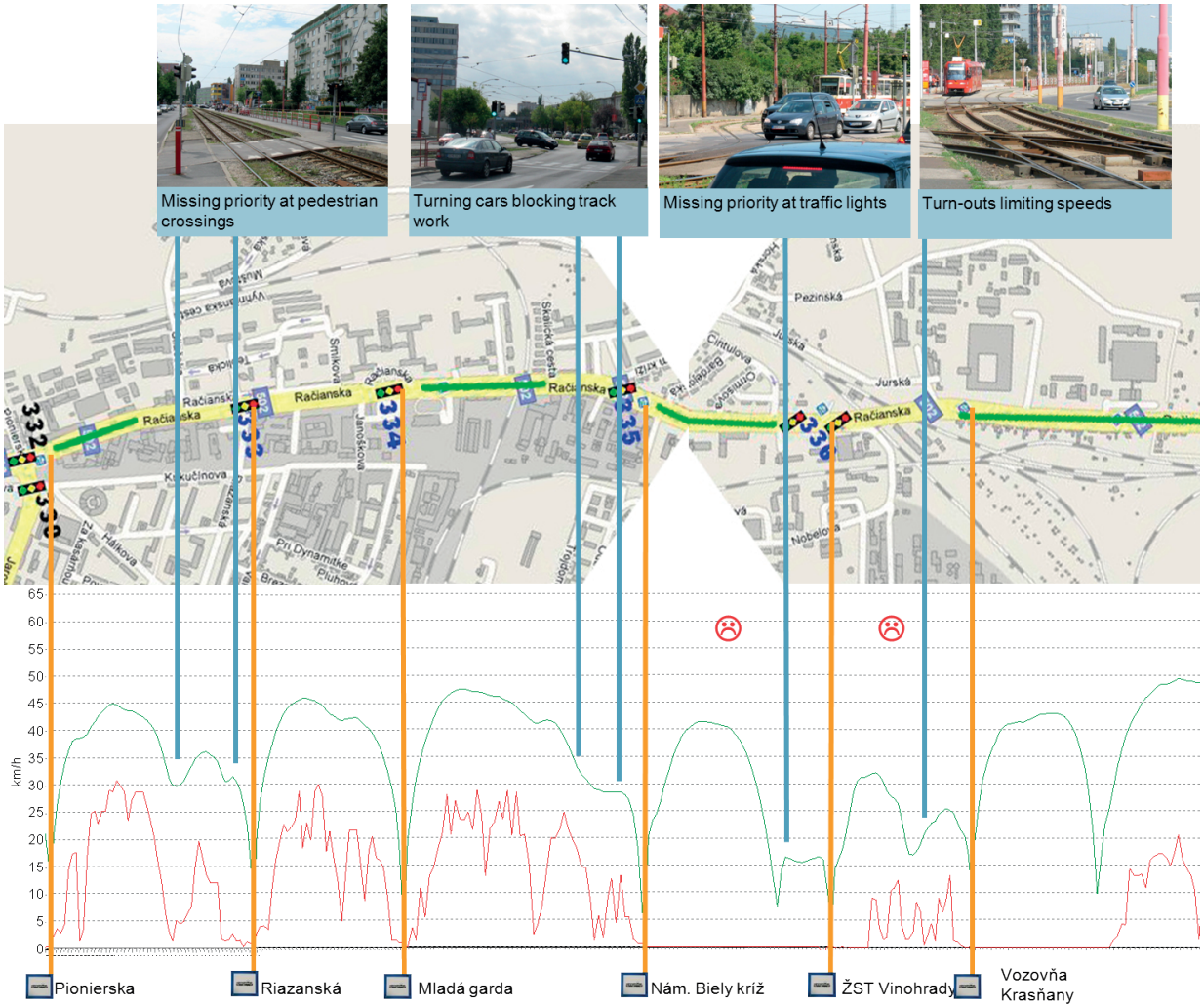

Fig. 1 Realised driving times on Racianska corridor and reasons for interferences and delays

Fig. 2 Speed limitations on Racianska corridor caused by track alignment, switches and insufficient maintenance

leading to reduced waiting time for car drivers and walkers. Finally, this leads to a higher degree of red light acceptability as unnecessary waiting time at red signals disappear.

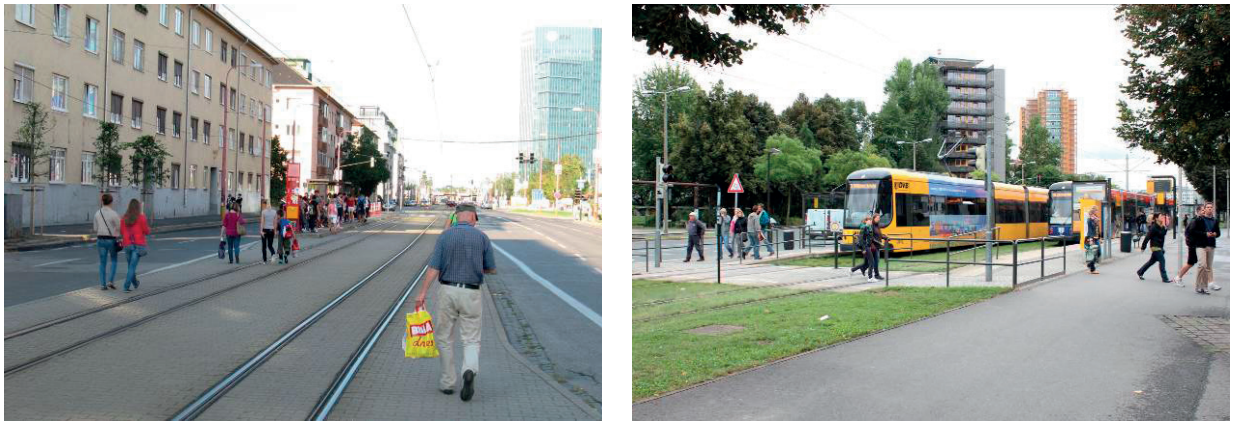

Fig. 3 Station in Bratislava without any passenger guiding system and insufficient waiting capacity, best practice station design in Dresden/Germany

Fig. 4 Unsignalized intersection on Vajnorska branch and "railway crossing" in Dresden/Germany

3. Priority at signalized intersections

The priority at signalized intersections is one of the most important measurements for a modern and reliable public transport. Every public transport vehicle needs only 5 sec green period – but in the right time. Precise interventions lead to minor interferences for individual transport. A well done priority of public transport is useful for public transport users and has only low impact on other transport modes. Therefore, a precise detection with up to 5 detection points transmitting information of line number and corresponding routing is essential [6].

Integral part of the project was the simulation of public transport priority at three signalized intersections using transport modelling software "ptv VISSIM". Besides trams, buses were considered as well. This can be realised by TETRA radio communication between public transport vehicles and the priority equipment on-site instead of fixed way-side detectors. Two out of three intersections are relatively simple junctions with a high degree of freedom. The third one (Racianska / Jarosova) is more complicated as the traffic light system is coupled with another intersection and a railway crossing.

Average waiting times public transport at intersection Vajnorska / Bojnicka — Table 2

Access from	Lines	Current Average Waiting Time (s)	Average Waiting Time (s) with Priority
East	Tram 2 and 4	19	0
South	Bus 65	16	4
West	Tram 2 and 4	24	1
West	Bus 57	43	4
North	Bus 65	11	3

Average waiting times car traffic at intersection Vajnorská / Bojnicka Table 3

Access from	Direction	Current Average Waiting Time (s)	Average Waiting Time (s) with Priority
East	Right	1	0
	Straight	38	34
	Left	44	39
South	Right	5	12
	Straight	32	48
	Left	39	50
West	Right	51	39
	Straight	20	21
	Left	15	15
North	Right	2	2
	Straight	28	34
	Left	41	48

The results prove the effectiveness of the priority at intersections with a high level of freedom. Table 2 shows the results of the optimisation at the intersection Vajnorska / Bojnicka for peak hour traffic conditions.

Not only public transport waiting times are reduced but also the range of waiting times. This is crucial for an improved reliability of public transport operations. The results show additionally that a sophisticated traffic light control does not have negative impact on individual transport or the overall capacity of the intersections. Table 3 shows the average waiting time for individual transport at the intersection Vajnorska / Bojnicka for peak hour traffic conditions.

The results of the sample intersections can be easily adapted to other intersections in Bratislava and elsewhere.

4. Conclusions

Following key pieces of advice can be extracted from this study:

- Introduction of a priority program at intersections is highly recommended. The technical solution should be identical for tram and buses. The implementation strategy should start at smaller intersections which usually have more degrees of freedom. This ensures reasonable results with comparatively low investment costs.
- Reconstruction of track sections with poor conditions is necessary. Bratislava public transport company has to be provided with sufficient funding in order to maintain the infrastructure regularly before speed reductions appear.
- Introduction of tram priority at pedestrian crossings is highly recommended.
  Reduction of unsignalized intersections and crossings: Remaining intersections should be equipped with traffic lights ensuring a strong priority for trams – similar like trains on railway crossings.
- Reconstruction of stations in order to provide safe and comfortable waiting and access areas. An implementation strategy for the construction of interchanging hubs should be accompanied by a re-design of the public transport network. The parallel alignment of trams and buses – both local and regional – should be reduced to a minimum.
- Updating the track alignment on essential sections: Changing curve radii or the location of switches and stations in order to increase the allowed speed.

Within the framework of this UNDP GEF project a sample implementation of tram priority will be realised at two street crossings, namely Racianska / Pekna cesta and Vajnorska / Bojnicka by the end of 2013. The project pushes the idea of public transport priority in Bratislava successfully. It is recommended to extend the project´s approach to main bus and trolleybus lines as well. A transfer to other Slovak and European cities can be realised easily.

References

[1] European Environment Agency: *Greenhouse Gas Emission Trends and Projections in Europe 2012*, EEA-Report, No. 6/2012, Copenhagen

[2] Global Environment Facility: Detail of GEF Project #3433, http://www.thegef.org/ gef/project_detail?projID=3433, last visit: 24/04/2013

[3] Dopravny Podnik Bratislava a.s. (Ed.): *Internal Timetables for Tramlines 1, 2, 3, 4, 5, 7, 11*, 2011, Bratislava

[4] Hamburg-Consult: *Planung und EDV im offentlichen Personennahverkehr*, http://www.hamburg-consult.de/leistungen/planung-edv-im-oeffentlichen-personennahverkehr/#edvc, last visit: 15/06/2013

[5] Dopravny Podnik Bratislava a.s.: *Bratislava Trams Driving Times*, 2011, Bratislava

[6] SMITH, H. R.; HEMILY, B., IVANOVIC, M.; FLEMING, G.: *Transit Signal Priority: A Planning and Implementation Handbook*, Washington, 2005.

https://doi.org/10.26552/com.C.2013.4.96-99

Monika Rolkova *

PARTICIPATIVE MANAGEMENT STYLE AND ITS RELATION TO EMPLOYEE WILLINGNESS TO ACCEPT JOB OFFER IN THE SAME COMPANY ONCE AGAIN

Participative management style is based on the involvement of employees in decision-making and problem-solving in the company, as well as on supporting their high autonomy and own initiative. The article describes outcomes of the research which examines the interaction between the management style and willingness of employees to accept job offer in the current company once again if they were asked in the future. Results confirmed that there is highly significant correlation between the belief of employees they would accept the job offer in the same enterprise again and their satisfaction with current management style as well as use of the elements of participative management style.

Keywords: *Participative management style, manager, demotivation, job offer, decision - making.*

1. Introduction

Participative management style is not a new style of management. It was presented in the book of American professor Douglas McGregor - The Human Side of Enterprise in 1960, which is a classic piece of company bureaucracy and human nature research. McGregor described two different approaches to the management of people: Theory X and Y: X theory which says that the average person has an innate aversion to work and tries to avoid it as much as possible, and because of this innate reluctance should be mostly forced to work, managed, controlled, and sometimes it is necessary to threat employees with penalties to begin to spend adequate effort leading to the achievement of business objectives. Theory Y assumptions say the contrary, that external control and the punishment of employees are not the only possibilities to achieve business goals. In order to accomplish the tasks, one is able to learn self-control and self-management. Commitment to achieving goals depends on the rewards connected to their attainment. The most interesting of these rewards - the satisfaction of the ego and the need for self - realization may be a direct result of efforts to achieve business objectives. In terms of modern industrialized life, the possibilities of the intellect of the average person are only partially used [1].

The current work environment is too bureaucratic and hierarchical, very often with lack of proper management. Business is too focused on the fact that people should not do any mistakes, rather than support them in achieving exceptional results. Superiors treat employees like children who do not think by themself and do not understand anything. Each activity must be approved by several superiors, each activity must be documented carefully. The rules are therefore adjusted so that no one has to do nothing wrong - but even nothing exceptional. In other words, the current model of people management in most companies does not stimulate innovations and the search for higher value-added [2].

The behavior of managers to employees is the factor that has the greatest impact on employee motivation. Managerial behavior leading to demotivation is in most cases unnecessary - not related to the "objective" conditions of work. It is the result of management mistakes and mostly of the lack of attention devoted to business training and selection of executives [3].

2. Participative management style

In this article we examine the participatory management style that in some companies has the form of so - called freedom at work. According to research studies, the concept of participative management style is currently used by 3 - 5 % of enterprises only [4], which due to its effectiveness is considered to be too low.

Participative style can be defined as a management style based on informing employees about important aspects of business development and their participation in decision-making and solving business problems, especially those that concern them. The main aim is to use their potential, knowledge, motivation, increase their job satisfaction and strengthen their identification with the company, but at the same time to gain their understanding of the new measures or changes in the company [5].

Participative style does not mean that a manager requests subordinates ideas and opinions, which are then used for decision-making. Participative decision goes further - employees are involved to participate in the management and development of the company, where openness, trust, consensus - building and

* **Monika Rolkova**
Department of Economics, Faculty of Operation and Economics of Transport and Communications, University of Zilina, Slovakia,
E-mail: monika.rolkova@fpedas.uniza.sk

mutual respect are the norms [6]. Subordinates have enough space to present their own initiative and independence in carrying out tasks. The manager encourages participation in decision-making of subordinates.

Currently, there are companies in which participative style goes even further - nothing is required, employees can decide what, when, where and how they will do. They can decide when to work, determine the amount of their salary, and elect their own bosses. These companies are usually the leaders in their respective fields of business and are the examples of one of the strongest trend in today's business world. The best examples of freedom at work are companies: Google, Semco, Zappos, W.L.Gore & Associates, Harley & Davidson or Martinus in Slovakia. In the free enterprises it is important to have two-way communication, where most decisions are taken by consensus (the right side of continuum in Fig. 1).

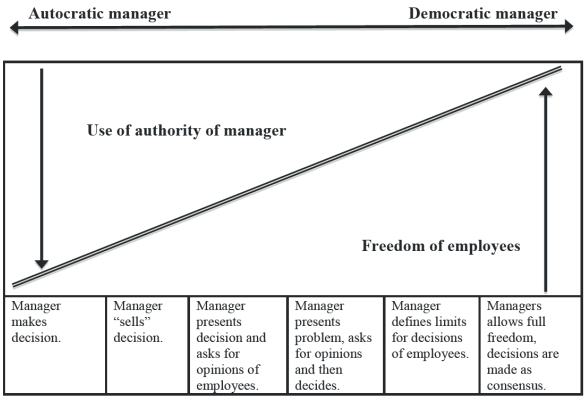

Fig. 1 The Management Behaviour Continuum. Source: self - processed based on [7]

The organization World Blu, which brings together free companies, provides 10 principles of organizational democracy, by which it assesses its members [8]:

1. *Purpose and Vision* - A democratic organization is clear about why it exists (its purpose) and where it is headed and what it hopes to achieve (its vision). These act as its true North, offering guidance and discipline to the organization's direction.
2. *Transparency* - stops the "secret society" mentality. Democratic organizations are transparent and open with employees about the financial health, strategy, and agenda of the organization.
3. *Dialogue + Listening* - Instead of the top - down monologue or dysfunctional silence that characterizes most workplaces, democratic organizations are committed to having conversations that bring out new levels of meaning and connection.
4. *Fairness + Dignity* - Democratic organizations are committed to fairness and dignity, not treating some people like "somebodies" and other people like "nobodies."
5. *Accountability* - Democratic organizations point fingers, not in a blaming way but in a liberating way. They are clear about who is accountable to whom and for what.
6. *Individual + Collective* - In democratic organizations, the individual is just as important as the whole, meaning employees are valued for their individual contribution as well as for what they do to help achieve the collective goals of the organization.
7. *Choice* - Democratic organizations thrive on giving employees meaningful choices.
8. *Integrity* - Integrity is the name of the game, and democratic companies have a lot of it. They understand that freedom takes discipline and also doing what is morally and ethically right.
9. *Decentralization* - Democratic organizations make sure power is appropriately shared and distributed among people throughout the organization.
10. *Reflection + Evaluation* - Democratic organizations are committed to continuous feedback and development and are willing to learn from the past and apply lessons to improve the future.

According to our prediction based on literature review, participative management style and democracy at work lead to better employee performance. Several studies support this opinion. The studies for example confirmed that satisfied employees are more likely to have low absenteeism and low turnover [9 and 10] Petty, McGee and Cavender in 1984 based on meta – analysis, demonstrated a strong relationship between job satisfaction and employee performance [11]. The findings of multiple regression analysis show that managers´use of participative management style is positively associated with high levels of job satisfaction [11].

3. Methodology

The type of research used in our study is a mapping research. It is a research project to describe and classify the investigated phenomena. This type of quantitative research doesn't require the formulation of scientific hypotheses, but the researcher should formulate the research questions [12].

We decided to focus attention on exploring elements of management style, which is a causal variable applied to business productivity. The main aim of the research was to explore how the elements of management style influences the satisfaction of subordinates. In this article we present two research questions from the study only.

As the research sample, we chose employees on subordinate positions in large international enterprises. We obtained respondents by intentional selection from the following sectors: electricity, gas and telecommunications. Selected companies are long-term existing enterprises in the market and the management of human capital is at a very high level there. We chose them because we wanted to focus the research on companies where human capital management don't deal with the basic problems but it is quite well developed already.

The basic research sample was 39 200 employees of selected sectors – according to information from Statistical Office of the Slovak Republic. The selected sample was calculated by Sample

Size Calculator - free online tool of Creative Research Systems. For calculation of sample size we use confidence level of 95%.

All of 200 respondents (Table 1) who filled in the questionnaire work currently on below manager level positions. As a research tool, we decided to use the questionnaire because of the necessary number of respondents and the importance of anonymity needed for examining sensitive issues in the manager – subordinate relationship. In our research we tried to obtain information through a questionnaire of attitudes and opinions on the behavior of their managers. The questionnaire was distributed online – the link to webpage with questionnaire was sent via e-mail. The response rate was approximately 50 %. We cannot confirm the exact number of employees that got the questionnaire because of snowball technique of targeting respondents – employees that were contacted by us, sent the questionnaire to their colleagues etc.

We created the items in the questionnaire based on literature findings about participative management style and measured them on a four – point Likert type scale (*yes - rather yes - rather no - no*). For statistical testing we used the Kendall's Tau correlation coefficient b - results are shown in Table 2 below.

As potentially problematic aspects in our research can be perceived difficult generalisation on the population of all employees in enterprises in Slovakia due to specific research sample of utilities selected by non-probability sampling. Another limitation is using of questionnaire as a research tool – for example the same sense of each question for all respondents can be a possible problem.

4. Results

Research question Q1: *Is the satisfaction of employees with management style related to their willingness to accept the job offer in the same company again?*

(Correlation of questions: "Would you accept a job offer in this company again?" and "Are you satisfied with the management style used by your manager?")

Research question Q2: Is *the use of elements of participative management style related to willingness of employees to accept the job offer in the same company again?*

(Correlation of question: "Would you accept a job offer in this company again?" and total of 15 items in the questionnaire that represents participatory management style – for example level of control, opportunity for own initiative and creativity, autonomy in decision – making, motivation, trust, use of employee potential etc.)

Respondents (non - management employees) Table 1.

Gender	Amount	%
Man	96	48.0
Woman	104	52.0
Total	200	100.0

Source: self-processed

Correlation is significant at the significance level of 0.01, which means that:

- the willingness to accept job offer in the same company was positively associated with subordinate satisfaction with the management style,
- the willingness to accept job offer in the same company again in the future was positively associated with the level of managers´ use of participative management style.

In this case, we confirm the theoretical prediction that management style is an important factor that affects subordinates, as research results show, it is closely related to whether the subordinates would accept the job offer in the same company again. The results show that the employees who believe in managers´ use of participative management style report higher level of willingness to accept an offer to work in the company again.

5. Conclusion

This study examined the influence of management style on employee willingness to accept the job offer in the same company again and the relationship between use of participative management style and employee willingness to accept the job offer again. It demonstrated highly positive relationship between the variables.

Several limitations of the research should be noted. The sample size is small but we believe that similar results would be confirmed even in a larger sample. We must admit that the snowball technique is not the most representative way of choosing respondents either.

In practice, we often see the resistance of managers towards participative management style as they believe that if they focus on people development and facilitating their independence, their performance will suffer. We incline to the view that human

Correlations Table 2.

			Management style	Participative management style
Kendall's tau_b	Accepting of job offer in the same company	Correlation coefficient	,564**	,596**
		p	.000	.000

Source: self-processed

resources are the most important means to achieve results. The company cannot be successful without the financial and material resources, but human resources should be an active element that sets the other ones in motion and keep them going. The difference is, whether the performance is achieved by encouraging co - operation and activities of the human factor, it means "with people" or "against them". An effective manager has the highest performance due to effective leading style. He uses individual motivation, reinforces the sense of group loyalty and identification with the organization. The ideal situation is when maximum performance is accompanied by employee satisfaction, good relationships within the group and a positive team spirit at work [13]. Researches show that satisfied employees are more productive in the long run than unhappy and dissatisfied. They don't have so many absences, are less likely to leave the company and work more than what their duties are. Our research aimed to contribute to a deeper knowledge of the attributes and relations of participative management style. We confirmed that the willingness of employees to accept the job offer in the same company again is significantly related to their satisfaction with management style, as well as using of elements of participative management style. We consider this style as the most appropriate style of management for the future of business. The companies should consider including participative management and employee empowerment techniques as components of management development and education programs.

References

[1] CARNEY, B. M., GETZ, I.: *Freedom at Work (in Czech),* Praha: PeopleComm, 2011. ISBN 978-80-904890-1-1.

[2] URIGA, J.: How the Work Will Look Like in Ten Years (in Slovak), *Trend*, 12.5.2011, pp.14-17. ISSN 1336-2674.

[3] URBAN, J.: How to Prevent Employee Demotivation (in Czech), *Human Resources Management,* No. 4, 2011, pp. 31. ISSN 1801-4690.

[4] *Management Study Guide: A Basic Understanding of Participative Management.* 2012, [online]: <http://www.managementstudyguide.com/participative-management.htm>

[5] URBAN, J.: Goals and Methods of Employee Participation (in Czech), *Mzdy & personalistika v praxi*, No. 7, 2005. [online] cit. 1.8.2012: <http://www.mzdovapraxe.cz/archiv/dokument/doc-d1193v1169-cile-a-metody-zamestnanecke-participace/>.

[6] JINDRA, J.: *Management Alphabet – Participative Management Style (in Czech),* Metodicky portal RVP 3.11.2008, [online] cit. 7.7.2012: <http://clanky.rvp.cz/clanek/s/Z/2743/ABECEDA-MANAGEMENTU--PARTICIPATIVNI-STYL-RIZENI.html/ >.

[7] CEJTHAMR, V., DEDINA, J.: *Management and Organizational Behaviour (in Czech),* Praha: Grada Publishing 2010. ISBN 978-80-247-3348-7.

[8] WORLD BLU: 10 *Principles of Organisational Democracy*. World Blu, 2012, cit. 30.6.2012, [online]: <http://www.worldblu.com/democratic-design/principles.php>.

[9] EBY, L.T., FREEMAN, D.M., RUSH, M.C., LANCE, C.E.: Motivational Bases of Affective Organizational Commitment: A Partial Test of an Integrative Theoretical Model, *J. of Occupational and Organizational Psychology*, vol. 72, 1999, pp. 463-483, ISSN: 2044-8325.

[10] PIERCE, J. L., RUBENFELD, S. A., MORGAN, S.: Employee Ownership: A Conceptual Model of Process and Effect, *Academy of Management Review*, vol. 16, 1991, pp. 121-144, ISSN 0363-7425.

[11] KIM, S.: Participative Management and Job Satisfaction: Lessons for Management Leadership, *Public Administration Review*, No. 3-4, 2002, pp. 231-241, ISSN 1540-6210.

[12] PAVLICA, K.: *Social Research, Company and Management (in Czech),* Praha : Ekopress, 2000. ISBN 80-86119-25-4.

[13] STEPANIK, J.: *The Most Often Mistakes and Failures of Managerial Praxis (in Czech),* Praha: Grada Publishing, 2010. ISBN 978-80-247-2494-2.

COMMUNICATIONS – Scientific Letters of the University of Zilina
Writer's Guidelines

1. Submitted papers must be unpublished and must not be currently under review for any other publication.
2. Submitted manuscripts should not exceed 8 pages including figures and graphs (in Microsoft WORD – format A4, Times Roman size 12, page margins 2.5 cm).
3. Manuscripts written in good English must include abstract and keywords also written in English. The abstract should not exceed 10 lines.
4. Submission should be sent: By e-mail – as an attachment – to one of the following addresses: komunikacie@uniza.sk or holesa@uniza.sk (or on CD to the following address: Zilinska univerzita, OVaV – Komunikacie, Univerzitna 1, SK-10 26 Zilina, Slovakia).
5. Uncommon abbreviations must be defined the first time they are used in the text.
6. Figures, graphs and diagrams, if not processed in Microsoft WORD, must be sent in electronic form (as JPG, GIF, TIF, TTF or BMP files) or drawn in high contrast on white paper. Photographs for publication must be either contrastive or on a slide.
7. The numbered reference citation within text should be enclosed in square brackets. The reference list should appear at the end of the article (in compliance with ISO 690).
8. The numbered references (in square brackets), figures, tables and graphs must be also included in text – in numerical order.
9. The author's exact mailing address, full names, E-mail address, telephone or fax number, the name and address of the organization and workplace (also written in English) must be enclosed.
10. The editorial board will assess the submitted paper in its following session. If the manuscript is accepted for publication, it will be sent to peer review and language correction. After reviewing and incorporating the editor's comments, the final draft (before printing) will be sent to authors for final review and minor adjustments
11. Submission deadlines are: September 30, December 31, March 31 and June 30.

COMMUNICATIONS

SCIENTIFIC LETTERS OF THE UNIVERSITY OF ZILINA
VOLUME 15

Address of the editorial office:
Zilinská univerzita
Office for Science and Research
(OVaV)
Univerzitna 1
SK 010 26 Zilina
Slovakia

E-mail: komunikacie@uniza.sk

Each paper was reviewed by two reviewers.

Journal is excerpted in Compendex and Scopus.

It is published by the University of Zilina in
EDIS – Publishing Institution of Zilina University
Registered No: EV 3672/09
ISSN 1335-4205

Published quarterly

Single issues of the journal can be found on:
http://www.uniza.sk/komunikacie

ICO 00397 563
November 2013